

# Design and Analysis of Hybrid Power System and IoT SCADA System for Remote Sites

Written by

© Wajahat Khalid

A Thesis Submitted to the School of Graduate Studies in partial fulfillment of  
the requirements for the degree of

Master of Engineering

Faculty of Engineering and Applied Science

Memorial University of Newfoundland

October 2024

# Abstract

In many developing countries, fossil fuels remain the primary energy source for power generation due to their relative affordability and availability. However, this reliance on fossil fuels significantly contributes to CO<sub>2</sub> emissions and environmental issues, such as floods driven by climate change. Additionally, the cost of power generation from fossil fuels is often high, posing economic challenges. Therefore, there is an urgent need to transition towards renewable energy sources, which offer a more sustainable and cost-effective solution. To address this issue, the design and analysis of hybrid power systems for remote sites have been carried out in Pakistan. These sites are in isolated areas without access to electricity and other infrastructure, where power is generated by burning fossil fuels. This practice is a significant source of CO<sub>2</sub> emissions and contributes to flooding. The aim is to integrate renewable energy sources, such as solar energy, with traditional generators to mitigate emissions and enhance energy access in remote sites in Pakistan.

The system is designed using a DC-DC converter, Maximum Power Point Tracking, LCL filter, and a DC-AC inverter. Utilizing software tools like PVsyst 7.4 and HOMER Pro-3.18.1 the study evaluates system sizing, energy consumption patterns, sensitivity analysis, and optimization strategies tailored to site-specific data. The analysis of connected and peak loads demonstrates the system's promise of providing reliable electricity with minimal environmental impact. The estimated capital cost and energy generation per unit underscore its economic feasibility. Dynamic modeling of the proposed hybrid power system has been performed using MATLAB R2023b, and validation through Hardware in the Loop examines the system's behavior in response to variations in solar irradiance and temperature, offering insights into operational efficiency and reliability.

For monitoring and control, an Internet of Things-based Supervisory Control and Data Acquisition system has been developed. Utilizing Blynk alongside Arduino Nano, GSM SIM800L, and ESP-32, the

system integrates essential components like ZMPT101B voltage sensor, ACS712 current sensors, MPPT for optimizing power output, a relay, battery bank, buck converter, and PV panels. Operating on both GSM and Wi-Fi, it ensures seamless data transfer. Data transmission between Arduino Nano, GSM SIM800L, and ESP-32 employs Universal Asynchronous Receiver/Transmitter (UART) serial communication protocols, programmed in Arduino IDE 1.8.19 using C++. As an open-source SCADA platform, it enables remote load management via the Blynk app and console, compatible with Android and iOS, using Transmission Control Protocol/Internet Protocol (TCP/IP) and Hypertext Transfer Protocol (HTTP) protocols for data exchange. Real-world testing validated its reliability across GSM and Wi-Fi networks, demonstrating robust performance in rural environments. Live data monitoring and control through the Blynk app showcased its capabilities. With a budget-friendly cost of CAD 35.52 and minimal power consumption at 3.462 W, this approach underscores IoT's potential to enhance efficiency and user engagement within renewable energy management systems.

The thesis demonstrates that the designed hybrid power system is economically feasible, reliable, and safe, which will help reduce carbon emissions and provide low-cost electricity.

# Acknowledgments

First, thanks to Allah Almighty who gave me strength and enabled me to sail through this fantastic journey of a master's in electrical engineering. I express my sincere gratitude to my supervisor, Dr. Mohsin Jamil, and co-supervisor Dr. Ashraf Ali Khan, whose immense knowledge and expertise in electrical power and renewable energy provided generous support and invaluable assistance throughout my master's degree. They were helpful, accommodating, and responsive whenever I sought their advice regarding my research. I also extend my thanks to the School of Graduate Studies and the Engineering and Applied Sciences department for their unwavering support. Additionally, my external supervisor, Dr. Qasim Awais, has been instrumental in helping me gather the selected site data and providing technical support in designing the SCADA system.

My appreciation also goes to my colleagues and friends, especially Mr. Muhammad Waqas , for their camaraderie, constructive discussions, and moral support. Your encouragement and understanding were crucial in overcoming the challenges encountered during this journey.

A heartfelt thank you goes to my family, despite being thousands of miles away, for their unwavering love, patience, and support. To my parents, for their sacrifices and constant belief in my abilities, and to my wife and children, Muhammad Taha Khalid, Uswa Wajahat, and Abdul Hadi Wajahat, for their endless encouragement and understanding. The sacrifices you all made, including time apart and the additional responsibilities you shouldered, were significant and deeply appreciated. Your love and support have been my pillars of strength throughout this journey.

# List of Figures

Figure 1. 1 Sector-wise CO <sub>2</sub> emissions of Pakistan [10].....	3
Figure 1. 2 Solar Irradiance Level of Pakistan [15]. .....	5
Figure 1. 3 An overview of IoT-based PV SCADA System.....	11
Figure 2. 1The energy mix of Pakistan [10].....	19
Figure 2. 2 Sketch of the natural gas transmission and distribution pipeline network. ....	20
Figure 2. 3 Solar resources (Global Horizontal Irradiance) of Pakistan [14]. ....	22
Figure 2. 4 Google Earth view of the selected site.....	23
Figure 2. 5 Selected site Solar GHI and clearness index. ....	24
Figure 2. 6 Electrical consumption of the selected site.....	25
Figure 2. 7 Monthly electricity generation by the proposed HPS.....	26
Figure 2. 8 HOMER Pro simulated diagram of proposed HPS. ....	27
Figure 2. 9 MATLAB/Simulink Model of the proposed HPS. ....	28
Figure 2. 10 a) Variations in Solar Irradiance (b) Variations in Temperature (c, d) Solar Panel output Current (I) and Voltage (V) due to variations in Solar Irradiance and Temperature. ....	29
Figure 2. 11 (a) %SOC of the battery bank (BB) (b) Battery bank voltage (c) Battery bank current. ....	30
Figure 2. 12 (a) Voltage delivered to the load in three phases (V <sub>peak</sub> ). (b) Current supplied to load across three phases. ....	31
Figure 2. 13 Real-time trial setup using OPAL-RT. ....	32
Figure 2. 14 OPAL-RT generated a three-phase load current.....	32
Figure 2. 15 OPAL-RT generated a three-phase load voltage. ....	33
Figure 3. 1 gCO <sub>2</sub> emissions by different types of fossil fuels [7]. ....	39
Figure 3. 2 Categories and trends of CO <sub>2</sub> emissions in Pakistan [11].....	40
Figure 3. 3 Pakistan's % energy supply by source [12]. ....	40

Figure 3. 4 Solar irradiance levels in Pakistan [21].	42
Figure 3. 5 A view of the site captured from above on Google Maps.	46
Figure 3. 6 Actual perspective of the selected site.	47
Figure 3. 7 Selected site solar GHI and clearness index.	48
Figure 3. 8 Selected site solar azimuth and zenith angle [34].	48
Figure 3. 9 Monthly electricity usage pattern at the chosen location.	50
Figure 3. 10 Diagram illustrating the proposed hybrid power system.	51
Figure 3. 11 Circuit diagram representing a photovoltaic cell.	52
Figure 3. 12 Buck converter (DC-DC).	53
Figure 3. 13 MATLAB modeled maximum power point tracking.	55
Figure 3. 14 Incremental Conductance Algorithm flow chart.	55
Figure 3. 15 I-V and P-V curves of selected PV panel.	57
Figure 3. 16 LCL filter's circuit diagram.	58
Figure 3. 17 Three-phase multi-level inverter schematic diagram.	60
Figure 3. 18 Orientation of the PV Panels.	61
Figure 3. 19 PVsyst simulation outcomes for the proposed system.	62
Figure 3. 20 The operational procedure of the HOMER Pro software in sequential order.	64
Figure 3. 21 Optimization results of HOMER Pro.	64
Figure 3. 22 Results of electricity generation by optimal designing of the HPS in HOMER Pro.	66
Figure 3. 23 MATLAB Simulink dynamic model for the proposed hybrid power system.	69
Figure 3. 24 (a) Variations in solar irradiance, (b) variations in temperature, (c) PV panel output voltage, and (d) PV panel output current due to variations in solar GHI and temperature.	71
Figure 3. 25 (a) %SOC of battery bank, (b) voltage of battery bank, and (c) current of battery bank.	72
Figure 3. 26 (a) Voltage is delivered to the load in three phases (RMS). (b) Current supplied to load across three phases (RMS).	73

Figure 3. 27 Hardware structure of the simulator. ....	74
Figure 3. 28 OPAL-RT hardware setup. ....	75
Figure 3. 29 Three-phase output load voltage because of experimental validation. ....	75
Figure 3. 30 Three-phase output load current as a result of experimental validation. ....	76
Figure 4. 1 Electricity demand and Generation of Pakistan [7]. ....	85
Figure 4. 2 (a) Structure of SCADA System. (b) Layer Scheme of SCADA system. ....	87
Figure 4. 3 Site overview from Google Maps [27]. ....	91
Figure 4. 4 Brief of the proposed SCADA system. ....	93
Figure 4. 5 Pin layout of Arduino nano [29]. ....	94
Figure 4. 6 Pin layout of the ESP32 [38]. ....	98
Figure 4. 7 Flow chart of SCADA System Working. ....	100
Figure 4. 8 Circuit Diagram of proposed SCADA system using Arduino Nano and GSM Sim800L. ....	101
Figure 4. 9 Blynk App setup using Arduino Nano and GSM SIM800L. ....	103
Figure 4. 10 Hardware setup using Arduino Nano and GSM SIM800L. ....	105
Figure 4. 11 Display of FIDs values on LCD. ....	106
Figure 4. 12 PV system FIDs values on the Blynk App Dashboard. ....	106
Figure 4. 13 PV system FIDs Monitoring on the Blynk App mobile interface. ....	107
Figure 4. 14 Circuit Diagram of proposed SCADA system using Arduino Nano and ESP-32. ....	109
Figure 4. 15 PV Panels installation at the rooftop of the ECE building. ....	111
Figure 4. 16 Experimental setup at MUN ECE Building. ....	112
Figure 4. 17 FIDs parameters on the LCD in the “OFF”. state. ....	112
Figure 4. 18 The status of the Blynk web dashboard interface in the “OFF” and “ON” states. ....	113
Figure 4. 19 Monitoring and Control of PV system on Blynk Console Dashboard using ESP-32 and Arduino Nano. ....	114
Figure 4. 20 PV system parameters under reduced sunlight. ....	115

Figure 4. 21 Status of DC Voltage and DC current. .... 115

Figure 4. 22 Notification of PV system parameters via SMS under testing conditions..... 117

Figure 4. 23 Arduino IDE code of the Twilio API..... 118



# List of Tables

Table 2. 1 Transmission Pipeline Network Details (SNGPL). .....	20
Table 2. 2 Electrical Load detail of the selected site.....	24
Table 2. 3 Hybrid Power System Optimization Results by HOMER Pro.....	26
Table 2. 4 Variations of Solar Irradiance on Optimization Results. ....	27
Table 3. 1 Economic loss impact due to floods in Pakistan in 2022 [15]. .....	41
Table 3. 2 Specifics regarding the electrical load at the chosen location.....	49
Table 3. 3 Various operational scenarios of the Incremental Conductance Algorithm. ....	56
Table 3. 4 Details of renewable energy generation and consumption based on predefined parameters.....	62
Table 3. 5 Specifications of battery used in HPS. ....	65
Table 3. 6 Specifications of PV panel used in HPS. ....	65
Table 3. 7 Per unit cost of components used in HPS. ....	66
Table 3. 8 Results of system optimization in HOMER Pro. ....	67
Table 3. 9 Sensitivity analysis of the system design by variations in the solar GHI. ....	67
Table 3. 10 Scenarios of variations in solar irradiance and temperature in MATLAB Simulink.....	70
Table 4. 1 An overview of prior work in the field of IoT SCADA.....	88
Table 4. 2 A detailed comparison of the proposed SCADA system with previous work. ....	89
Table 4. 3 Technical specifications of Arduino Nano.....	95
Table 4. 4 Technical specifications of the ESP-32.....	98
Table 4. 5 FIDs connections with Arduino Nano and GSM SIM800L.....	102
Table 4. 6 Price and Power consumption of elements used in the SCADA system. ....	120

# Table of Contents

<b>Abstract .....</b>	<b>I</b>
<b>Acknowledgments.....</b>	<b>III</b>
<b>List of Figures .....</b>	<b>IV</b>
<b>List of Tables.....</b>	<b>VIII</b>
<b>Table of Contents .....</b>	<b>9</b>
<b>Chapter 1 Introduction .....</b>	<b>1</b>
1.1 Background.....	1
1.2 Site Selection .....	5
1.3 Hybrid Power System Components.....	6
1.3.1 Photovoltaic Modules.....	7
1.3.2 Battery Storage.....	8
1.3.3 Inverters (DC to AC).....	8
1.3.4 Maximum Power Point Tracking (MPPT).....	8
1.3.5 Diesel Generator.....	9
1.3.6 Buck Converter .....	9
1.3.7 Monitoring and Control System.....	10
1.4 IoT-Based SCADA for PV System .....	10
1.4.1 SCADA Platform .....	12
1.5 Problem Statements .....	12
1.6 Research Objectives.....	14

<b>Bibliography .....</b>	<b>15</b>
<b>Chapter 2.....</b>	<b>17</b>
<b>Hybrid Power System Design and Dynamic Modeling of Signal Repeater Station on Natural Gas Transmission Network.....</b>	<b>17</b>
<b>Abstract .....</b>	<b>18</b>
2.1 Introduction.....	18
2.2 Site Selection .....	23
2.2.1 Solar Irradiance .....	23
2.2.2 Analysis of Electrical Load .....	24
2.3 Design and Optimization of a Hybrid Power System.....	25
2.4 Dynamic Modeling and Simulation.....	27
2.5 Experimental Validation.....	31
2.6 Conclusion and Future Work.....	33
<b>Chapter 3 .....</b>	<b>36</b>
<b>Dynamic Simulation and Optimization of Off-Grid Hybrid Power Systems for Sustainable Rural Development .....</b>	<b>36</b>
<b>Abstract .....</b>	<b>37</b>
3.1 Introduction.....	37
3.2 Site Selection and Description.....	45
3.2.1 Solar Horizontal Irradiance .....	47
3.2.2 Analysis of Electrical Load .....	49
3.3 Designing of Hybrid Power System .....	50
3.3.1 Overview and Mathematical Modeling of Elements in the HPS .....	51
3.4 Performance Analysis and Optimization of the Intended Hybrid Power System .....	60

3.4.1	Performance Analysis of System Using PVsyst Software .....	60
3.4.2	Orientation.....	61
3.4.3	Simulation in PVsyst.....	61
3.4.4	HOMER Pro Simulation and Optimization .....	63
3.5	Dynamic Modeling of Proposed Hybrid Power System in MATLAB/Simulink.....	68
3.6	Experimental Validation Using Hardware in Loop.....	73
3.7	Findings .....	76
3.8	Conclusion.....	77
<b>Chapter 4</b>	.....	<b>83</b>
<b>Open Source IoT-Based SCADA System for PV Monitoring and Control Using HTTP and TCP/IP Protocols</b>	.....	<b>83</b>
<b>Abstract</b>	.....	<b>84</b>
4.1	Introduction.....	84
4.2	Literature Review and Proposed System Comparison .....	88
4.3	Site and System Description.....	90
4.3.1	Site Description .....	90
4.3.2	PV System Description .....	91
4.3.3	System Description .....	92
4.3.4	Components used in the proposed SCADA system.....	93
4.4	Implementation Approach.....	99
4.5	SCADA-based PV System Design Using Arduino Nano and GSM SIM800L.....	100
4.5.1	Schematic Design.....	100
4.5.2	Blynk App Setup .....	102

4.5.3	Arduino Code Development.....	103
4.5.4	Hardware Setup and Commissioning with Blynk App .....	105
4.6	SCADA-based PV System Design Using Arduino Nano and ESP-32.....	108
4.6.1	Schematic Design.....	108
4.6.2	Arduino IDE Code Development for ESP-32 .....	109
4.6.3	Hardware Setup .....	111
4.6.4	Notification of PV system parameters .....	116
4.7	Discussion.....	118
4.8	Conclusion.....	120
	<b>Arduino- ESP-32 Code (Appendix A) .....</b>	<b>122</b>
	<b>References .....</b>	<b>125</b>
	<b>Chapter 5 .....</b>	<b>130</b>
	<b>Conclusion and Future Work.....</b>	<b>130</b>
5.1	Conclusion.....	130
5.2	Research Contribution/Problem Solutions .....	132
5.3	Future Work.....	133
	<b>Articles in Refereed Publications.....</b>	<b>134</b>
	<b>Refereed Conference Publications.....</b>	<b>134</b>

# Chapter 1 Introduction

## 1.1 Background

Access to modern energy services is crucial for meeting fundamental social needs and fostering economic development. Modern energy sources, especially electricity, and gas, influence productivity, health, education, access to clean water, and communication services. A strong link exists between per capita energy consumption economic growth and other indicators of a modern lifestyle. Higher electricity usage is often associated with an improved quality of life and well-being. Studies suggest that energy's vital role and the focus on energy accessibility are major drivers of economic growth, poverty alleviation, and the reduction of income inequality[1]. In 2021, global energy demand surged by 4.5%, five times higher than in 2020. Most energy production still relies on fossil fuels, leading to a 4.5% increase in coal demand, a 3.2% rise in natural gas, and a 1.3% uptick in liquid fuels, resulting in a 5% increase in CO<sub>2</sub> emissions. During the same period, renewable energy demand grew by only 3%. As of 2019, 80.2% of the global energy mix came from fossil fuels, 11.2% from renewable sources, and 8.6% from nuclear and other energy sources. In 2009, 80.3% came from fossil fuels, 8.7% from renewables, and 11% from other sources[2].

Pakistan, with the world's 6th largest population, is growing at an annual rate of 2.4% and is projected to reach 333.1 million by 2050. Additionally, urbanization is expected to hit 52% by 2025. The country's electricity demand has been increasing at an average rate of 8% per year. In 2018, Pakistan generated a total of 120,785 GWh of electricity but faced a shortfall of about 30%, requiring an additional 51,765 GWh to meet the demand-supply gap for that year[3]. Per capita electricity consumption in Pakistan is approximately 449 kWh, significantly below the global average. The country experienced an electricity shortage estimated at 1,000-2,000 MW in 2007, which escalated to around 7,000 MW by 2015. This shortfall has forced many industries to shut down or reduce their production, while residential consumers in both urban and rural areas endure power outages of about 12 hours daily during the summer. Without substantial intervention, the electricity crisis may worsen in the coming years due to rising demand and

inconsistent supply[4]. Pakistan primarily relies on natural gas and furnace oil for electricity generation with GHG emissions projected to increase from 347 Mt CO<sub>2</sub>-eq in 2011 to 4,621 Mt CO<sub>2</sub>-eq by 2050[5]. Pakistan has an untapped electricity generation potential of 100,000 MW from Thar coal, 56,000 MW from hydro, 150,000 MW from wind, and approximately 50,000 MW from solar energy[6].

The majority of electricity generation is derived from fossil fuels, leading to significant greenhouse gas emissions. Natural gas is the leading fuel in Pakistan, comprising 45% of the primary energy demand. This reliance on natural gas provides a relatively cleaner alternative to coal and oil, reducing the overall carbon footprint of the energy sector. However, the increasing demand and depleting reserves pose challenges to sustainability and energy security. To address these issues, Pakistan is exploring alternative energy sources and enhancing its natural gas infrastructure to ensure a stable and efficient power supply[7]. Sui Northern Gas Pipelines Limited (SNGPL) and Sui Southern Gas Company (SSGC) are the two major natural gas distribution companies in Pakistan. SNGPL operates in the northern regions, encompassing Punjab, Khyber Pakhtunkhwa, and parts of Azad Kashmir, with an extensive network spanning over 94,000 kilometers. SSGC, on the other hand, serves the southern regions, including Sindh and Baluchistan, and manages a pipeline network exceeding 44,000 kilometers. Both companies play crucial roles in ensuring the distribution of natural gas across Pakistan, supporting residential, commercial, and industrial sectors, and contributing significantly to the country's energy infrastructure[8].

In 2014, the power sector was responsible for a significant portion of global greenhouse gas emissions. According to the IEA (2017), this included 90% CO<sub>2</sub>, 1% N<sub>2</sub>O, 9% CH<sub>4</sub>, and 14% other gases. Climate change impacts various aspects such as weather patterns, household income, poverty, agricultural and forest products, and local livelihoods. Environmental changes have immediate effects on multiple sectors in Pakistan, including water availability, crop patterns, livestock, forests, biodiversity, and coastal zones. Consequently, climate change is one of the most complex and dangerous environmental challenges. To mitigate its impacts, the global community aims to limit the increase in global temperatures to 2°C by the end of this century[9].

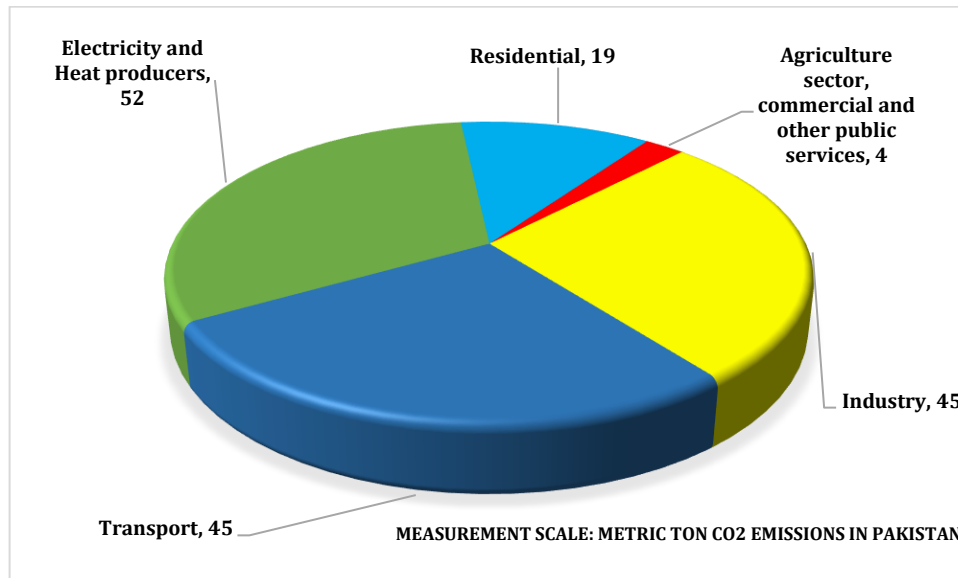


Figure 1. 1 Sector-wise CO2 emissions of Pakistan [10].

Figure 1.1 shows the sector-wise share of CO<sub>2</sub> emissions in Pakistan. Deforestation in Pakistan, driven by the need to meet energy demands, has significantly exacerbated the country's flood risk. The removal of forests, which act as natural barriers against floodwaters, has left vast areas vulnerable to severe flooding. This deforestation has not only increased the frequency and intensity of flood events but also contributed to soil erosion and reduced groundwater recharge. Pakistan has a long history of floods, experiencing nearly 19 major events over the past 60 years. These floods have cumulatively inundated over 594,700 km<sup>2</sup>, impacted 166,075 villages, and resulted in direct economic losses amounting to approximately \$30 billion. Tragically, these events have also led to the loss of 10,668 lives[11].

The Khyber Pakhtunkhwa (KPK) province in Pakistan has been frequently affected by devastating floods, causing widespread destruction and hardship. These floods have severely damaged infrastructure, including roads, bridges, and homes, displacing thousands of residents and disrupting daily life. The agricultural sector, a primary livelihood source in KPK, suffers extensive losses, with crops and livestock being washed away. Additionally, floods have led to significant soil erosion and contamination of water sources, exacerbating health risks. The recurring nature of these floods highlights the urgent need for improved flood management strategies and infrastructure resilience in the region[12].



With a population of nearly 235.8 million in 2022 and a total land area of 796,095 km<sup>2</sup>, Pakistan faces significant demographic and geographic challenges. Current projections indicate that the population will continue to grow, reaching approximately 403 million by 2050. Over 63% of the population resides in rural areas, where improving living standards is constrained. These limitations compel rural households, and to some extent urban households, to rely on biomass energy resources for cooking and heating. According to the International Energy Agency (IEA 2019), more than 2.8 million households in Pakistan lack access to clean fuel energy, and 14% of the world's population does not have electricity for cooking and heating[13].

A hybrid power system, combining renewable energy sources such as solar with traditional energy sources, is essential for addressing CO<sub>2</sub> emissions and electrification challenges in rural areas. By integrating photovoltaic panels, wind turbines, and sometimes small-scale hydroelectric systems with backup diesel generators or battery storage, these systems can provide a reliable and continuous power supply. This approach significantly reduces reliance on fossil fuels, thereby lowering CO<sub>2</sub> emissions. Moreover, hybrid systems can be tailored to the specific needs and resources of rural communities, offering a sustainable and cost-effective solution for electrification. This not only improves the quality of life by providing consistent access to electricity but also supports economic development and reduces the environmental impact associated with traditional energy sources.

Pakistan has substantial solar energy potential due to its high solar radiation levels, with an average solar irradiance of 5.5 to 7.0 kWh/m<sup>2</sup> per day, translating to approximately 1,800 to 2,200 kWh/m<sup>2</sup> annually. Baluchistan, with irradiance levels often exceeding 7.0 kWh/m<sup>2</sup> per day, stands out for its exceptional solar resources. Sindh also enjoys high solar irradiance, averaging around 6.0 to 6.5 kWh/m<sup>2</sup> per day, especially in its arid regions. Punjab benefits from 5.5 to 6.0 kWh/m<sup>2</sup> per day, while Khyber Pakhtunkhwa experiences similar levels of 5.5 to 6.0 kWh/m<sup>2</sup> per day. Gilgit-Baltistan and Azad Jammu and Kashmir have slightly lower irradiance, ranging from 5.0 to 6.0 kWh/m<sup>2</sup> per day. With an estimated solar power potential of around 2.9 million MW, Pakistan is well-positioned to harness solar energy to

meet its growing energy demands and reduce reliance on fossil fuels[14]. Figure 1.2 shows the Solar Irradiance level of Pakistan.

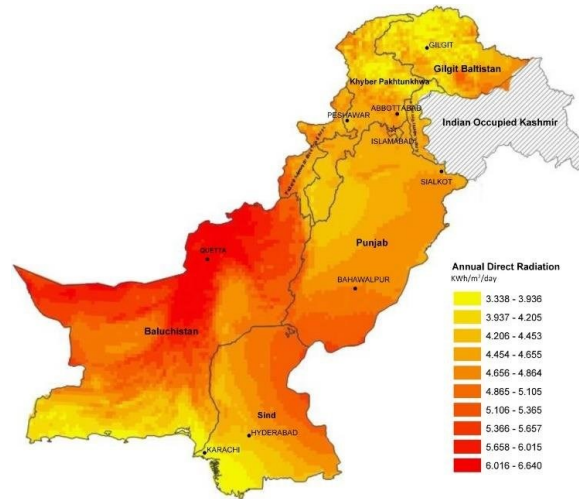


Figure 1. 2 Solar Irradiance Level of Pakistan [15].

A hybrid power system, combining renewable energy sources such as solar with traditional energy sources, is essential for addressing CO2 emissions and electrification challenges in rural areas. By integrating photovoltaic panels, wind turbines, and sometimes small-scale hydroelectric systems with backup diesel generators or battery storage, these systems can provide a reliable and continuous power supply. This approach significantly reduces reliance on fossil fuels, thereby lowering CO2 emissions. Moreover, hybrid systems can be tailored to the specific needs and resources of rural communities, offering a sustainable and cost-effective solution for electrification. This not only improves the quality of life by providing consistent access to electricity but also supports economic development and reduces the environmental impact associated with traditional energy sources.

## 1.2 Site Selection

Selecting the right site for setting up a PV (photovoltaic) system is crucial for maximizing energy production and ensuring long-term efficiency. Key considerations include the site's solar exposure, with a preference for locations that receive ample sunlight throughout the year. The angle and orientation of the installation area should be optimized to capture the maximum solar irradiance. Additionally, the site should be free from shading by nearby structures, trees, or other obstructions that could block sunlight[16].

In this research, two remote sites have been selected details of which are given below:

- A natural gas repeater station is situated on the Sui Northern Gas Pipelines Limited Transmission Network in a remote area of Kotmomin, Punjab, Pakistan. Due to its isolated location, there is no access to the grid, and the critical transmission operations are currently powered by diesel generators. The site's GPS coordinates are 32°12'09"N 72°59'03"E. Solar radiation data for this location, as illustrated in Figure 5, has been sourced from NASA's database through the HOMER Pro software. The data indicates that the site receives sufficient sunlight, with levels ranging from 3.080 to 7.140 kWh/m<sup>2</sup>/day. Additionally, the clearness index values, which measure the proportion of sunlight relative to sky coverage, range from 0.534 to 0.648.
- The second selected site, **Berru Bandi**, is a small community of ten houses located in the rural area of Abbottabad District, approximately 25 kilometers from Abbottabad city. This site is situated on top of a mountain at coordinates 34°16'38"N 73°15'18"E and at 1456.79 meters above sea level. Accessing the site is challenging due to a lack of road access and basic amenities. The site receives adequate solar radiation, with values ranging from 2.79 kWh/m<sup>2</sup>/day to 7.46 kWh/m<sup>2</sup>/day, indicating sufficient sunlight energy availability. The clearness index, a dimensionless measure ranging from 0 (completely overcast sky) to 1 (clear sky), varies from 0.546 to 0.694 at this location, reflecting favorable conditions for solar energy generation.

### 1.3 Hybrid Power System Components

An off-grid hybrid power system (HPS) is designed to operate independently from the main utility grid, providing reliable electricity in remote or rural areas where grid access is unavailable or unreliable. Here's a breakdown of its components and operation:

- **Renewable Energy Sources:** Solar panels generate electricity from sunlight and wind, respectively.

- **Battery Storage:** Stores excess energy produced by renewable sources, ensuring a continuous power supply during periods of low energy generation (e.g., night or calm weather).
- **Inverters:** Convert the direct current (DC) generated by the solar panels and wind turbines into an alternating current (AC) most household appliances use.
- **Charge Controllers:** Manage the flow of electricity from renewable sources to the batteries, preventing overcharging and optimizing battery lifespan.
- **Diesel Generator:** Provides backup power to ensure reliability during extended periods of low renewable energy production.
- **Monitoring and Control Systems:** Include sensors and software to track system performance, manage energy distribution, and ensure efficient operation.
- **Power Converters and Protection Devices:** Ensure compatibility and safety within the system by adjusting voltage levels and protecting against faults.

### 1.3.1 Photovoltaic Modules

PV (photovoltaic) modules, commonly known as solar panels, are essential components in solar energy systems, converting sunlight into electrical energy. They are composed of multiple solar cells made from semiconductor materials, typically silicon, which generate electric current when exposed to sunlight through the photovoltaic effect. Key features to consider when selecting PV modules include their efficiency ratings, power output, temperature coefficient, and durability. Efficiency ratings indicate how well the module converts sunlight into usable electricity. Power output, measured in watts, indicates the amount of electricity generated under standard test conditions. The temperature coefficient shows how the module's performance changes with temperature, which is crucial for areas with high-temperature

fluctuations. Durability is often ensured by weather-resistant materials and robust construction, allowing the modules to withstand environmental stresses like wind, rain, and hail. PV modules come in various types, including monocrystalline, polycrystalline, and thin film, each with distinct advantages and trade-offs

### **1.3.2 Battery Storage**

Battery storage in HPS is essential for storing excess energy from renewable sources like solar panels during peak production periods. This stored energy ensures a reliable power supply during times of low or no renewable energy production, such as at night or in calm weather. Batteries also provide backup power in off-grid systems, ensuring uninterrupted electricity. Integrated with charge controllers and inverters, they optimize energy management by regulating charging and discharging cycles, thus maximizing efficiency and extending battery lifespan. This capability enhances grid stability by smoothing fluctuations in energy output and supports energy independence in off-grid applications.

### **1.3.3 Inverters (DC to AC)**

In an HPS, a DC to AC inverter is crucial for converting direct current (DC) from renewable sources like solar panels and wind turbines into alternating current (AC) electricity. This conversion allows AC power to be supplied to household appliances, industrial machinery, and grid-tied applications, matching the utility grid's AC specifications. Inverters facilitate efficient energy distribution and seamless integration of renewable energy into power grids, enhancing flexibility and stability. Modern HPS inverters include advanced features like grid synchronization to ensure electricity is synchronized with the grid's frequency and phase, maximizing energy utilization and ensuring safe operation. They may also offer monitoring and control functionalities to optimize energy production, manage battery storage, and maintain system performance in various environmental conditions.

### **1.3.4 Maximum Power Point Tracking (MPPT)**

Maximum Power Point Tracking (MPPT) is a vital technology in HPS that optimizes energy output from

renewable sources like solar panels and wind turbines. MPPT controllers adjust the operating voltage and current to extract maximum power under varying conditions, such as changes in sunlight intensity or wind speed, ensuring peak system efficiency. By continuously optimizing the electrical characteristics, MPPT maximizes energy harvest and improves overall system performance, crucial for reliable power supply and system sustainability. This technology is particularly beneficial in HPS by increasing energy yield, reducing fossil fuel dependency, and supporting grid stability in both off-grid and grid-tied configurations. MPPT controllers enhance return on investment by ensuring that renewable sources operate at their highest potential.

### **1.3.5 Diesel Generator**

In HPS, diesel generators provide a reliable backup power source during periods of low renewable energy generation or high demand. They are crucial in off-grid setups for maintaining power during extended cloudy or low wind conditions and can also supplement renewable sources in grid-tied systems. Diesel generators are equipped with automatic start-up and shutdown features, integrated with system controllers to switch seamlessly between power sources. They operate most efficiently at specific load capacities, optimizing fuel use and reducing emissions. Proper sizing and management of diesel generators are essential to enhance overall system efficiency and minimize environmental impact.

### **1.3.6 Buck Converter**

In HPS, a buck converter efficiently manages DC voltage from renewable sources like solar panels, wind turbines, and battery storage. It steps down higher DC voltages to match the load or battery charging requirements, optimizing energy transfer and minimizing power losses. By regulating output voltage with a transistor or MOSFET, buck converters achieve high efficiency, often exceeding 90%. When integrated with MPPT controllers, they maximize energy capture from solar panels. Buck converters are essential for effectively integrating renewable energy and stable system performance.

### **1.3.7 Monitoring and Control System**

In HPS, the monitoring and control system is vital for optimizing the performance of renewable energy sources, storage, and backup generators. It uses sensors and software to collect and analyze real-time energy production and consumption data. Operators use this data to monitor system health, detect issues, and adjust parameters for efficient energy management. Automated algorithms manage interactions between components, while remote access allows for proactive maintenance. Historical data analysis supports performance evaluation and informed decision-making.

#### **1.3.7.1 Voltage Sensor (ZMPT101B)**

The ZMPT101B is a voltage transformer module used in HPS to measure AC voltages up to 250V. It converts AC voltage into a proportional DC output, enabling precise monitoring of components like inverters and generators. With high accuracy and low power consumption, it supports effective energy management and system reliability. Its compact size and microcontroller compatibility make it ideal for monitoring and control systems.

#### **1.3.7.2 Current Sensor (ACS712)**

The ACS712 current sensor measures AC or DC currents up to 30A in HPS. The Hall effect provides a voltage output proportional to the current, allowing for bidirectional measurement and easy integration with microcontrollers. It enables precise management of energy consumption, battery rates, and fault detection in components like inverters and charge controllers. Its compact size and accuracy make it ideal for reliable current measurement.

## **1.4 IoT-Based SCADA for PV System**

An IoT-based SCADA (Supervisory Control and Data Acquisition) system for PV systems integrates Internet of Things (IoT) technology with traditional SCADA principles to enhance monitoring, control,

and management capabilities. This system utilizes sensors and IoT devices to collect real-time data on solar panel performance, environmental conditions, and energy production metrics.

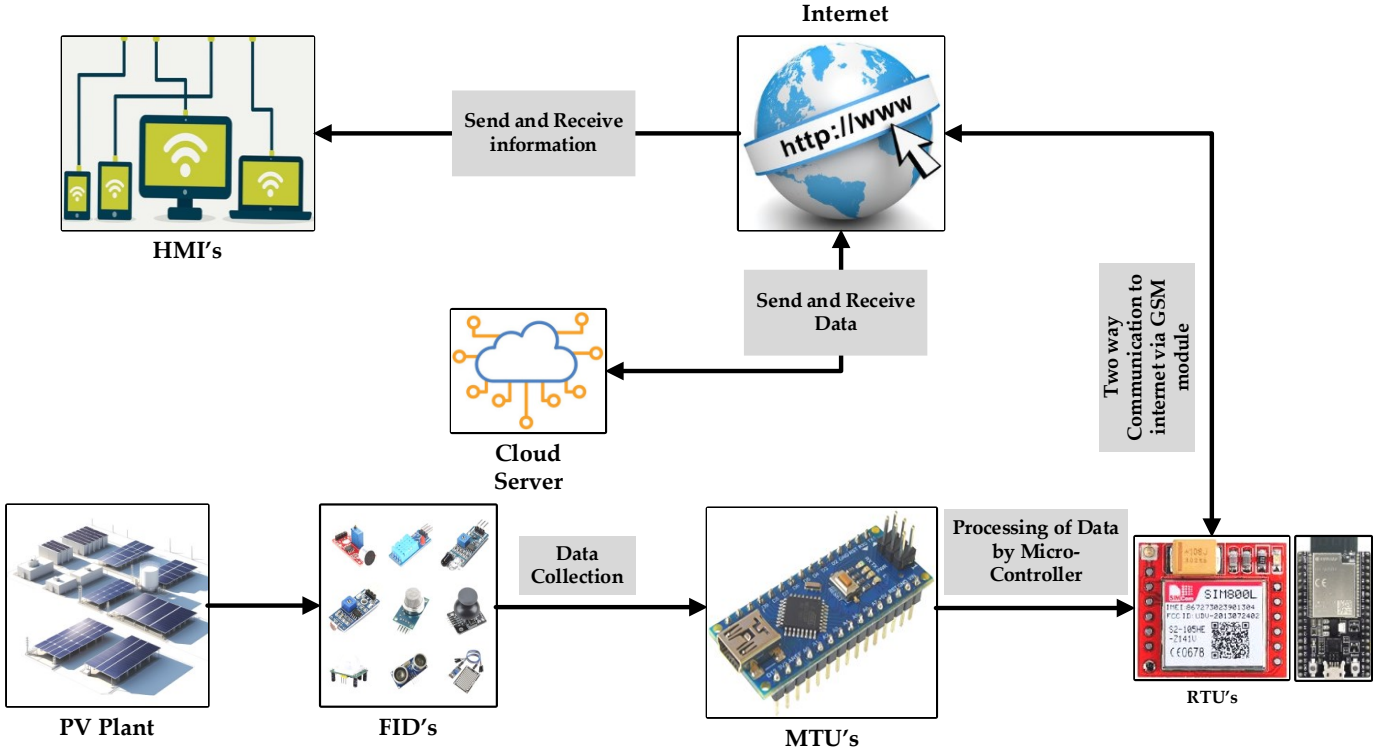


Figure 1. 3 An overview of IoT-based PV SCADA System.

Through cloud-based platforms, operators can remotely access and analyze this data, enabling proactive maintenance, optimizing energy efficiency, and identifying performance anomalies or faults promptly. Automated alerts and predictive analytics further enhance system reliability by allowing operators to respond swiftly to changing conditions or potential issues. By leveraging IoT connectivity, the SCADA system provides scalable and flexible solutions for PV systems, supporting sustainable energy practices and maximizing the yield of solar energy installations[18]. Figure 1.3 shows an overview of IoT-based PV system configuration.



## 1.4.1 SCADA Platform

A SCADA (Supervisory Control and Data Acquisition) platform centralizes the monitoring and control of industrial processes or infrastructure. It collects real-time data from sensors on variables like temperature and pressure and allows operators to interact through a human-machine interface (HMI) to monitor and adjust settings. Data is stored for analysis and reporting, providing insights into performance and optimization. SCADA ensures reliable communication over LAN/WAN or cloud, with robust security measures to protect data and system integrity. A SCADA system can be conceptualized across four main layers:

- **Sensing Layer:** At the bottom layer, the sensing layer consists of sensors, meters, and remote terminal units (RTUs) that collect real-time data from industrial processes or infrastructure. These devices monitor parameters such as temperature, pressure, and flow rates.
- **Device Layer:** Above the sensing layer, the device layer encompasses controllers and actuators that receive commands from the SCADA system and perform actions based on the received data. This layer interfaces directly with physical equipment and machinery.
- **Cloud Layer:** The cloud layer facilitates data storage, processing, and analysis in cloud-based environments. It leverages cloud computing infrastructure to store large volumes of SCADA data securely and provide scalable computing resources for advanced analytics and machine learning applications.
- **Service Layer:** At the topmost layer, the service layer includes SCADA servers, human-machine interfaces (HMIs), and application services that enable operators to monitor processes, visualize data, and control operations remotely. This layer also supports integration with enterprise systems and external services for comprehensive operational management and decision-making.

## 1.5 Problem Statements

Electricity is indispensable to modern society, serving as the lifeblood of industrialization, technological

advancement, and daily convenience. It powers homes, hospitals, schools, and industries, enabling essential services such as lighting, heating, and communication. Access to reliable electricity is therefore crucial for societal development, economic prosperity, and improving standards of living across the globe.

Clean energy initiatives are pivotal for global sustainability efforts, offering environmentally friendly alternatives to traditional fossil fuels. Technologies such as solar power play a crucial role in reducing carbon emissions and mitigating climate change impacts. By transitioning to clean energy sources, communities and industries can improve air quality, reduce reliance on finite resources, and promote sustainable development. Embracing clean energy technologies represents a significant step towards achieving global energy goals while preserving natural ecosystems and fostering a more resilient and equitable future for all. The cost of renewable energy has become increasingly competitive with electricity generated from fossil fuels in recent years. Technological advancements and economies of scale have driven down the costs of renewable energy sources such as solar. Lower operational and maintenance expenses contribute to their overall affordability compared to traditional fossil fuel plants.

The mitigation of floods caused by deforestation in rural areas due to meeting energy needs can be effectively addressed by integrating strategies with a shift towards renewable energy sources. Transitioning towards renewable energy sources like solar reduces reliance on wood and biomass, alleviating deforestation pressures and preserving ecosystems.

This study aims to create cost-effective, open-source IoT-based SCADA systems for HPS capable of monitoring and controlling essential parameters. The designed system is user-friendly, operating seamlessly on both mobile devices and web consoles. This stands in contrast to the expensive proprietary SCADA systems currently prevalent in the market. Many utility companies opt for comprehensive solutions from multiple suppliers, often priced beyond the means of small and medium-sized organizations, leading to reliance on single suppliers. Addressing this challenge involves configuring and programming open-source SCADA systems to effectively monitor and manage photovoltaic (PV) systems. This

approach aims to democratize access to SCADA capabilities, facilitating wider adoption and fostering innovation in technologies for monitoring renewable energy systems.

Therefore, this study aims to present an efficient solution for an HPS that incorporates diverse renewable energy sources. The objective is to reduce the cost per unit of electricity and mitigate carbon emissions. Furthermore, dynamic modeling has been utilized to analyze the system's performance under both steady-state and transient conditions, complemented by real-time Hardware in the Loop simulation. To enable economical monitoring, a SCADA system has been developed to show real-time parameters and provide user-friendly control of electrical appliances, empowering users to both monitor data and manage operations efficiently.

## **1.6 Research Objectives**

The problem statement and motivation mentioned in the previous section led to the establishment of the following key objectives of this research. These are given below.

1. To mitigate greenhouse gas emissions and reduce flooding in developing countries by evaluating their potential to generate electricity from solar energy
2. Design an HPS for two distinct sites in rural areas of Pakistan to produce low-cost electricity while ensuring system reliability.
3. Examine the dynamics of HPS underload variations and sudden changes in irradiance and validate the designed system in real-time using Hardware-in-the-Loop (HIL) testing.
4. Design and implement an open-source, low-cost IoT-based SCADA system for remote monitoring and control of system parameters, utilizing various communication protocols.

# Bibliography

- [1] S. A. Sarkodie and S. Adams, 'Electricity access, human development index, governance and income inequality in Sub-Saharan Africa', *Energy Rep.*, vol. 6, pp. 455–466, Nov. 2020, doi: 10.1016/j.egy.2020.02.009.
- [2] M. A. Raza, K. L. Khatri, and A. Hussain, 'Transition from fossilized to defossilized energy system in Pakistan', *Renew. Energy*, vol. 190, pp. 19–29, May 2022, doi: 10.1016/j.renene.2022.03.059.
- [3] N. H. Mirjat, M. A. Uqaili, K. Harijan, G. D. Valasai, F. Shaikh, and M. Waris, 'A review of energy and power planning and policies of Pakistan', *Renew. Sustain. Energy Rev.*, vol. 79, pp. 110–127, Nov. 2017, doi: 10.1016/j.rser.2017.05.040.
- [4] A. Mengal, N. H. Mirjat, G. D. Walasai, S. A. Khatri, K. Harijan, and M. A. Uqaili, 'Modeling of Future Electricity Generation and Emissions Assessment for Pakistan', *Processes*, vol. 7, no. 4, p. 212, Apr. 2019, doi: 10.3390/pr7040212.
- [5] N. Abas, A. Kalair, N. Khan, and A. R. Kalair, 'Review of GHG emissions in Pakistan compared to SAARC countries', *Renew. Sustain. Energy Rev.*, vol. 80, pp. 990–1016, Dec. 2017, doi: 10.1016/j.rser.2017.04.022.
- [6] A. A. Durrani, I. A. Khan, and M. I. Ahmad, 'Analysis of Electric Power Generation Growth in Pakistan: Falling into the Vicious Cycle of Coal', *Eng*, vol. 2, no. 3, pp. 296–311, Jul. 2021, doi: 10.3390/eng2030019.
- [7] M. Shahbaz, H. H. Lean, and A. Farooq, 'Natural gas consumption and economic growth in Pakistan', *Renew. Sustain. Energy Rev.*, vol. 18, pp. 87–94, Feb. 2013, doi: 10.1016/j.rser.2012.09.029.
- [8] S. Kanwal, M. T. Mehran, M. Hassan, M. Anwar, S. R. Naqvi, and A. H. Khoja, 'An integrated future approach for the energy security of Pakistan: Replacement of fossil fuels with syngas for better environment and socio-economic development', *Renew. Sustain. Energy Rev.*, vol. 156, p. 111978, Mar. 2022, doi: 10.1016/j.rser.2021.111978.
- [9] B. Lin and M. Y. Raza, 'Analysis of energy related CO<sub>2</sub> emissions in Pakistan', *J. Clean. Prod.*, vol.

219, pp. 981–993, May 2019, doi: 10.1016/j.jclepro.2019.02.112.

[10] M. U. Malik, Z. U. Rehman, A. Sharif, and A. Anwar, ‘Impact of transportation infrastructure and urbanization on environmental pollution: evidence from novel wavelet quantile correlation approach’, *Environ. Sci. Pollut. Res.*, vol. 31, no. 2, pp. 3014–3030, Dec. 2023, doi: 10.1007/s11356-023-31197-x.

[11] S. M. H. Shah, Z. Mustaffa, F. Y. Teo, M. A. H. Imam, K. W. Yusof, and E. H. H. Al-Qadami, ‘A review of the flood hazard and risk management in the South Asian Region, particularly Pakistan’, *Sci. Afr.*, vol. 10, p. e00651, Nov. 2020, doi: 10.1016/j.sciaf.2020.e00651.

[12] F. E. L. Otto *et al.*, ‘Climate change increased extreme monsoon rainfall, flooding highly vulnerable communities in Pakistan’, *Environ. Res. Clim.*, vol. 2, no. 2, p. 025001, Jun. 2023, doi: 10.1088/2752-5295/acbfd5.

[13] H. Yousaf, A. Amin, A. Baloch, and M. Akbar, ‘Investigating household sector’s non-renewables, biomass energy consumption and carbon emissions for Pakistan’, *Environ. Sci. Pollut. Res.*, vol. 28, no. 30, pp. 40824–40834, Aug. 2021, doi: 10.1007/s11356-021-12990-y.

[14] M. Irfan, Z.-Y. Zhao, M. Ahmad, and M. C. Mukeshimana, ‘Solar Energy Development in Pakistan: Barriers and Policy Recommendations’, *Sustainability*, vol. 11, no. 4, p. 1206, Feb. 2019, doi: 10.3390/su11041206.

[15] S. Akhtar, M. K. Hashmi, I. Ahmad, and R. Raza, ‘Advances and significance of solar reflectors in solar energy technology in Pakistan’, *Energy Environ.*, vol. 29, no. 4, pp. 435–455, Jun. 2018, doi: 10.1177/0958305X18758487.

[16] S. Zambrano-Asanza, J. Quiros-Tortos, and J. F. Franco, ‘Optimal site selection for photovoltaic power plants using a GIS-based multi-criteria decision making and spatial overlay with electric load’, *Renew. Sustain. Energy Rev.*, vol. 143, p. 110853, Jun. 2021, doi: 10.1016/j.rser.2021.110853.

[17] ‘<https://www.superstrate.net/pv/limit/tandem.html>’.

[18] G. Yadav and K. Paul, ‘Architecture and security of SCADA systems: A review’, *Int. J. Crit. Infrastruct. Prot.*, vol. 34, p. 100433, Sep. 2021, doi: 10.1016/j.ijcip.2021.100433.

## Chapter 2

# Hybrid Power System Design and Dynamic Modeling of Signal Repeater Station on Natural Gas Transmission Network

## Preface

*A version of this manuscript has been peer-reviewed, accepted, and presented in the conference proceedings of the IEEE 2024 12th International Conference on Smart Grid. The paper has also been published on the IEEE Xplore Database as a part of the IEEE ICSMARTGRID 2024 conference proceedings (doi: 10.1109/icSmartGrid61824.2024.10578153). I am the primary author, and have carried out most of the research work, performed the literature reviews, and carried out the system design, modeling, and analysis of the results. I also prepared the first draft of the manuscript and subsequently revised the final manuscript based on the feedback from the supervisor. The Co-author, Dr. Mohsin Jamil supervised the research and provided the research guide, reviewed and corrected the manuscript, and contributed research ideas in the actualization of the manuscript.*

# Abstract

This paper explores the design and dynamic modeling of a Hybrid Power System (HPS) for Repeater Stations on Natural Gas transmission pipeline networks. These stations transmit crucial data, such as gas flow rates and pressure readings, from remote areas to central control centers. Given their remote locations, ensuring a reliable power supply is crucial. Using the advanced software tool HOMER Pro, the study explores optimization methods tailored to site-specific details. With careful analysis, considering a connected load of 33.65 kWh/d and a peak load of 11.33 kW, the proposed hybrid power system presents a reliable solution for electricity supply while reducing environmental impact. The estimated capital cost of \$24,987 and Cost of Energy (COE) of \$0.199 per unit underscore the system's economic feasibility, supporting its potential for widespread adoption. The system design undergoes dynamic modeling with MATLAB/Simulink R2022b (MATLAB 9.13) to assess its performance and reliability. Experimental validation includes hardware-in-the-loop (HIL) testing using OPAL-RT Technologies' real-time OP5707XG simulator.

**Keywords:** Natural Gas transmission network, Repeater Station, Hybrid Power System (HPS), HOMER Pro, COE, dynamic simulation.

## 2.1 Introduction

Energy is essential for human welfare and is pivotal in economic development and fostering growth. Ensuring access to reliable energy resources is a significant global challenge, especially in developing nations lacking secure energy supplies[1]. It is commonly recognized that energy is the benchmark for measuring economic growth and improving everyone's living level [2]. Access to energy is a fundamental pillar of modern society, closely associated with advancements in health, education, and social well-being [3]. Energy can originate from fossil fuels such as crude oil, coal, and uranium, or renewable sources like radiant energy, Thermal power, Organic fuel, Hydroelectric, and wind energy [4]. Natural gas (NG) stands out among fossil fuel sources due to its lower emissions density and reduced sustainability effect during

generation and consumption, particularly when compared to oil and coal [5]. Natural gas holds a critical position in energy production. Global consumption of natural gas (NGC) is projected to surge by over 40% from 2018 to 2050, driven primarily by electricity generation and industrial sector demands[6]. Natural gas is often far from where it's needed, so it's transported by trucks carrying liquefied natural gas (LNG) or through pipelines. Pipelines are crucial due to the large volume of gas, requiring a well-developed Transmission Pipeline Network (TPN) to meet growing demand. As the gas moves through the TPN, it passes through various components like compressor stations, valve assemblies, repeater stations, and sales meter stations, regulating pressure and ensuring it reaches its destination[7]. Figure 2.1 Shows the dependency of Pakistan’s energy production on Natural Gas. Pakistan has faced a severe energy crisis for the past decade, particularly in natural gas supply. The discovery of significant reserves in Sui, Baluchistan, in 1952 led to the establishment of gas infrastructure for domestic, industrial, and electricity generation purposes. The transmission and Distribution of Natural gas are managed by two State-owned Sui Twin Companies namely Sui Northern Gas Pipelines Limited (SNGPL) and Sui Southern Gas Company Limited (SSGCL) [9].

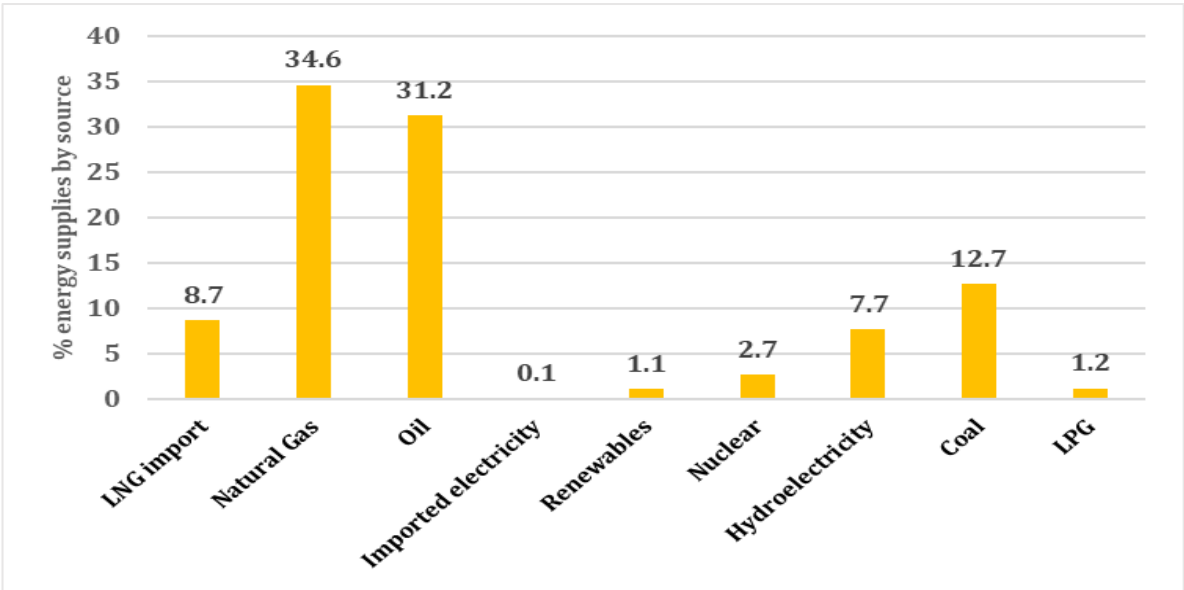


Figure 2. 1The energy mix of Pakistan [10].

The natural gas transmission network includes compressor stations, valve assemblies, and repeater stations, strategically placed in far-flung locations to support nationwide gas transmission. Table 2.1 presents a detailed Sui Northern Gas Pipelines Transmission network overview.



Table 2. 1 Transmission Pipeline Network Details (SNGPL).

Description	Present Status
Transmission Network length	9285 Km
Maximum Pipeline Diameter	42 inches
Minimum Pipeline Diameter	4 inches
Number of Valve Assemblies	466
Number of Sales Meter Stations	412
Number of Repeater Stations	85
Number of Compressor Stations	11

Figure 2.2 depicts a schematic of the natural gas transmission and distribution network, spanning from exploration to the end consumer.

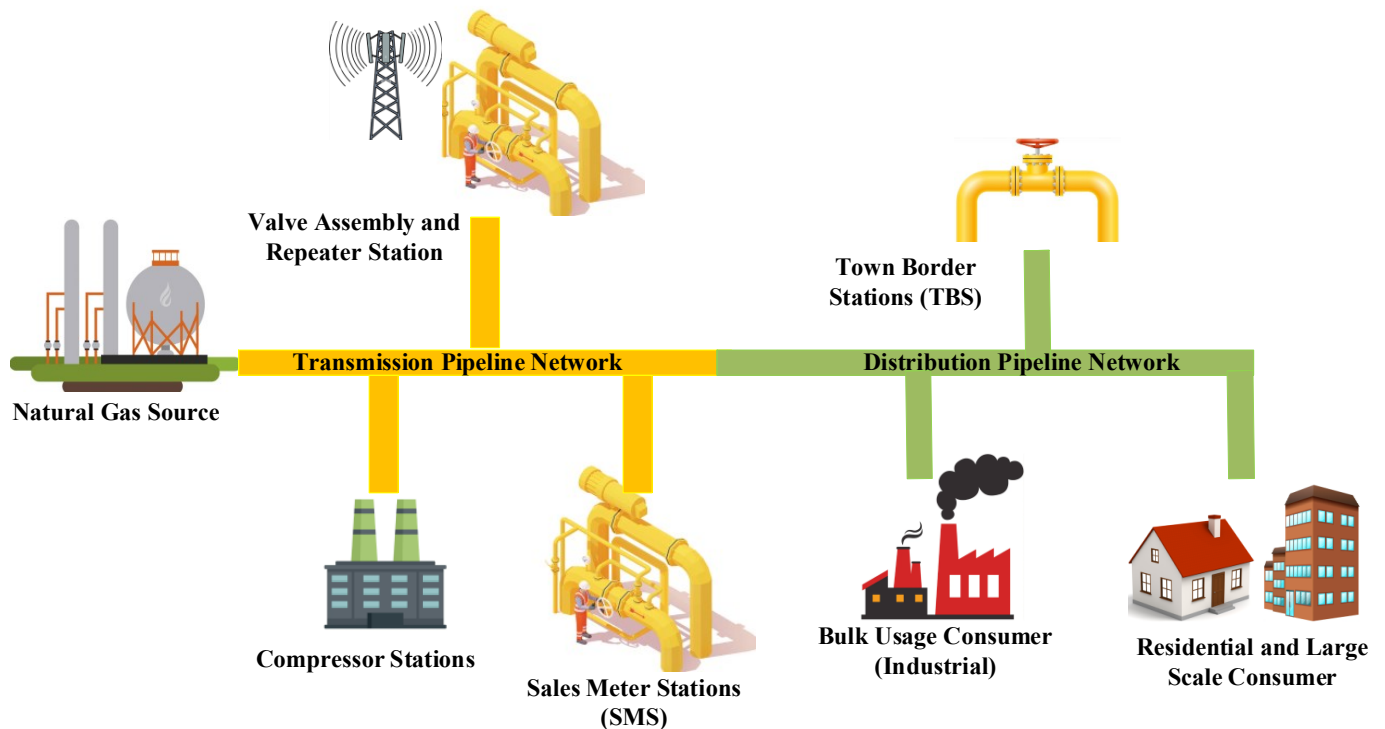


Figure 2. 2 Sketch of the natural gas transmission and distribution pipeline network.

Repeater stations are essential in Transmission Pipeline networks, enabling real-time monitoring and control of gas pressure, volume, and flows, and transmitting radio waves for wireless communication within

the Organization. This ensures constant communication with the Gas Control Center and allows station officials to promptly respond to any emergencies or ruptures. As depicted in Table 1, the transmission network of Sui Northern Gas Pipelines comprises 85 repeater stations. These stations are strategically positioned in remote areas where the gas pipelines pass through, as they cannot traverse urban areas. This ensures their placement where there is no access to the electricity grid. To fulfill their energy needs, these repeater stations utilize natural gas to power generators, which, despite being costly and unreliable, also contribute to CO<sub>2</sub> emissions.

A considerable segment of the populace in Pakistan, especially in rural regions, remains deprived of electricity access, resorting to fossil fuel combustion to fulfill their energy needs. The circumstance is concerning, with just 60% of the nation's inhabitants linked to the power grid. At present, Pakistan grapples with a deficit in power supply ranging from 3-5 GW[10]. Pakistan's energy crisis arises from heavy reliance on costly thermal resources like coal, oil, and natural gas, exacerbated by shortages. Hydroelectricity's share has declined significantly, while renewables meet only 0.3% of energy needs. Solar energy emerges as a promising solution, offering competitive pricing globally. Solar PV capacity reached 402 GW by 2017, with projections indicating a further increase by almost 580 GW, driving renewable electricity capacity growth[11]. The global shift towards renewable energy is increasingly crucial as traditional sources struggle to keep pace with rising energy demands, resulting in shortages. However, the variability of solar radiation and wind speeds, influenced by changing weather patterns, poses challenges for renewable energy systems, causing fluctuations in output. To address this issue, hybrid renewable energy (HRE) systems, which combine various renewable sources, offer a promising solution for enhancing efficiency and reliability[12].

Solar energy, derived from sunlight, is available directly or indirectly from sunlight-generated heat. Outside the Earth's atmosphere, solar radiation averages 1367 W/m<sup>2</sup>, reducing due to atmospheric effects to a peak intensity of about 1 kW/m<sup>2</sup> at sea level. Pakistan, located within the Latitude and Longitude ranges 24°N and 37°N and 62°E and 75°E, receives solar radiation ranging from 5 to 7 kWh/m<sup>2</sup>/day over 95% of its territory, with a continuity factor exceeding 85%. The mean global irradiation on a horizontal surface in

Pakistan is around 200–250 W/m<sup>2</sup>, with 8 to 10 hours of sunshine daily[13].

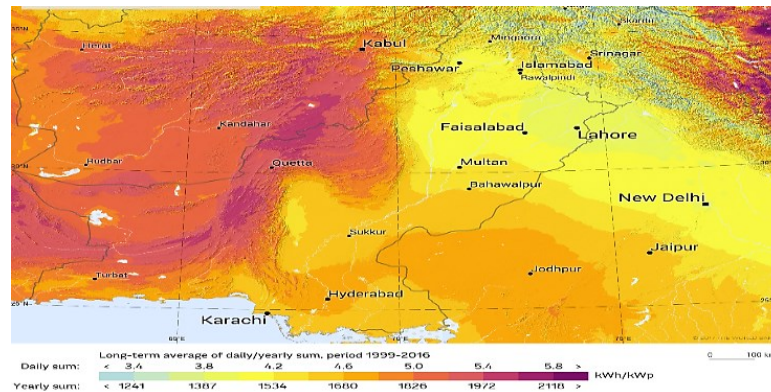


Figure 2. 3 Solar resources (Global Horizontal Irradiance) of Pakistan [14].

Over the last few years, many studies have been conducted in the domain of renewable energy. Irfan et al.[15] evaluate off-grid solar PV feasibility for rural electrification in Punjab, Pakistan. They find ample solar irradiance in rural areas, with optimized tilt angles for enhanced energy output. Ahmed et al.[16] utilized PV\*SOL software to simulate rooftop PV applications on university buildings. Results show the potential generation of 5389.2 MWh/year with an annual specific yield of 1336.6 kWh/kWp. Environmental analysis indicates PV utilization can save 63,727.05 tons of CO<sub>2</sub>, 1.89 tons of CH<sub>4</sub>, 0.27 tons of N<sub>2</sub>O, 970.05 tons of SO<sub>2</sub>, and 590.12 tons of NO emissions over 25 years. Aziz Baig et al.[17] proposed a PV system tailored to individual household load profiles, comprising PV panels and a battery bank. The paper outlines the solar energy potential, load profiles, and optimal system configuration. Additionally, it describes the microgrid setup, connections, and technical details of Peer-to-Peer energy trading for potential financial returns.

The primary emphasis of these investigations lies in the design and optimization of renewable energy solutions for rural and urban electrification, with minimal attention given to the electrification of natural gas infrastructure. Hence, this research aims to demonstrate the optimization and evaluation of a stand-alone Hybrid Power System essential for powering a remote Natural Gas Transmission Pipeline repeater station in Pakistan, with a focus on ensuring system reliability. The primary goal of this research is to design and

fine-tune the suggested Hybrid Power System by utilizing HOMER Pro software. This involves identifying the optimal capability and layout of essential elements to fulfill energy needs. Key steps include assessing the consumption profile, evaluating the availability of sustainable resources, integrating energy storage solutions, and analysis of techno-economical solutions and the impact of variations of Solar irradiance on the Cost of Energy (COE) as well as the overall cost of the proposed system. The dynamic modeling and simulation of the intended system by using MATLAB/Simulink to access system performance along with experimental validation on the real-time simulator OPAL-RT Simulator.

## 2.2 Site Selection

Site selection is crucial for hybrid power systems, impacting performance by assessing renewable resources and load profiles. Environmental and economic factors influence viability, aiming for optimal energy generation, minimal impact, and cost-effectiveness. The selected is a repeater station on the Transmission network of Sui Northern Gas Pipelines located at a remote location of Kotmomin with coordinates of  $32^{\circ}12'09''\text{N } 72^{\circ}59'03''\text{E}$ . The satellite view of the site on Google Earth is shown in Figure 2.4.



Figure 2. 4 Google Earth view of the selected site.

### 2.2.1 Solar Irradiance

Global Horizontal Irradiance (GHI) measures total solar radiation on a horizontal surface, crucial for solar energy assessment. Influenced by time, location, and atmospheric conditions, accurate GHI analysis aids in system design and performance optimization. GHI data guides solar energy technology deployment,

ensuring efficient utilization across diverse geographic regions.

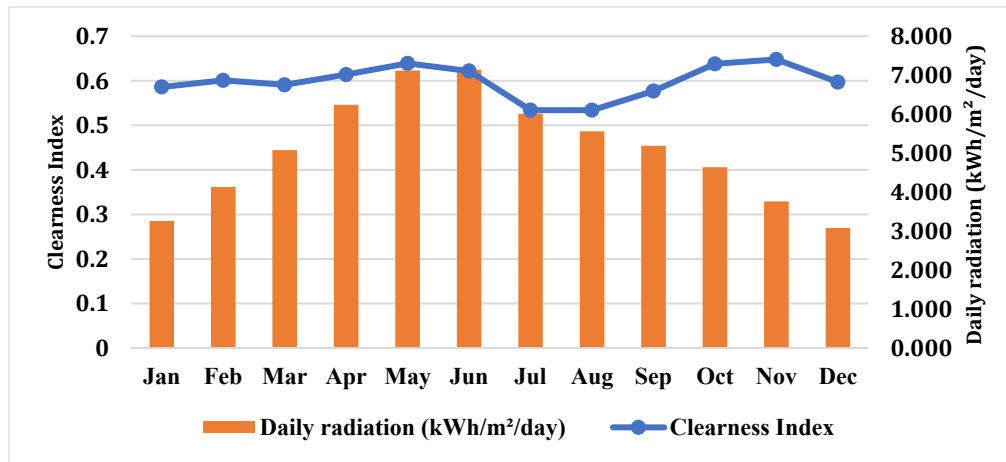


Figure 2. 5 Selected site Solar GHI and clearness index.

The chosen location's solar radiation data is shown in Figure 2.5. is sourced from NASA's database via HOMER Pro software, showing sufficient sunlight levels ranging from 3.080 to 7.140 kWh/m<sup>2</sup>/day. Clearness index values, indicating sky coverage to sunlight intensity, range from 0.534 to 0.648 at the selected sites.

## 2.2.2 Analysis of Electrical Load

The electrical load plays a crucial role in hybrid power systems, greatly influencing their design, functionality, and overall effectiveness. Table 2.2 shows the details of the electrical load at the selected site. The diversity factor in electrical loads assesses how the peak demands of various devices align with the system's maximum demand.

Table 2. 2 Electrical Load detail of the selected site.

Appliances Description	Number of Units	Rated Power Watts (W)	Total Connected Load (kW)
Ceiling Fan	20	120	2.4
Air Conditioner	2	5200	10.4
Refrigerator	1	750	0.75
Reverse Osmosis Plant	1	2000	2
Cathodic Protection System	1	3000	3
SCADA Remote site Computers	4	250	1
Water Pump	1	1500	1
LED Lights	100	30	3
<b>Total Connected Load</b>			<b>23.55</b>

A higher factor suggests less simultaneous usage, potentially allowing for smaller capacity requirements. It reflects load distribution and impacts system sizing and efficiency. Equation 1. describes the formula for the diversity factor.

$$\text{Diversity Factor} = \frac{\sum \text{Individual maximum demand}}{\text{maximum demand of the aggregated system}} \quad (1)$$

Considering the diversity factor, the Hybrid Power System is configured to accommodate a peak load of 11.33 kW. Figure 2.6 illustrates the monthly electricity consumption pattern at the chosen location.

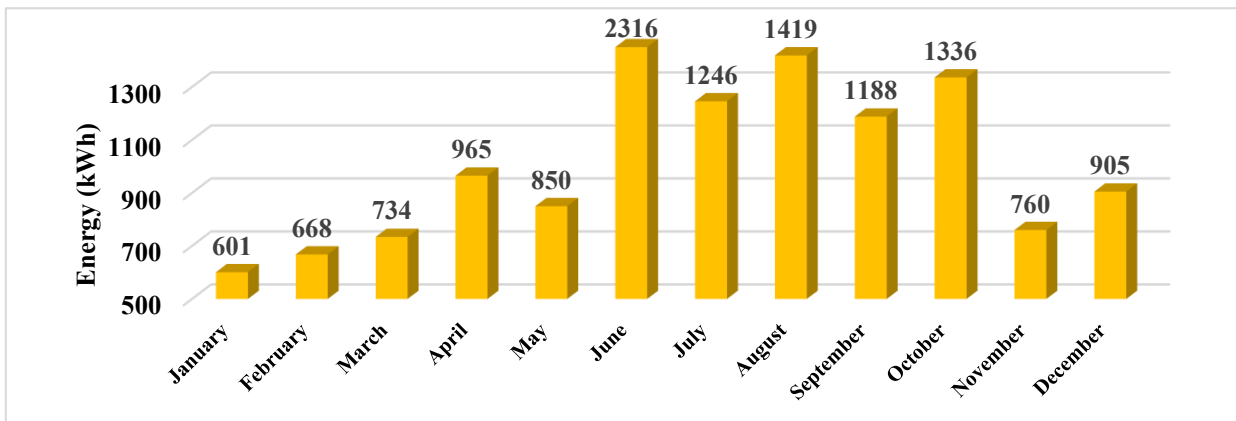


Figure 2. 6 Electrical consumption of the selected site.

## 2.3 Design and Optimization of a Hybrid Power System

The design of a hybrid power system for the selected site is done using HOMER Pro software. HOMER Pro software, a product of collaboration between the National Renewable Energy Laboratory and HOMER Energy, specializes in optimizing microgrid designs for various settings including rural regions, islands, military installations, and connected buildings. Its suite of tools evaluates both engineering and economic factors, comparing existing systems with proposed ones[18]. The HOMER Pro software inputs the solar irradiance, temperature profile, and load profile of the chosen site. The system comprises two buses: AC and DC. The Gas Generator is linked to the AC bus, operating within the range of 220V to 210V to fulfill the energy requirements of the Hybrid Power System and connected loads. Meanwhile, the Solar Panels and battery bank (BB) are connected to the DC bus, operating at 360V. Figure 8. depicts the essential components for designing and optimizing the Hybrid Power System using HOMER Pro. The software

evaluates 1047 solutions, selecting the best based on technical, economic, and environmental factors.

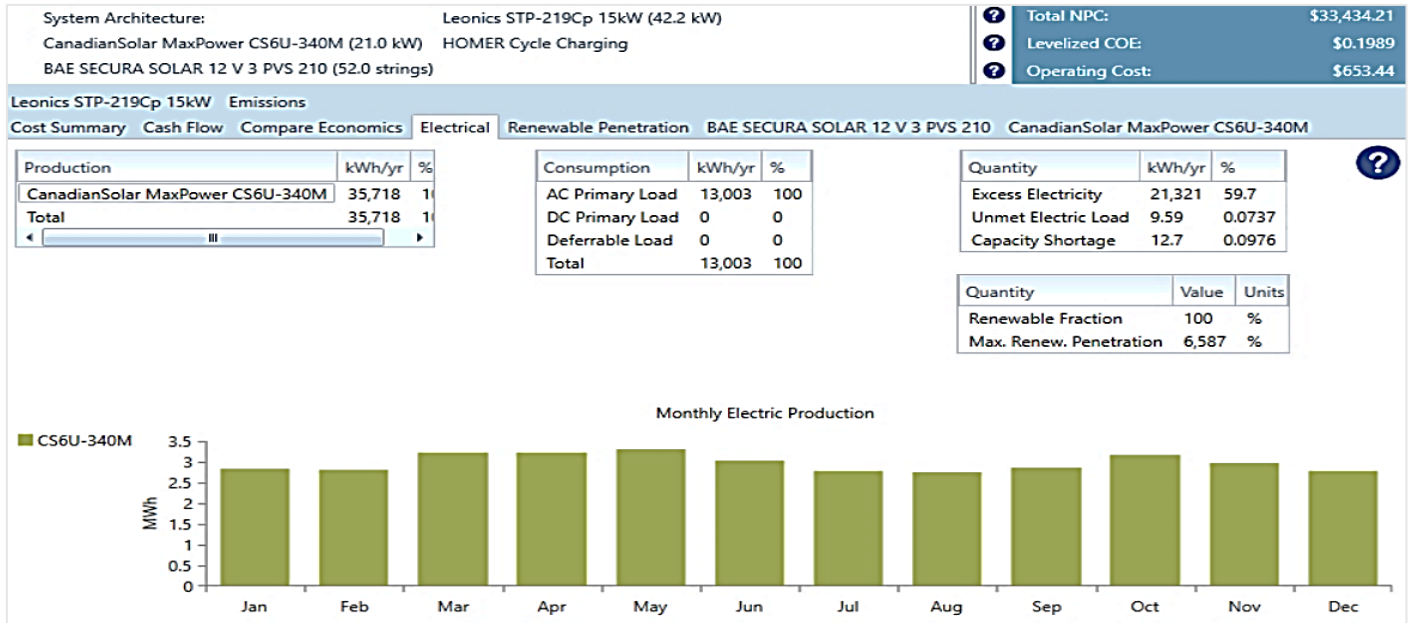


Figure 2. 7 Monthly electricity generation by the proposed HPS.

Table 2. 3 Hybrid Power System Optimization Results by HOMER Pro.

System Design	PV (kW)	Gas Gen-set (kW)	Battery Bank (No. of Batteries)	Converter AC-DC (kW)	NPC (USD)	COE (USD/kWh)	Operating Cost (USD/Year)	Initial Capital (USD)
Solar Panel-BB-Converter	21		52	42.2	33,434	0.199	653.44	24,987
PV-Gen-set-BB-Converter	17.2	13	20	10.4	72,297	0.430	499.97	65,834
BB-Gen-set-Converter		13	25	14.9	178,181	1.06	9,290	58,087
Gen-set		13			447,757	2.66	30,614	52,000

The optimal values presented in Table 2.3 were derived using HOMER Pro, which evaluates various system configurations to find the most feasible solution. Specifically, HOMER Pro simulates combinations of PV systems, battery banks, and converters, calculating Net Present Cost (NPC), Cost of Energy (COE), operating costs, and initial capital. The selected configuration—21 kW PV, 52 batteries, and a 42.2 kW converter—provided the lowest NPC of \$33,434 and COE of \$0.199 per kWh, balancing efficiency and cost-effectiveness. Alternative configurations resulted in higher NPCs and COEs, making them less viable in the long term.

Table 2. 4 Variations of Solar Irradiance on Optimization Results.

Case	Solar Irradiance Variations (kWh/m <sup>2</sup> /day)	System Design	PV (kW)	Battery Bank (No. of Batteries)	Converter (kW)	NPC (\$)	COE (\$/kWh)	Operating Cost (\$/Year)	Initial Capital (\$)
1	+40%	PV-BB-Converter	18	45	12.5	25,618	0.152	514.73	18,964
2	+20%	PV-BB-Converter	18	52	14.9	27,649	0.164	554.53	20,480
3	<b>Ideal case</b>	PV-BB-Converter	21	52	42.2	33,434	0.199	653.44	24,987
4	-30%	PV-BB-Converter	26.7	56	20.8	35,687	0.212	714.66	26,448
5	-50%	PV-BB-Converter	36.4	56	14.7	41,833	0.249	844.62	30,914

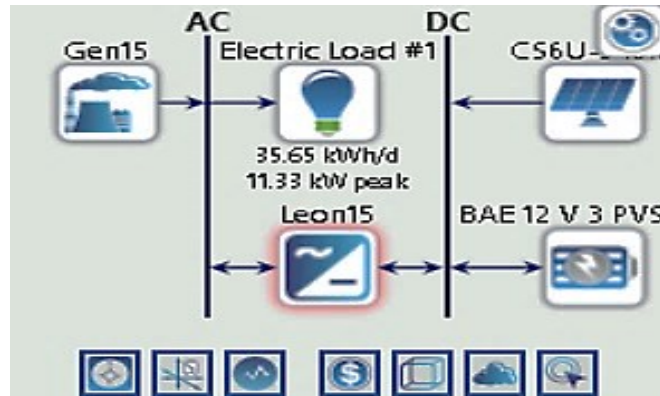


Figure 2. 8 HOMER Pro simulated diagram of proposed HPS.

Figure 2.7 illustrates monthly electricity generation from the system, projected to produce 35,718 kWh annually with a renewable fraction of 100% and a 59.7% surplus. Table 2.3 details HOMER Pro's optimization, with 52 batteries, 61 PV panels, a Net Present Cost (NPC) of \$33,434, and a Cost of Energy (COE) of \$0.199. Other combinations are unfeasible due to high COE, NPC, and initial costs. Table 2.4 shows the impact of irradiance variations on the Cost of Energy (COE) in a Hybrid Power System. Higher sunlight levels may require larger setups, while lower levels can increase costs. A 40% increase in irradiance leads to COE, NPC, operating, and initial cost reductions of approximately 23-24%. Conversely, a 50% decrease results in COE, NPC, operating, and initial cost increases of around 5-10%.

## 2.4 Dynamic Modeling and Simulation

Dynamic modeling and simulation are crucial for assessing system functionality. MATLAB/Simulink simulations analyze the hybrid power system's behavior, focusing on power quality, voltage fluctuations, and load effects.



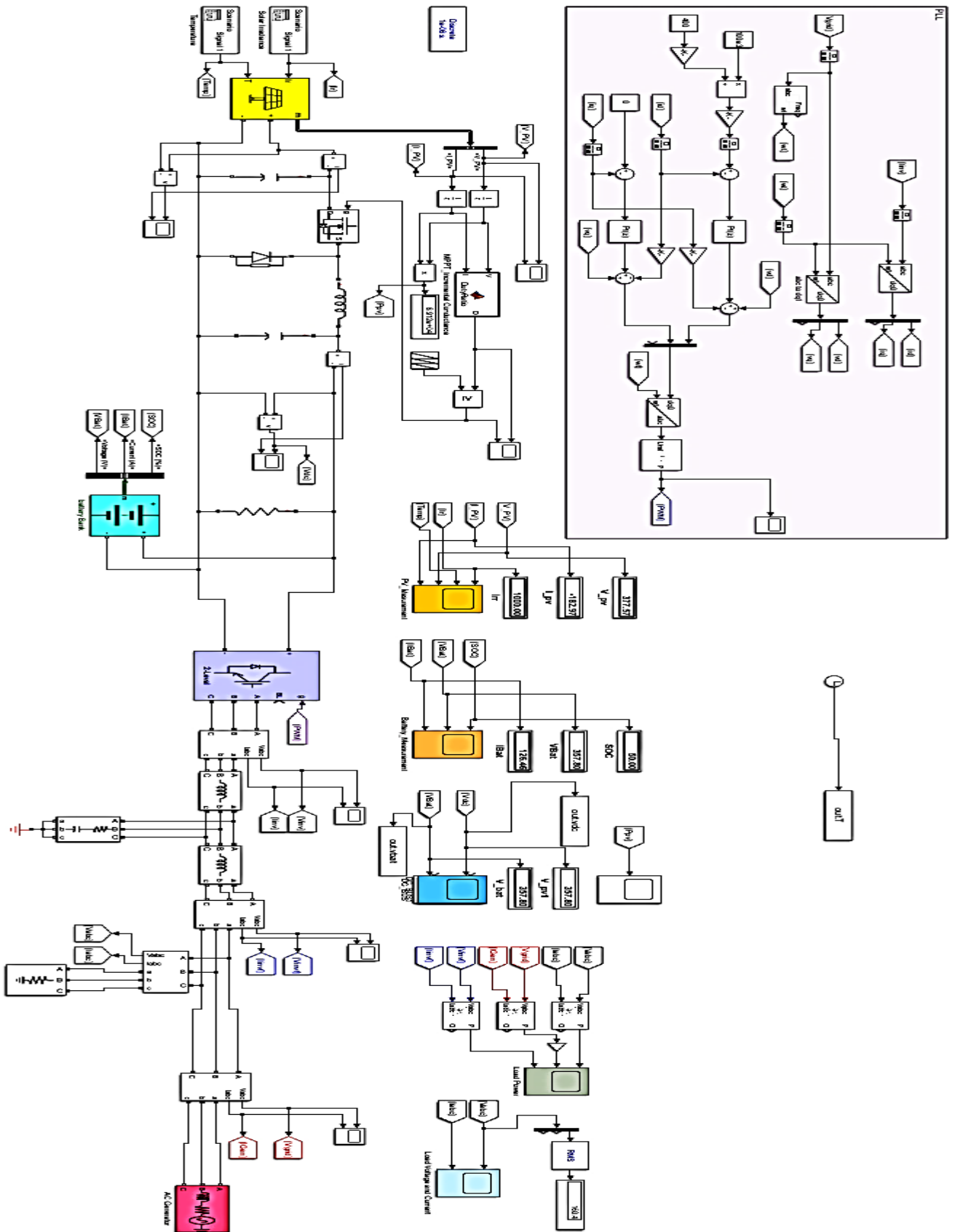


Figure 2. 9 MATLAB/Simulink Model of the proposed HPS.

They study how the PV system responds to changes in solar irradiance and temperature. Standard irradiance is set at 1000 W/m<sup>2</sup> and simulated solar cell temperatures range from 25°C to 60°C. Higher temperatures can boost current output in the semiconductor, illustrating the complex relationship among irradiance, temperature, voltage, and current, affecting system performance and efficiency. Figure 2.9 shows the MATLAB/Simulink model of the proposed Hybrid Power System.

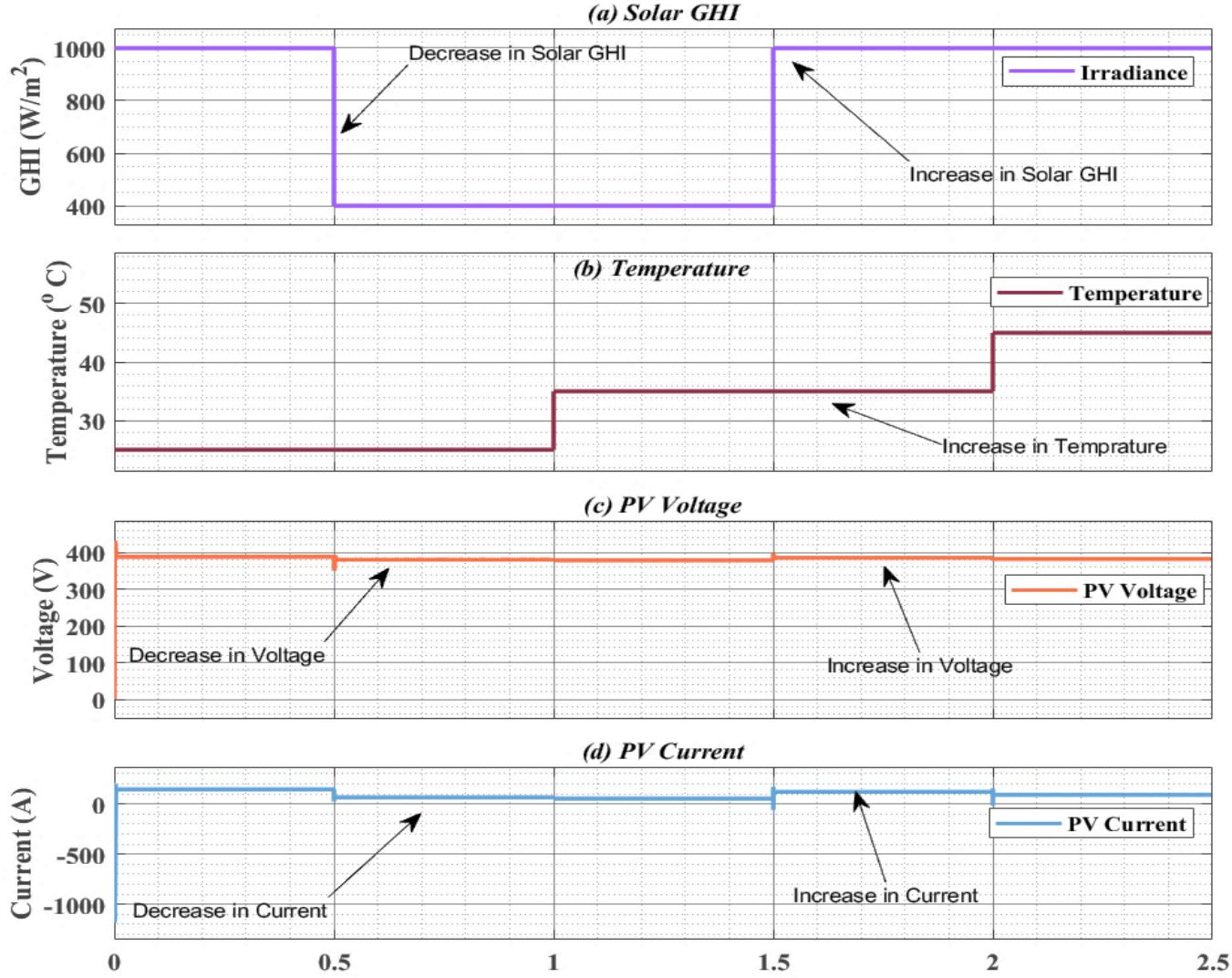


Figure 2. 10 a) Variations in Solar Irradiance (b) Variations in Temperature (c, d) Solar Panel output Current (I) and Voltage (V) due to variations in Solar Irradiance and Temperature.

Adjustments to the PV array's solar GHI and temperature in MATLAB/Simulink illustrate their impact on output voltage and current. Initially, under standard conditions with 1000 W/m<sup>2</sup> GHI and 25°C temperature, Figure 2.10 depicts variations in GHI and temperature.

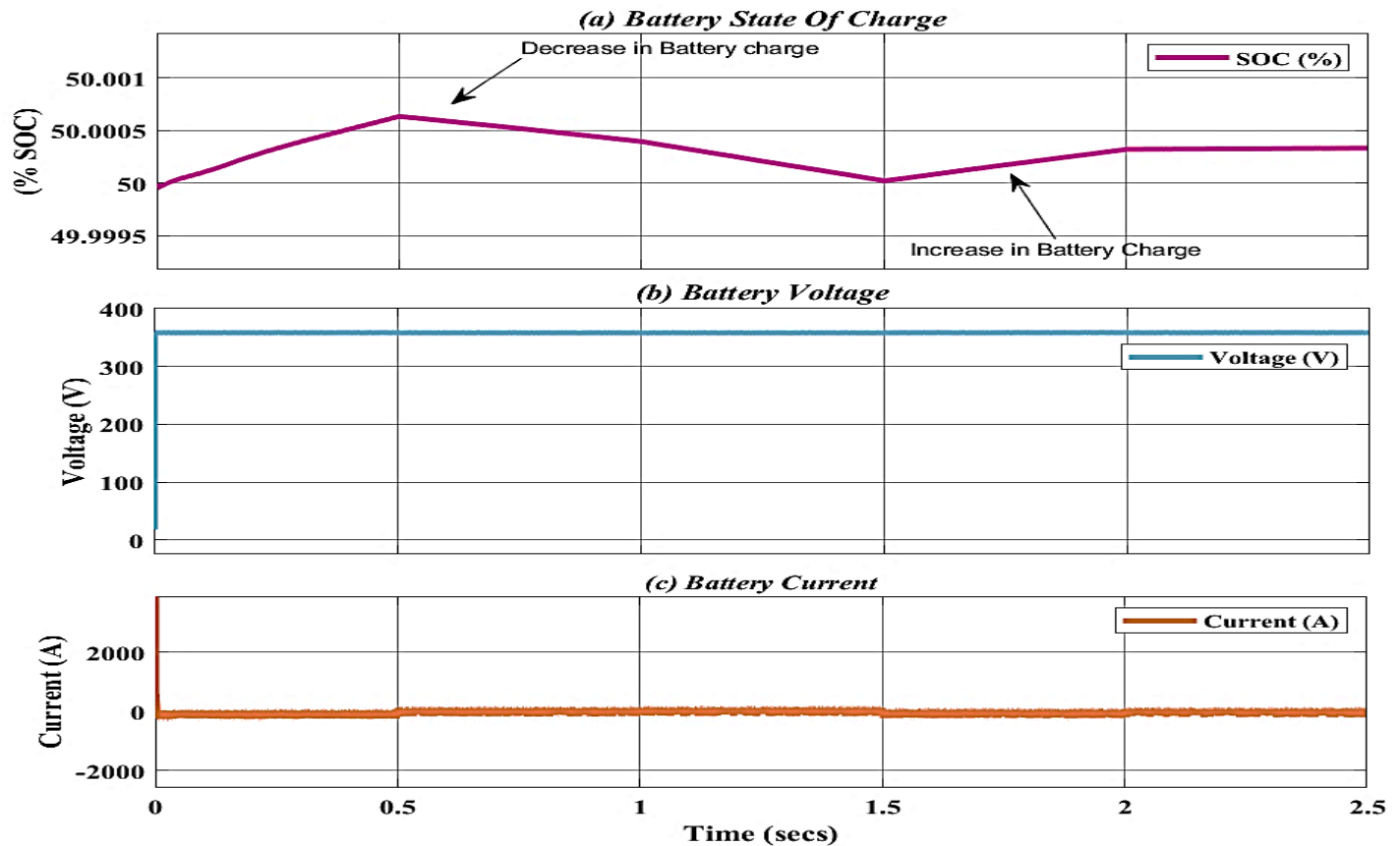


Figure 2. 11 (a) %SOC of the battery bank (BB) (b) Battery bank voltage (c) Battery bank current.

Subsequently, at 0.5 seconds, GHI reduced to  $400 \text{ W/m}^2$ , and temperature increased to  $35^\circ\text{C}$ , decreasing voltage and current. At 2 seconds, with a temperature of  $55^\circ\text{C}$  and GHI at  $1000 \text{ W/m}^2$ , current and voltage decreased due to higher temperature, while GHI increased voltage output. This analysis enhances understanding of the system's behavior in varied environmental conditions, aiding performance optimization.

Changes in irradiance and temperature significantly influence battery charging in photovoltaic systems. Higher irradiance levels boost charging currents and voltages, while lower levels decrease them. Temperature also affects charging rates, with higher temperatures speeding seconds causing battery discharge until 1.5 seconds, followed by recharge as irradiance rises from up the process due to enhanced chemical reactions. In Figure 2.11, a shift in irradiance at 0.5 400 to  $1000 \text{ W/m}^2$  after 1.5 seconds, stabilizing at 2 seconds.

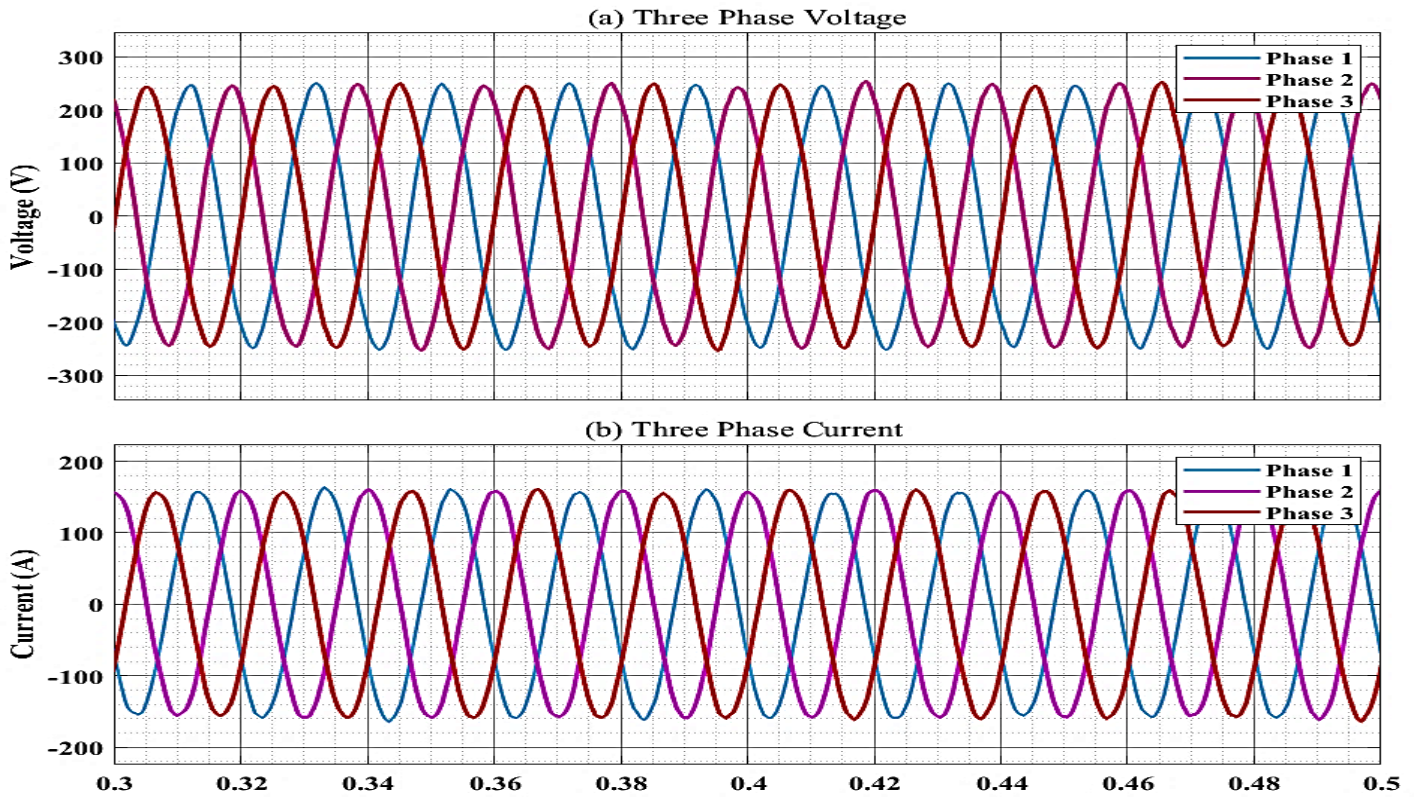


Figure 2. 12 (a) Voltage delivered to the load in three phases ( $V_{peak}$ ). (b) Current supplied to load across three phases.

## 2.5 Experimental Validation

Validation of a Hybrid Power System in real-time is vital for real-world reliability and efficiency. This is achieved through Hardware-in-the-Loop (HIL) analysis, combining physical hardware with simulation models. OPAL-RT Technologies' OP5707XG simulator is pivotal, representing real-world conditions and interactions efficiently on Virtex-7 Field Programming Gate Analysis platforms. Figure 2.13 shows the real-time experimental setup of the OPAL-RT simulator. The experimental data obtained from OPAL-RT Technologies' real-time OP5707XG simulator, depicted in Figures 2.14 and 2.15, validate a Simulink model. Employing OPAL-RT Technologies' OP5707XG simulator to execute a Simulink model enables real-time verification of three-phase current and voltage waveforms. These findings demonstrate the system's resilience in maintaining a stable power supply amidst varying input factors like solar irradiance, temperature fluctuations, and alterations in load.

The experimental validation used the OPAL-RT OP5707XG real-time simulator, which precisely replicates dynamic voltage and current responses across three phases. Integrated with MATLAB/Simulink, it models the hybrid system of PV panels, battery storage, converters, and a diesel generator. The setup includes AC and DC buses, with the gas generator on the AC bus and the solar panels and battery bank on the DC bus, ensuring the system meets energy needs under varying conditions. Simulations tested system behavior under different solar irradiance and temperature conditions, with real-time data on load response.

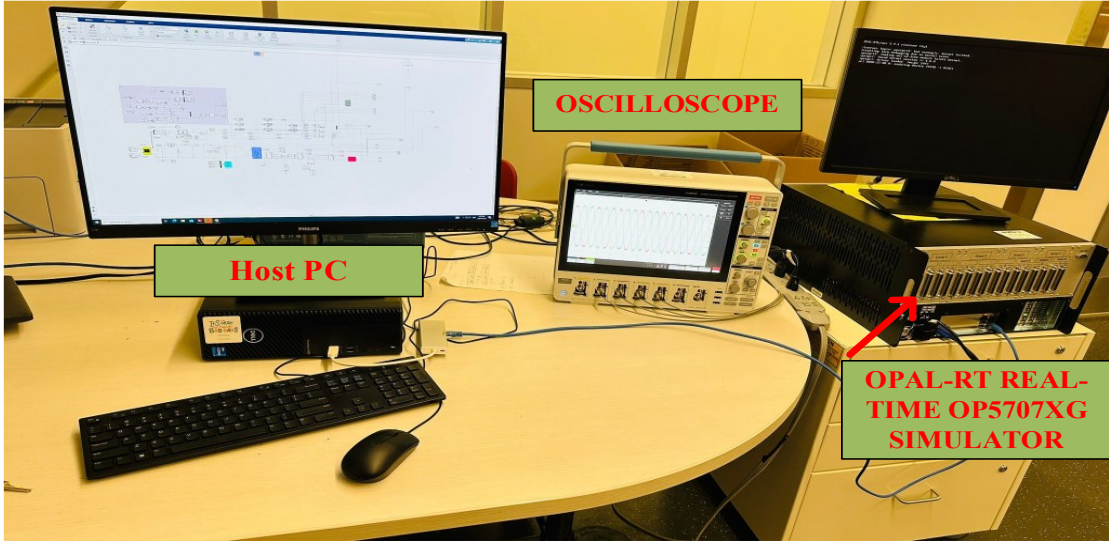


Figure 2. 13 Real-time trial setup using OPAL-RT.

The system's stability across diverse conditions underscores its reliability for critical infrastructure applications, ensuring a consistent energy supply.

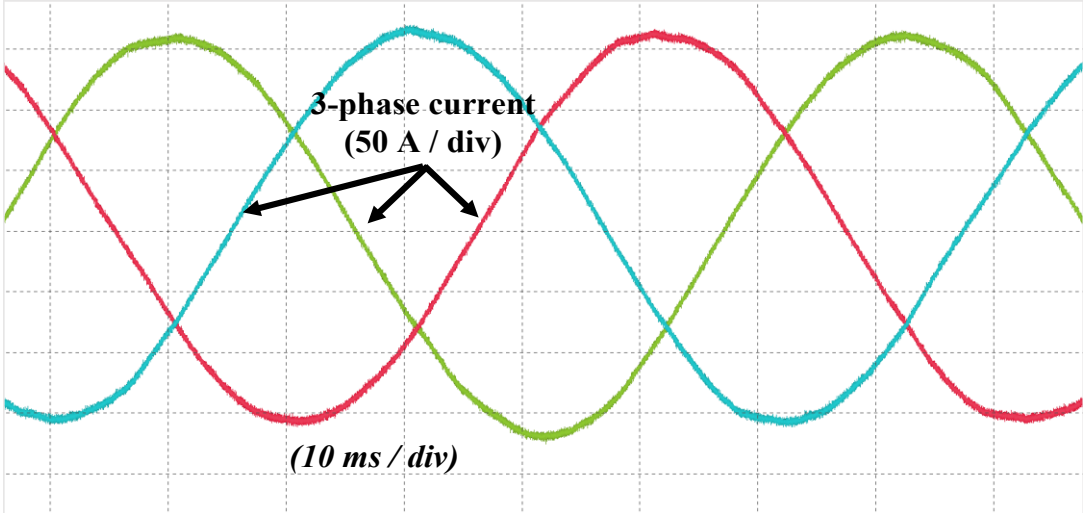


Figure 2. 14 OPAL-RT generated a three-phase load current.

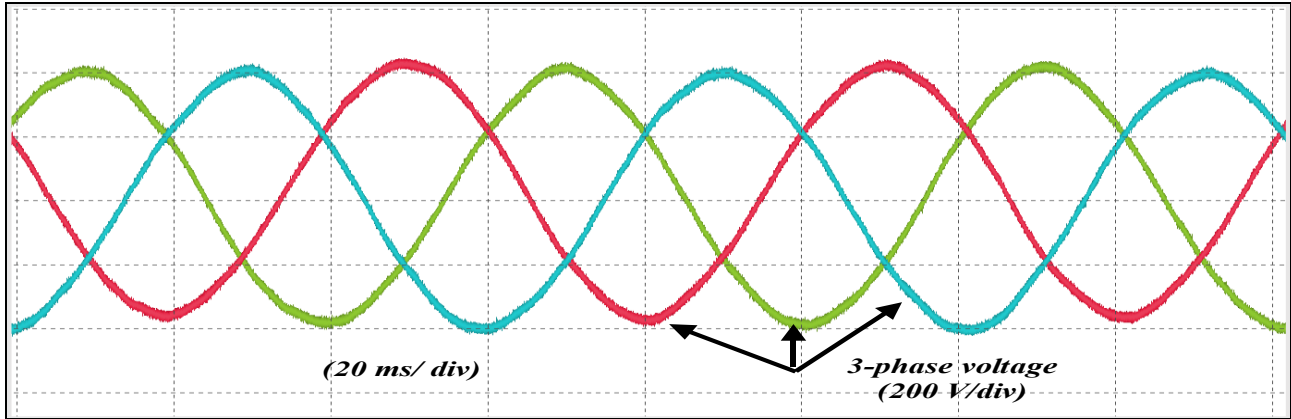


Figure 2. 15 OPAL-RT generated a three-phase load voltage.

## 2.6 Conclusion and Future Work

In summary, this study introduces an innovative strategy to manage the energy requirements of distant natural gas transmission pipeline repeater stations by designing and optimizing a hybrid power system. Utilizing HOMER Pro software, the system integrates photovoltaic panels, a DC-AC inverter, a natural gas generator (Genset), a battery bank (BB), and electrical loads. Through extensive simulations, the optimal system achieves 100% renewable energy fraction and zero CO<sub>2</sub> emissions. The hybrid power system aims for a cost of energy of \$0.199, an annual operating cost of \$653.44, a Net Present Cost of \$33,434, and an initial capital cost of \$24,987. Analysis of Solar Irradiance variations demonstrate their impact on energy cost and system total cost, highlighting the system's sensitivity to solar radiation changes. Additionally, dynamic modeling and simulation conducted with MATLAB/Simulink and real-time experimental validation via OPAL-RT simulator confirm the system's reliability in providing consistent power. Overall, the Hybrid Power System offers sustainable and cost-effective energy solutions, catering to the energy needs of isolated repeater stations and enhancing energy infrastructure sustainability.

For forthcoming research, the author aims to conduct an implementation of a SCADA system for real-time monitoring of PV panel and battery bank current and voltage, as well as site conditions through IoT or open-source platforms.

## References

- [1] A. Shahsavari and M. Akbari, 'Potential of solar energy in developing countries for reducing energy-related emissions', *Renew. Sustain. Energy Rev.*, vol. 90, pp. 275–291, Jul. 2018, doi: 10.1016/j.rser.2018.03.065.
- [2] M. P. Bakht, Z. Salam, A. R. Bhatti, U. Ullah Sheikh, N. Khan, and W. Anjum, 'Techno-economic modeling of the hybrid energy system to overcome the load shedding problem: A case study of Pakistan', *PLOS ONE*, vol. 17, no. 4, p. e0266660, Apr. 2022, doi: 10.1371/journal.pone.0266660.
- [3] World Bank. *The welfare impact of rural electrification: a reassessment of the costs and benefits - an IEG impact evaluation (English)*. Washington, DC: 2008.
- [4] M. U. Etokakpan, S. A. Solarin, V. Yorucu, F. V. Bekun, and S. A. Sarkodie, 'Modeling natural gas consumption, capital formation, globalization, CO2 emissions and economic growth nexus in Malaysia: Fresh evidence from combined cointegration and causality analysis', *Energy Strategy Rev.*, vol. 31, p. 100526, Sep. 2020, doi: 10.1016/j.esr.2020.100526.
- [5] Tester, Jefferson W., et al. *Sustainable energy: choosing among options*. MIT Press, 2012.
- [6] M. Yousaf Raza and B. Lin, 'Natural gas consumption, energy efficiency and low carbon transition in Pakistan', *Energy*, vol. 240, p. 122497, Feb. 2022, doi: 10.1016/j.energy.2021.122497.
- [7] A. D. Woldeyohannes and M. A. A. Majid, 'Simulation model for natural gas transmission pipeline network system', *Simul. Model. Pract. Theory*, vol. 19, no. 1, pp. 196–212, Jan. 2011, doi: 10.1016/j.simpat.2010.06.006.
- [8] '<https://www.iea.org/countries/Pakistan/energy-mix>'.
- [9] S. Kanwal, M. T. Mehran, M. Hassan, M. Anwar, S. R. Naqvi, and A. H. Khoja, 'An integrated future approach for the energy security of Pakistan: Replacement of fossil fuels with syngas for better environment and socio-economic development', *Renew. Sustain. Energy Rev.*, vol. 156, p. 111978, Mar. 2022, doi: 10.1016/j.rser.2021.111978.
- [10] U. Zafar, T. Ur Rashid, A. A. Khosa, M. S. Khalil, and M. Rashid, 'An overview of implemented

- renewable energy policy of Pakistan’, *Renew. Sustain. Energy Rev.*, vol. 82, pp. 654–665, Feb. 2018, doi: 10.1016/j.rser.2017.09.034.
- [11] M. Irfan, Z.-Y. Zhao, M. Ahmad, and M. Mukeshimana, ‘Solar Energy Development in Pakistan: Barriers and Policy Recommendations’, *Sustainability*, vol. 11, no. 4, p. 1206, Feb. 2019, doi: 10.3390/su11041206.
- [12] S. Guo, Q. Liu, J. Sun, and H. Jin, ‘A review on the utilization of hybrid renewable energy’, *Renew. Sustain. Energy Rev.*, vol. 91, pp. 1121–1147, Aug. 2018, doi 10.1016/j.rser.2018.04.105.
- [13] M. K. Farooq and S. Kumar, ‘An assessment of renewable energy potential for electricity generation in Pakistan’, *Renew. Sustain. Energy Rev.*, vol. 20, pp. 240–254, Apr. 2013, doi: 10.1016/j.rser.2012.09.042.
- [14] ‘<https://solargis.com/maps-and-gis-data/download/pakistan>’.
- [15] M. Irfan, Z. Zhao, M. Ahmad, and A. Rehman, ‘A Techno-Economic Analysis of Off-Grid Solar PV System: A Case Study for Punjab Province in Pakistan’, *Processes*, vol. 7, no. 10, p. 708, Oct. 2019, doi: 10.3390/pr7100708.
- [16] A. Ahmed *et al.*, ‘Investigation of PV utilizability on university buildings: A case study of Karachi, Pakistan’, *Renew. Energy*, vol. 195, pp. 238–251, Aug. 2022, doi: 10.1016/j.renene.2022.06.006.
- [17] M. J. Aziz Baig, M. T. Iqbal, M. Jamil, and J. Khan, ‘Design and Analysis of an Isolated DC-Microgrid for a Remote Community in Pakistan’, in *2021 IEEE 12th Annual Ubiquitous Computing, Electronics & Mobile Communication Conference (UEMCON)*, New York, NY, USA: IEEE, Dec. 2021, pp. 0712–0716. doi: 10.1109/UEMCON53757.2021.9666665.
- [18] M. A. A. Rahmat *et al.*, ‘An Analysis of Renewable Energy Technology Integration Investments in Malaysia Using HOMER Pro’, *Sustainability*, vol. 14, no. 20, p. 13684, Oct. 2022, doi: 10.3390/su142013684.



# Chapter 3

## Dynamic Simulation and Optimization of Off-Grid Hybrid Power Systems for Sustainable Rural Development

### Preface

*A version of this manuscript has been published in MDPI Electronics Journal, Volume 13, issue-13 (<https://doi.org/10.3390/electronics13132487>). I am the primary author, and have carried out most of the research work, performed the literature reviews, and carried out the system design, modeling, and analysis of the results. I also prepared the first draft of the manuscript and subsequently revised the final manuscript based on the feedback from the supervisor. The co-authors, Dr. Mohsin Jamil and Dr. Ashraf Ali Khan, supervised the research, acquired, and provided the research guide, reviewed and corrected the manuscript, and contributed research ideas in the actualization.*

# Abstract

This paper analyzes dynamic modeling for rural HPS to address GHG emissions' environmental impact on floods and climate change. The aim is to integrate renewable energy sources, such as solar energy, with traditional generators to mitigate emissions and enhance energy access in rural communities in Pakistan. The system is designed using a DC-DC converter, MPPT, LCL filter, and a DC-AC inverter. Utilizing software tools like PVsyst 7.4 and HOMER Pro-3.18.1, the study evaluates system sizing, energy consumption patterns, and optimization strategies tailored to site-specific data. The expected results include a reliable, environmentally friendly hybrid power system capable of providing consistent electricity to rural areas. The analysis of a connected load of 137.48 kWh/d and a peak load of 33.54 kW demonstrates the system's promise for reliable electricity with minimal environmental impact. The estimated capital cost of USD 102,310 and energy generation at USD 0.158 per unit underscores economic feasibility. Dynamic modeling and validation using HIL examine the system's behavior in response to variations in solar irradiance and temperature, offering insights into operational efficiency and reliability. The study concludes that the hybrid power system is scalable for rural energy access, which is a practical solution for achieving a 100% renewable energy fraction, significantly contributing to emission reduction and promoting sustainable energy practices

**Keywords-** GHG (greenhouse gas emissions); HPS (hybrid power system); LCL filter; DC-AC inverter; MPPT (maximum power point tracking); PVsyst and HOMER Pro; HIL (hardware in the loop)

## 3.1 Introduction

Energy is vital for enhancing human welfare, promoting economic advancement, and stimulating economic prosperity [1]. It is commonly recognized that energy is the benchmark for measuring economic growth and improving everyone's living level [2]. In contemporary society, energy ranks alongside fundamental human needs such as food, clothing, and shelter. It exerts both positive and negative influences

on humanity. From a utility perspective, energy facilitates the alleviation of arduous tasks by providing convenient access to larger quantities of affordable, safe, and clean energy sources [3]. Energy deficiency poses a significant challenge for many developing nations, stemming from issues like generation shortages, inefficient power transmission, and outdated distribution equipment. Consequently, affected countries resort to load shedding, a controlled measure of disconnecting the grid supply from specific regions for several hours daily; prolonged effects can significantly impact the economic advancement of a nation. The World Bank notes that persistent electricity shortages have adversely impacted economies in Pakistan, Sri Lanka, South Africa, and India. The energy systems of most nations, whether already developed or in the process of development, predominantly rely on fossil fuels. However, this reliance contributes significantly to environmental issues such as global warming and air pollution. These environmental concerns not only pose health risks but also impact the overall quality of life for affected populations [4]. As per the agenda of the Paris Agreement, leaders around the globe have agreed to restrain the increase in the average global temperature to stay “well below” 2 °C above pre-industrial levels and endeavor to remain below a warming of 1.5 °C [5]. Nearly 90% of the entire GHG emissions stem from CO<sub>2</sub> released through the combustion of fossil fuels [6].

Figure 3.1 illustrates that using fossil fuels generates CO<sub>2</sub> emissions, which are responsible for global warming and climate change and significantly impact our environment. Conversely, both developed and developing nations are fulfilling their energy needs by heavily depending on fossil fuels. This reliance not only harms the environment within their borders but also contributes to global climate change, which disproportionately affects underdeveloped countries. Located in Asia, Pakistan boasts the 10th largest economy in the region. Pakistan is grappling with significant challenges such as energy security and the environmental repercussions of energy consumption. Pakistan is heavily reliant on energy imports, accounting for nearly a third of its energy demand.

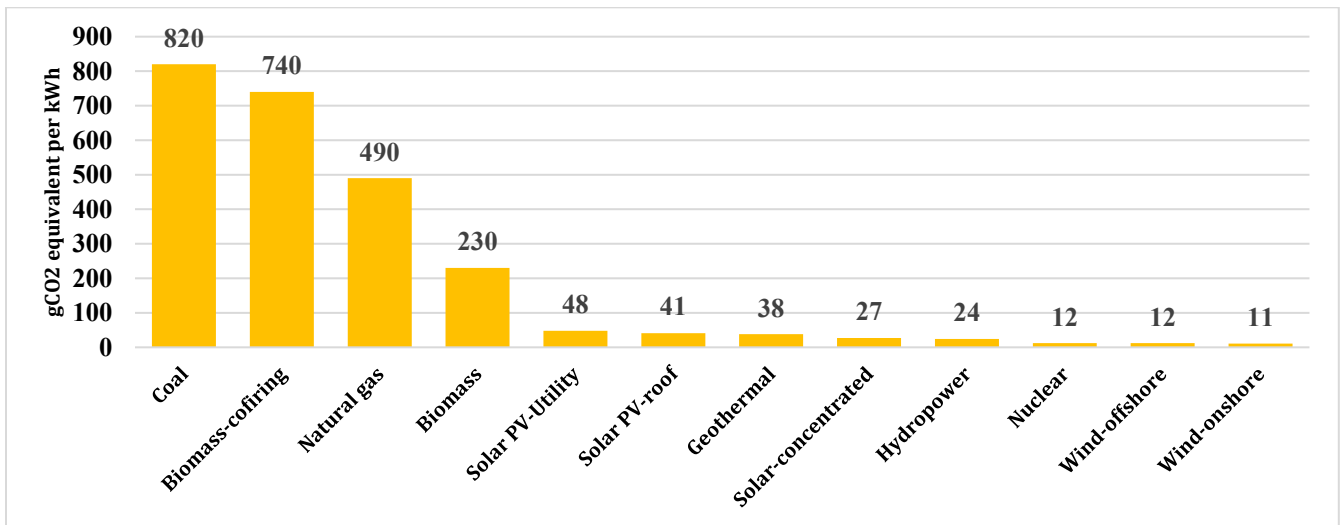


Figure 3. 1 gCO2 emissions by different types of fossil fuels [7].

In the fiscal year 2017–2018, energy imports amounted to approximately USD 14.4 billion, marking an increase from USD 10.9 billion in the preceding year. About 75% of the USD 3.5 billion surge in energy imports resulted from elevated energy prices, with only around 25% attributed to increased import volumes. This significant price escalation ripples through the entire energy supply chain, leading to elevated business costs and a higher cost of living in Pakistan. Such heavy dependence on imported energy is unsustainable for Pakistan’s economy, which has grappled with a persistent current account deficit for over two decades [8]. Pakistan has a global 0.8% share in CO2 emissions, and it has increased 114% since 2000 [9]. This alarming trend is underscored by a notable rise in the consumption of natural gas, coal, and electricity, increasing by 41%, 52%, and 11%, respectively, within Pakistan [10]. Figure 3.2 shows the categories and trends of CO2 emissions in Pakistan and the percentage of energy supply by source and Figure 3.3 shows the Pakistan’s energy supply by source.

Severe weather phenomena like heavy precipitation and flooding can inflict significant harm on both human communities and the natural world. The frequency of heavy precipitation events, which significantly contribute to flooding, has notably risen in various regions of the Northern Hemisphere in recent years, largely attributable to human-induced climate change and driven by heightened greenhouse gas emissions [13]. Global warming stands as a primary catalyst for shifts in global climate patterns. Pakistan,

ranking among the top ten nations affected by this aftermath phenomenon, is witnessing severe repercussions.

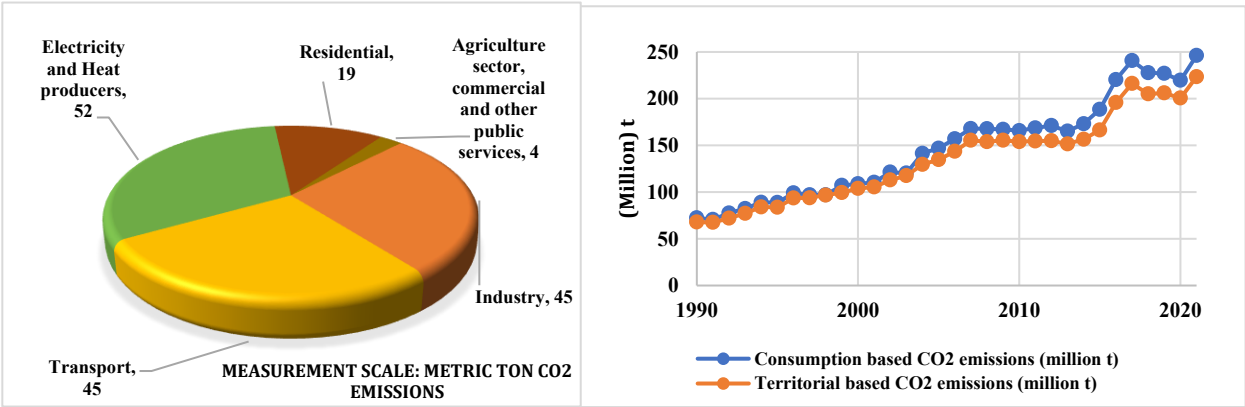


Figure 3. 2 Categories and trends of CO2 emissions in Pakistan [11].

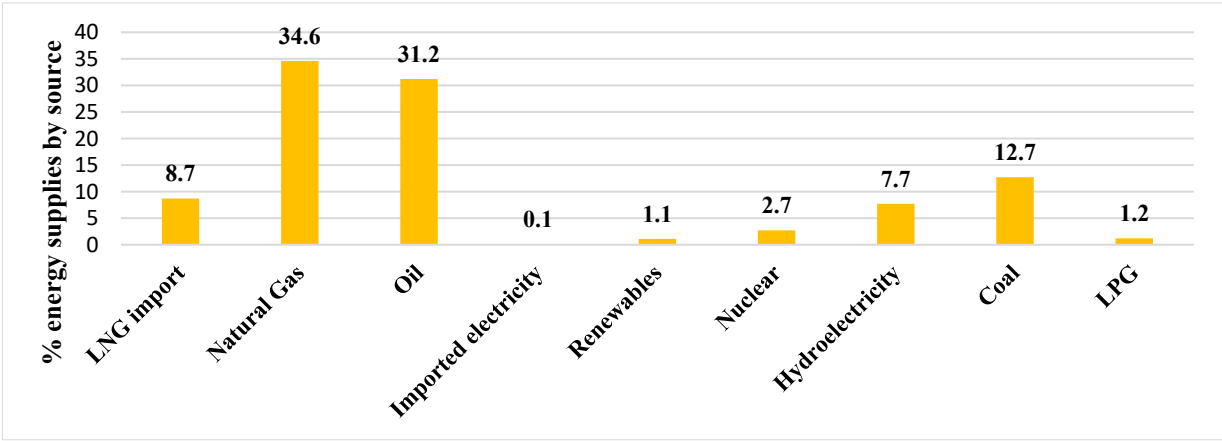


Figure 3. 3 Pakistan's % energy supply by source [12].

Presently, the country grapples with extreme flooding, impacting approximately 33 million individuals and destroying 1.5 million residences, along with USD 2.3 billion in crop losses. Furthermore, over 2000 km of roads have been damaged, impeding connectivity to provinces and major urban centers. Notably, record-high temperatures, such as 40 °C in various regions and a staggering 51 °C in Jacobabad, underscore the intensity of the situation [14].

The Khyber Pakhtunkhwa province in Pakistan has been a focal point for natural disasters, particularly floods, causing significant adverse effects on its land, infrastructure, healthcare, education, socio-economic development, and human lives. While efforts toward recovery are underway, the province still lags others in terms of progress. Situated amidst the Karakoram, Himalayas, and Hindu Kush Mountain

ranges, Khyber Pakhtunkhwa is home to glaciers and extensive high-altitude ice reserves. Table 1 shows the loss incurred on Pakistan’s economy due to the flooding.

Table 3. 1 Economic loss impact due to floods in Pakistan in 2022 [15].

<b>Province</b>	<b>Damage (Million USD)</b>	<b>Loss (Million USD)</b>	<b>Requirement for Rehabilitation (Million USD)</b>
Baluchistan	1625	2516	2286
KPK (Khyber Pakhtunkhwa)	935	658	780
Punjab	515	566	746
Sindh	9068	11,376	7860

These towering mountains, coupled with Pakistan’s major rivers, including the Indus River, give rise to steep waterways such as Swat, Kabul, Kunhar, and Panjkora, traversing the plains of Khyber Pakhtunkhwa [16]. Along with global warming issues, Pakistan is facing severe energy crises. Pakistan’s electricity industry grapples with several challenges, including a widening gap between supply and demand, frequent power cuts, escalating fuel import expenses, and rising environmental pollutants. To fulfill its commitments under the Paris Agreement to reduce carbon dioxide (CO<sub>2</sub>) emissions, Pakistan has introduced various incentives and mechanisms to promote renewable energy production. Therefore, it is imperative to conduct a long-term evaluation of these policy incentives and mechanisms to determine their effectiveness in achieving the CO<sub>2</sub> emissions reduction target [17]. A significant portion of the population, particularly in rural areas, lacks access to electricity and turns to the burning of fossil fuels to meet their energy demands. The situation is alarming, with only 60% of the country’s population connected to the grid. Presently, Pakistan is contending with a power supply shortage of 3–5 GW [18].

The adoption of renewable energy holds paramount significance globally due to the escalating energy consumption, surpassing the capabilities of traditional energy sources and leading to energy crises. However, the fluctuating nature of solar radiation and wind speed, influenced by climate and weather dynamics, poses challenges to the consistent operation of renewable energy systems, resulting in output fluctuations. To address this issue, hybrid renewable energy (HRE) systems, integrating multiple renewable

energy sources, emerge as a highly efficient solution with promising potential [19]. Ensuring adequate electricity supply in rural areas is crucial for fulfilling basic living requirements and fostering economic development. However, extending the grid over long distances through challenging geographical terrain is often economically impractical as a solution to this challenge. Internal combustion engines and diesel generators, known for their rapid response to fluctuating demand and relatively low initial investment costs, are commonly employed for electricity generation in remote regions. Nonetheless, the utilization of traditional fuels leads to the emission of pollutants. Moreover, given the unfavorable economic conditions, procuring and transporting fossil fuels for power generation purposes proves to be economically unviable [20].

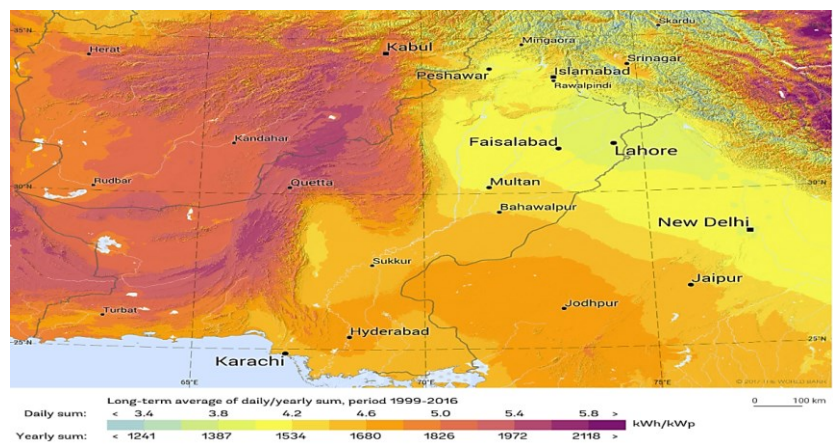


Figure 3. 4 Solar irradiance levels in Pakistan [21].

Pakistan’s abundant solar potential, with high irradiance levels ranging from 5.0 to 7.0 kWh/m<sup>2</sup>/day and 2200 to 2400 annual sunshine hours, offers a significant opportunity for electricity generation. Estimated at 2.9 million megawatts annually, solar energy exceeds current demand, presenting a sustainable solution for energy shortages. Government initiatives, including large-scale solar projects and residential subsidies, aim to harness this resource for environmentally friendly energy production and meet growing needs. Figure 3.4 shows the solar irradiance levels in Pakistan.

Numerous studies have investigated hybrid energy systems from various angles. Tamoor et al. [22] designed an on-grid photovoltaic system, particularly in the selection of a PV module type and size that can lead to notable energy losses within the system. The study compared PV units of different dimensions

and power rankings but with similar effectiveness in two chosen sites. Helioscope simulation software was employed to model these PV systems, enabling the analysis of their monthly and annual energy production as well as system losses. Nawab et al. [23] suggest a self-sufficient solar biogas microgrid designed for rural communities in the Lakki Marwat district, Pakistan, which is reliant on agriculture and livestock. HOMER Pro simulated the electric power system, while RET Screen analyzed its economics. The optimized system consists of a 30-kW photovoltaic system, a 37-kW biomass hybrid system, a 64-kWh battery storage capacity, and a 20-kW inverter, producing 515 kWh of electricity and 338.50 m<sup>3</sup> of biogas daily. Iqbal and Iqbal [24] conducted thermal modeling of a standard rural dwelling in Pakistan using BEopt to establish the hourly load profile. This load data was then utilized to design a stand-alone PV system using HOMER Pro. The proposed system comprises a 5.8 kW PV array along with eight batteries with a 12 V and 255 Ah capacity, coupled with a 1.4 kW inverter. The analysis indicates that this system is capable of primarily supporting lighting and appliance loads in a rural household. Xu et al. [25] examined the feasibility of electrifying rural areas in Sindh province, Pakistan, focusing on solar energy. The results indicate that these regions have favorable solar conditions for electricity generation. By optimizing tilt angles, the solar energy generation capacity can be significantly enhanced. An economic analysis reveals that off-grid solar PV systems offer electricity at PKR 6.87/kWh, which is far cheaper than conventional sources priced at PKR 20.79/kWh. Ur Rehman and Iqbal [26] presented the development of an off-grid PV system for a rural household in Pakistan, aiming to meet its year-round electrical needs, targeting a monthly generation of 40 kWh. Utilizing HOMER Pro software, the system's performance was simulated with location-specific solar data. It consists of four 140-watt solar panels, four 125 Ah batteries, a 1 kW inverter, and introduces a simple control and data-logging approach for monitoring. Elsaraf et al. [27] worked for the electrification of remote communities in Canada in which the energy systems are tailored to local consumption. Various renewable sources including solar thermal, PV, wind, hydroelectric, and fuel cells were utilized and the microgrid significantly reduced diesel usage by 71%, thus achieving a levelized cost of energy (LCOE) of  $-0.0245$  \$/kWh. Kumar et al. [28] designed and



installed an off-grid solar PV system in Pakistan's desert region, where approximately 95% of the area lacks electricity access. This endeavor includes a comprehensive sizing and cost analysis to determine suitable specifications for PV solar panels, battery capacity, inverter size, and a charge controller based on the anticipated loads. Ali et al. [29] presented an off-grid photovoltaic (PV) system tailored for a rural household in Pakistan, designed to meet its year-round electricity requirements with an anticipated monthly output of 40 kWh based on household electricity consumption data; the system's performance is evaluated through steady-state modeling using HOMER Pro software. The simulation results forecast the system's annual electrical output, accounting for solar irradiance, temperature, and humidity data specific to the chosen location. Rehmani and Akhter [30] investigated the electrification of a rural community using various renewable resources and conducted an economic analysis under different scenarios. It was found that in the scenario utilizing all available resources including PV, wind, and biomass, the levelized cost of energy decreased to Rs 14.40. Although there was a slight increase in the net present cost to Rs 14.6 million, the payback period was notably reduced to just 2.54 years.

While previous research has primarily concentrated on optimizing and designing photovoltaic systems for site electrification, there is a noticeable gap in addressing the environmental impact stemming from fossil fuel usage, which is a significant contributor to recent flooding in Pakistan. Furthermore, there is a limited exploration of the reliability of hybrid power systems concerning the proportion of renewable energy integrated. Therefore, this study aims to illustrate the optimization and analysis of the design of a stand-alone hybrid power system required for the electrification of a rural area in Khyber Pakhtunkhwa province of Pakistan because of the reliability of the hybrid power system. The key contributions of this research paper to the existing research are as follows:

- The projected HPS is designed with PVsyst and HOMER Pro software. This entails identifying system loss, the ideal capacity, and the setup of elements to fulfill the power requirements of a system. The

procedure encompasses investigating the load profile, evaluating the accessibility of renewable resources, integrating energy storage capacity, establishing the generator capacity, and employing a control system.

- Utilizing MATLAB Simulink r2023b, the dynamic modeling of the suggested hybrid power system is performed to assess its HPS behavior, voltage fluctuations, system load effects, and the quality of generated power across various settings, all tailored towards the selected site. The practical validation of the designed HPS is being performed by the OPAL-RT OP5707XG HIL real-time simulator.

- The decreases in CO<sub>2</sub> emissions through energy production from the hybrid power system contribute to environmental preservation, thereby lowering the likelihood of floods in Pakistan.

The structure of this study unfolds as outlined: Section 2 explores the factors considered in site selection. Section 3 details the scheme of the hybrid power system. Section 4 discusses the performance analysis and optimization of the HPS utilizing PVsyst and HOMER Pro. Section 5 illustrates the dynamic modeling and simulation of the proposed system using MATLAB Simulink, while Section 6 demonstrates the testing of the system's validity under consideration using HIL. Lastly, a thorough summary and discussion of the entire study are provided.

## **3.2 Site Selection and Description**

The site selection process is integral to the design of a hybrid power system, playing a pivotal role in determining its performance and effectiveness. Key considerations include assessing the readiness of renewable resources, for instance, solar irradiation, wind speed, and hydro potential. Understanding the site-specific load profile is essential for appropriately sizing and configuring system components to meet energy demand. Environmental factors, including terrain, climate conditions, and regulatory requirements, also influence system design. Economic viability hinges on factors such as installation costs, potential energy savings, and payback periods, all of which are influenced by site selection. Ultimately, a

well-chosen site maximizes energy generation potential while minimizing environmental impact and operational costs, laying a strong foundation for the hybrid power system’s success.

The selected site, “Berru Bandi”, is a small community consisting of 10 houses located in the rural area of Abbottabad District, approximately 25 km from Abbottabad City. Perched atop a mountain at coordinates  $34^{\circ}16'38''$  N  $73^{\circ}15'18''$  E and an altitude of 1456.79 m above sea level, accessing this site is challenging due to the lack of road access and basic amenities. As illustrated in Figure, approximately 66% of power in Pakistan is generated from natural gas and oil through power plants. The state-owned Sui companies, Sui Northern and Sui Southern, manage a combined network of 151,397 km (13,143 km of transmission and 138,254 km of distribution) for natural gas transmission and distribution [31]. Additionally, the NTDC (National Transmission and Dispatch Company) oversees an electricity network spanning 28,805 km [32]. Despite the extensive natural gas and electricity networks, providing an energy source to this remote area proves challenging due to its mountainous terrain and elevated location. Currently, residents rely on diesel generators ( $10 \times 5$  kW) to meet their energy needs, resulting in over 75,000 L of diesel fuel consumption, which ultimately results in CO<sub>2</sub> emissions that are harmful to the environment. Therefore, the most feasible solution for electrifying this rural community is the implementation of a hybrid power system. An overhead perspective of the location is illustrated in Figure 3.5 on Google Maps.

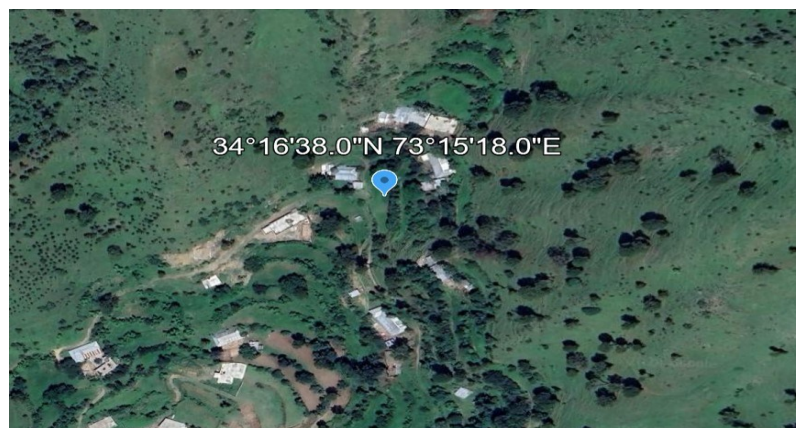


Figure 3. 5 A view of the site captured from above on Google Maps.

Figure 3.6 presents different real-life views of the selected site. As we can see in the aerial view in

Figure 5, there is an ample area available around the community, which is sufficient for the setup of solar PV panels and other elements of the hybrid power system.



Figure 3. 6 Actual perspective of the selected site.

### 3.2.1 Solar Horizontal Irradiance

Solar horizontal irradiance (SHI) holds a crucial role in assessing the solar prospective of a location and determining the feasibility of solar energy projects. It represents the total solar emission obtained per unit area at the Earth's surface in a horizontal plane, without considering the angle of incidence or orientation of surfaces. Moreover, SHI data are essential for conducting solar resource assessments, identifying suitable sites for solar projects, and making informed decisions regarding renewable energy investments. The solar horizontal irradiance data of the selected site are obtained using the NASA Surface Meteorology and Solar Energy Database, facilitated with HOMER Pro software. Figure 3.7 represents the value of solar radiation which ranges from 2.79 kWh/m<sup>2</sup> /day to 7.46 kWh/m<sup>2</sup> /day, which shows that there exists sufficient sunlight energy at the selected site. Similarly, the clearness index is a dimensionless number that ranges between 0 (when the sky is completely covered) to 1 (when there is perfect sun) whereas at selected sites it ranges between 0.546 to 0.694.

The energy output of a photovoltaic (PV) system is significantly influenced by weather conditions including wind speed, humidity levels, temperature changes, and solar irradiance, along with additional

factors like dust accumulation, localized heating, snow accumulation, and tiny fractures. However, the incline and orientation angles of PV setups are crucial in maximizing annual energy production. These angles directly impact the absorption of solar energy by the PV module surfaces, thereby affecting the performance of the installation [33]. The solar azimuth angle is the angular distance between the direction of the sun and a reference direction, typically measured clockwise from true north in the horizontal plane.

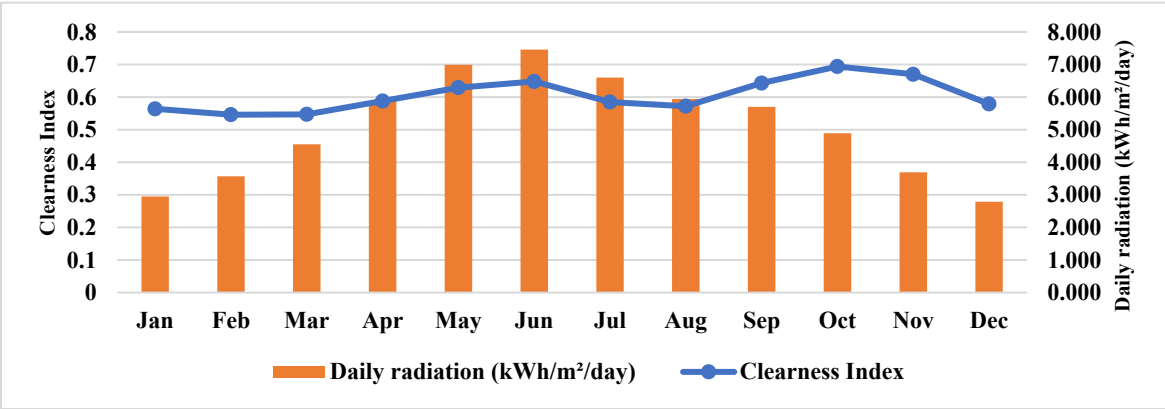


Figure 3. 7 Selected site solar GHI and clearness index.

It represents the direction along the horizon where the sun appears to rise and set. The solar azimuth angle changes throughout the day, as the position of the sun overhead shifts from east to west. It is an important parameter in solar energy applications, as it determines the alignment of solar panels for optimal sunlight exposure and energy capture. The solar elevation, solar azimuth, day length, and solar zenith angle were computed using the online software tool “Solargis”, as depicted in Figure 3.8.

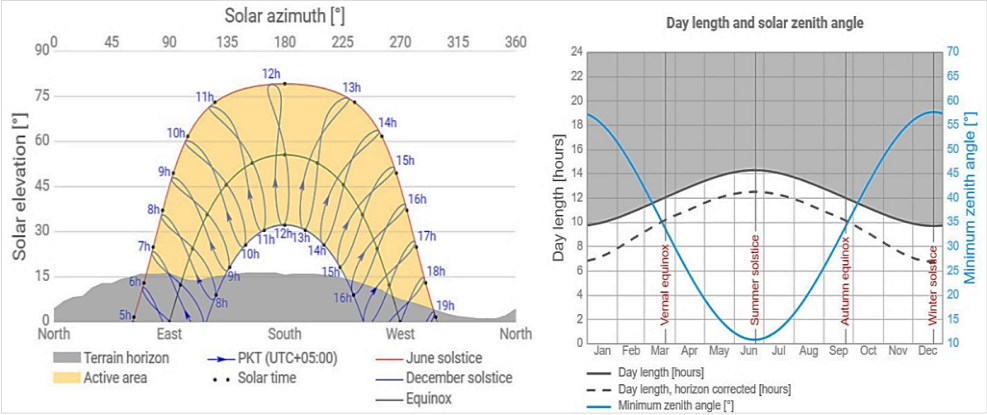


Figure 3. 8 Selected site solar azimuth and zenith angle [34].

### 3.2.2 Analysis of Electrical Load

The electrical load is of paramount importance in hybrid power systems, significantly shaping their design, operation, and overall efficiency. In the selected rural community, there are 10 houses with nearly identical electrical appliances. The details of these appliances, along with their connected loads, are presented in Table 3.2 below:

Table 3. 2 Specifics regarding the electrical load at the chosen location.

Appliances Description	Unit's Quantity	Installed Unit Load Rated Power	Aggregate Connected Load
		Watts (W)	(kW)
LED Lights	100	30	3
Ceiling Fan	30	75	2.25
Iron	8	1000	8
Washing Machine	10	700	7
Refrigerator	10	750	7.5
Television	10	200	2
Electric Heater	8	500	4
Electric Geyser	8	1000	8
Water Suction Pump	1	5000	5
<b>Total Connected Load</b>			<b>46.75 KW</b>

Energy load profiles provide insights into the consumption patterns of energy over time, capturing the interactions between different subsystems at various spatial and temporal scales. Due to diverse factors, individual households exhibit distinct energy demand patterns, with peak energy usage occurring at different times. As a result, when households are aggregated, the maximum demand from the group is typically lower than the sum of individual maximum demands due to the diversity in timing. Equation (1) shows the formula for the diversity factor.

$$\text{Diversity factor} = \frac{\sum \text{Individual maximum demand}}{\text{maximum demand of the aggregated system}} \quad (1)$$

This phenomenon reflects the likelihood that peak demands from different households do not coincide. Consequently, as more households are integrated into a system, the maximum demand per household

decreases. The greater the diversity factor, the less likely it is that households will have peak energy demands at the same time [35]. Considering the diversity factor, the hybrid power system is aimed at a peak load of 33.54 kW, and the system will be tailored accordingly. Figure 3.9 demonstrates the monthly electricity consumption pattern of the selected site.

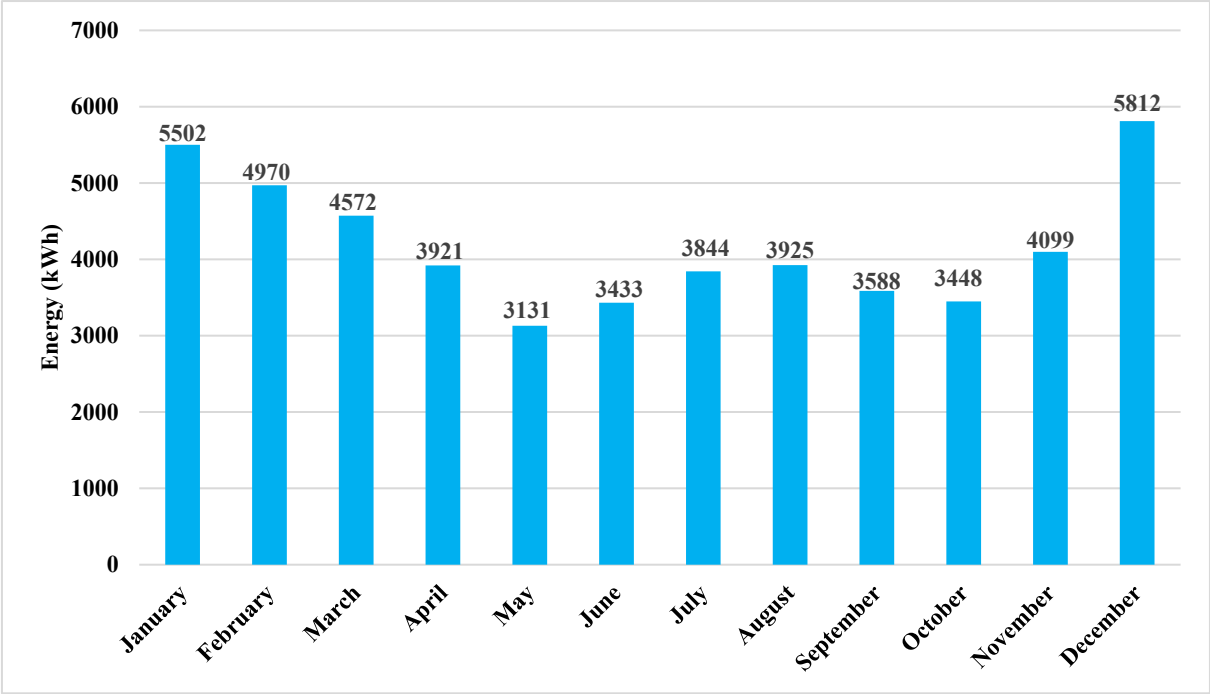


Figure 3. 9 Monthly electricity usage pattern at the chosen location.

### 3.3 Designing of Hybrid Power System

The hybrid power system (HPS) envisioned for the chosen location integrates multiple elements, such as a solar photovoltaic system, MPPT controller, battery bank, DC-DC buck converter, DC-AC inverter, LCL filter, AC power source, and diesel generator. This setup features both AC and DC buses for increased operational versatility and easier upkeep, ensuring uninterrupted power provision. Engineered with backup capabilities, the HPS ensures dependable and sustained energy delivery to facilitate smooth operations. Figure 3.10 depicts the schematic representation of the proposed hybrid power setup.

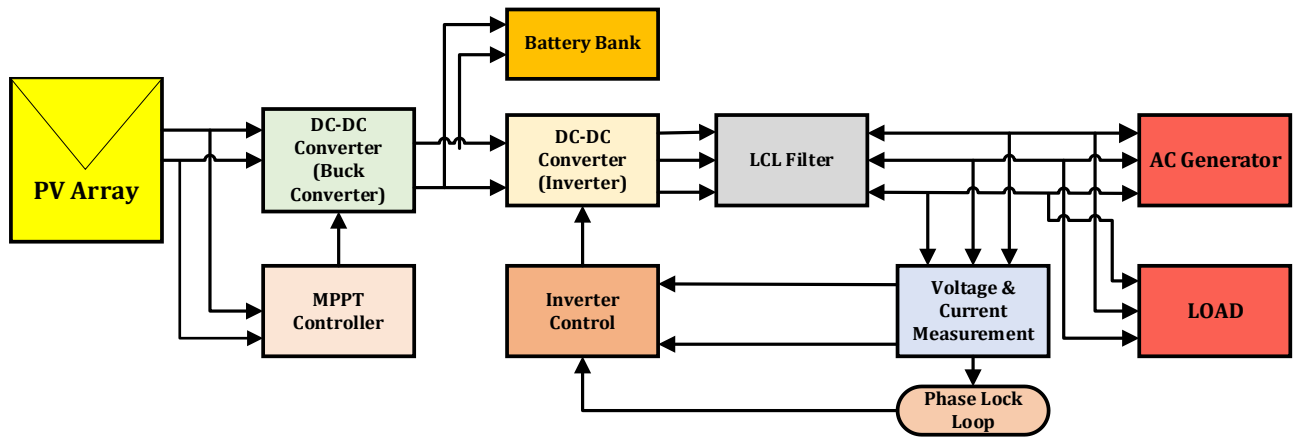


Figure 3. 10 Diagram illustrating the proposed hybrid power system.

### 3.3.1 Overview and Mathematical Modeling of Elements in the HPS

#### 3.3.1.1 Photovoltaic Structure

The primary goal of solar cells is to capture photons and transform light into electricity. The production of efficient solar cells is crucial for overcoming challenges in solar technology optimization. The system comprises numerous solar cells constructed from semiconductor materials like silicon. When sunlight interacts with these cells, it stimulates electrons, generating an electric current. The panels are typically arranged in arrays to generate higher power levels, and they are widely used in residential, commercial, and industrial applications to harness renewable solar energy for electricity generation [36]. Figure 3.11 shows the circuit diagram of the PV cell. The PV cell's equivalent circuit comprises an ideal current source parallel to a diode. When exposed to solar radiation, current flows from the ideal current source. If the load resistance exceeds that of the diode, the diode conducts current, increasing the voltage across its terminals but decreasing the current through the load. Conversely, if the diode's resistance is higher than the load's, electrons flow easily through the load, resulting in a higher current. However, the voltage difference across the terminals decreases. The ideal solar cell circuit also includes series resistance ( $R_s$ ) and shunt resistance ( $R_{sh}$ ). Shunt resistance accounts for losses when electrons move directly between terminals, like shorts. Series resistance represents current losses due to inefficient charge transfers within



the device.

$$I = I_{Gen} - I_D - I_{sh} \quad (2)$$

According to Equation (2), I represent the obtained current, where  $I_{Gen}$  is the produced current,  $I_D$  signifies the diode current, and  $I_{sh}$  is the current lost due to shunt resistance. To find out the  $I_D$  (diode current), the following equation is used:

$$I_D = I_0 \left\{ \exp\left[\frac{qV}{nkT}\right] - 1 \right\} \quad (3)$$

Here,  $I_0$  denotes the reverse leakage current, n stands for the ideal diode factor, q represents the charge constant, the Boltzmann constant is denoted by k, and the absolute temperature is represented by T.

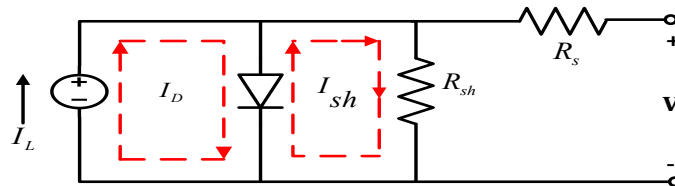


Figure 3. 11 Circuit diagram representing a photovoltaic cell.

### 3.3.1.2 Buck Converter (DC-DC)

A DC-DC buck converter is a type of power electronic device applied to step down the voltage level of a direct current (DC) power source. It operates by converting a higher input voltage to a lower output voltage while regulating the output current to match the load requirements. This is achieved by controlling the duty cycle of a switch (typically a transistor) in the converter circuit. During operation, the switch is rapidly turned on and off, allowing energy to flow from the input to the output in discrete intervals. The diagram depicting the buck converter circuit is illustrated in Figure 3.12. The key components of the converter include the transistor switch, and the output LC-type smoothing filter comprising elements L

and C, along with a discharge diode. The transistor switch is regulated by a pulse width modulation (PWM) generator, which produces a control signal determined by the calculated duty cycle values,  $d$ , computed by the MPPT controller.

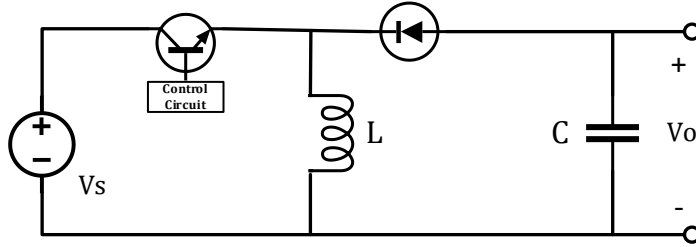


Figure 3. 12 Buck converter (DC-DC).

The initial calculation involves determining the duty cycle,  $D$ , using the maximum input voltage, as this results in the highest switch current which can be calculated using Equation (4):

$$D \text{ (maximum duty cycle)} = \frac{V_{out}}{V_{in(max)} \times \eta} \quad (4)$$

In the above equation, “ $\eta$ ” represents the efficiency of the converter. For the calculation of the values of inductance ( $L$ ) and capacitance ( $C$ ), the following equations (5) and (6) are used:

$$L = \frac{V_{out} \times (V_{in} - V_{out})}{\Delta I_L \times f_s \times V_{in}} \quad (5)$$

$$C_{out} = \frac{\Delta I_L}{8 \times f_s \times \Delta V_{out}} \quad (6)$$

$$\Delta I_L = \frac{V_{out} \times D}{f_L \times L} \quad (7)$$

The ripple current refers to the fluctuating or oscillating component of the current that flows through a

circuit or device, typically characterized by its alternating nature. In the above equation,  $\Delta I_L$  represents the inductor ripple current and it can be calculated by using Equation (7).

### **3.3.1.3 Maximum Power Point Track Control**

The performance of photovoltaic (PV) systems is directly affected by changing weather conditions, leading to fluctuations in their output. Solar irradiance, determined by the angle of sunlight, plays a vital role in adjusting the electrical characteristics of PV modules. While the voltage output of a PV module remains relatively stable, its output current is significantly influenced by variations in solar irradiance. To maximize the power extraction from the PV system, an MPPT controller is employed. MPPT technology is essential in modern power systems, ensuring that the maximum available power is efficiently delivered to loads, batteries, motors, and the power grid in off-grid and on-grid applications, correspondingly [37].

Figure 3.13 shows the diagram of MATLAB-designed MPPT. Overtime, various MPPT algorithms like Constant Voltage (VC), Fractional Open-Circuit Voltage (FOCV), Open Circuit Voltage with Pivot PV Cell (FOCV PVC), Fractional Short Circuit Current (FSCC), Look-up Table (LUT), Hill Climbing (HC), DC Link Capacitor (DCLC) and Incremental Conductance (IncCond) algorithms have been designed to optimize the power and efficiency of solar panels. Each method comes with its own set of advantages and disadvantages. In this paper, the Incremental Conductance Algorithm has been selected, as it tracks the MPP by evaluating the instantaneous conductance of the PV array with its incremental conductance. By dynamically adjusting the operating voltage and current, the ICA (Incremental Conductance Algorithm) ensures that the PV system operates at or near its MPP under varying environmental conditions, maximizing the efficiency and power output of the solar panels. The flow chart of the Incremental Conductance Algorithm is shown in Figure 3.14.

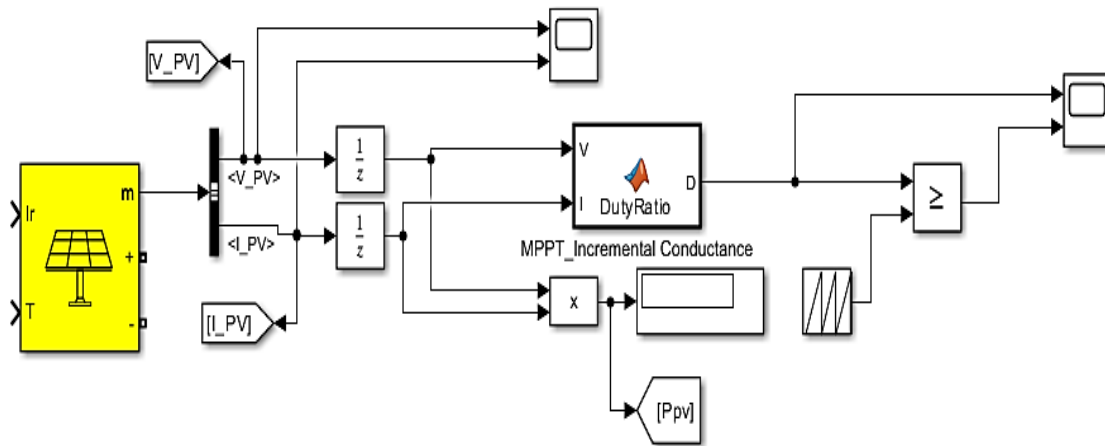


Figure 3. 13 MATLAB modeled maximum power point tracking.

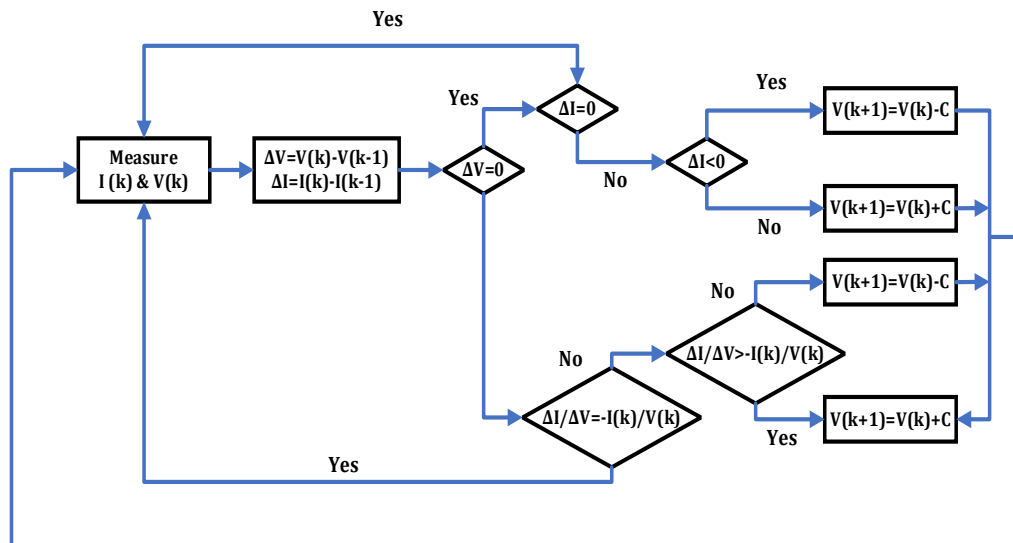


Figure 3. 14 Incremental Conductance Algorithm flow chart.

In the incremental conductivity method, adjustments to the terminal voltage of the array are made in line with the MPP voltage, leveraging the incremental and instantaneous conductivity of the PV module. Developed in 1993, this algorithm aimed to address limitations observed in the PO (perturbation and observation) algorithm. INC (Incremental conductance) aims to extend monitoring periods and enhance energy production, especially in expansive environments where irradiation levels fluctuate [38]. The system calculates the power and conductance of the PV by analyzing its output voltage and current. Based on these measurements, it determines the duty cycle necessary to operate the system at the MPP. When the ratio of the difference in PV power to the variance in voltage reaches zero, it signifies the attainment of the

MPP. This state can be characterized by Equations (8) and (9) provided below.

$$\frac{dP_{pv}}{dV_{pv}} = \frac{d(V_{pv} \cdot I_{pv})}{dV_{pv}} = I_{pv} + V_{pv} \frac{dI_{pv}}{dV_{pv}} = 0 \quad (8)$$

$$\frac{I_{pv}}{V_{pv}} = -\frac{dV_{pv}}{dI_{pv}} \cong -\frac{\Delta V_{pv}}{\Delta I_{pv}} \quad (9)$$

In the power voltage (P-V) curve of a photovoltaic system, the slope refers to the rate at which the power output changes concerning voltage. At the MPP, the slope of the curve is zero, indicating that a slight change in voltage does not affect power output. Table 3.3 shows various operational scenarios of the IC algorithm. As you move to the left of the MPP on the curve, the slope increases (positive), meaning that a small increase in voltage leads to a greater increase in power output. Conversely, as movement to the right of the MPP occurs, the slope decreases (negative), signifying that a small increase in voltage results in a smaller increase in power output. Table 3 outlines the various operational scenarios of the Incremental Conductance Algorithm:

Table 3. 3 Various operational scenarios of the Incremental Conductance Algorithm.

Condition	Setting Point	Results Achieved
$\frac{dI}{dV} = -\frac{I}{V}$	MPP = P	Functioning at MPP
$\frac{dI}{dV} > \frac{I}{V}$	MPP > P	The operational point is set to the maximum power point (MPP)
$\frac{dI}{dV} < \frac{I}{V}$	MPP < P	The operational point aligns with the maximum power point (MPP)

In Figure 3.15, the graphical representations of the current-voltage (I-V) and power-voltage (P-V) properties for the photovoltaic (PV) array utilized in this study across varying temperature levels have been described. The performance of PV panels is influenced by temperature and solar irradiance. Higher temperatures typically lead to a lower voltage but a higher current due to decreased bandgap energy. Conversely, increased solar irradiance boosts photon absorption, raising both current and voltage. These

variations are critical for optimizing PV system design and performance across different environmental conditions.

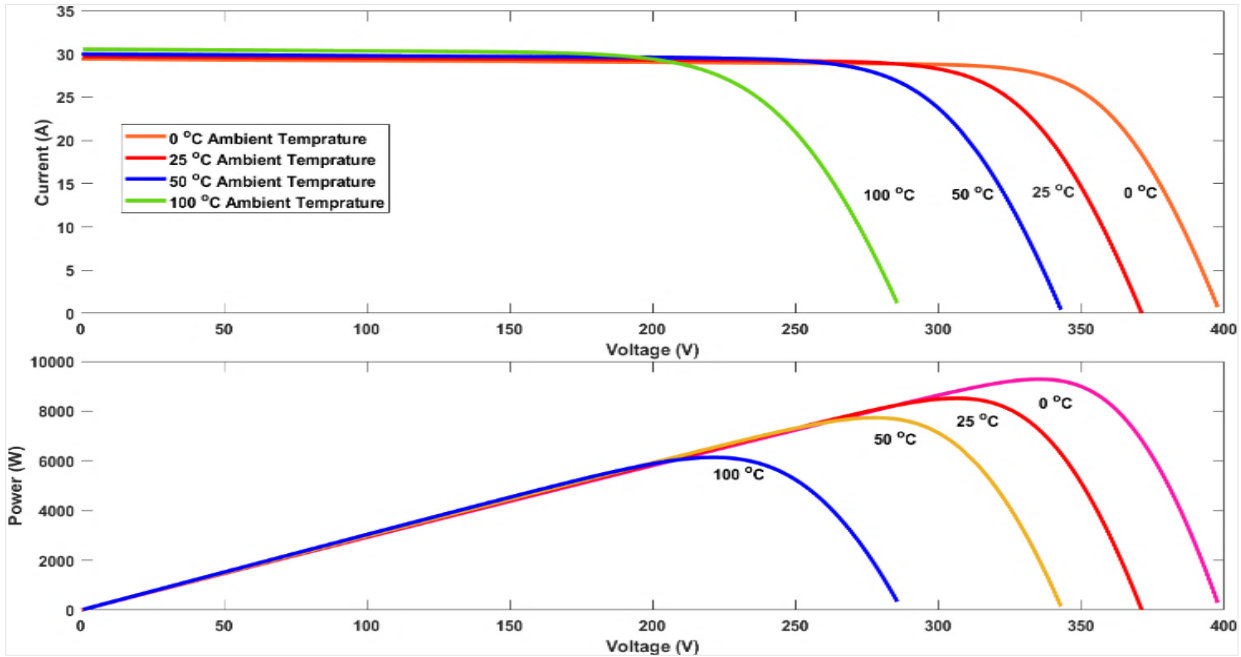


Figure 3. 15 I-V and P-V curves of selected PV panel.

### 3.3.1.4 LCL Filter

The widespread adoption of the LCL filter in contemporary power generation setups is attributed to its superior ability to reduce high-frequency noise, as well as its compact dimensions, and economical nature. The precise and appropriate parameter design for the LCL filter is crucial for cost-saving and enhancing filtering effectiveness [39]. Figure 3.16 illustrates the schematic representation of the LCL filter circuit. The LCL filter effectively reduces current ripples despite having small inductance values, but it can also introduce resonances and instability. Hence, it is crucial to precisely design the filter based on the converter's parameters.

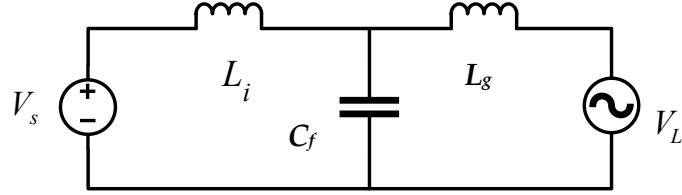


Figure 3. 16 LCL filter's circuit diagram.

One significant aspect of the filter is its cutoff frequency, which should be at least half of the converter's switching frequency to ensure sufficient attenuation within the converter's operational range. Equation (10) can be used to find the value of  $f_{res}$ :

$$f_{res} = \frac{1}{2\pi} \times \sqrt{\frac{L_i + L_g}{L_i \times L_g \times C_f}} \quad (10)$$

The initial stage in determining the filter components involves designing the inverter side inductance, denoted as  $L_i$  which can be calculated using the following Equation (11):

$$L_i = \frac{V_{dc}}{16 \times f_{sw} \times k \times I_{peak}} \quad (11)$$

The inverter-side inductor is tailored to restrict the ripple current to a specified level, typically 10% of the rated current ( $k = 0.1$ ). The capacitor in the filter should be sized to accommodate a grid power factor fluctuation of up to 5% ( $x = 0.05$ ). For calculating the value of the filter capacitance, the following equation is used (12):

$$C_f = \frac{x \times S_n}{\omega_{grid} \times V_n^2} \quad (12)$$

Here,  $S_n$  represents the nominal apparent power and  $V_n$  denotes the RMS voltage between lines; the inductor on the grid side is engineered to restrict the dominant harmonic current amplitude to a defined

threshold.

$$L_g = L_i \times \frac{k \times \frac{I_{DH}}{I_{limDH}} + 1}{L_i \times C_f \times \omega_{sw}^2 - 1} \quad (13)$$

In Equation (13),  $I_{DH}$  represents HOMER Pro, the amplitude of the dominant harmonics  $I_{limDH}$ , and is the desired amplitude level of the dominant harmonics. To minimize filter oscillations and instability, adding a resistor in the series with the capacitor is recommended, known as “passive damping”. While effective and straightforward, this approach increases heat losses and significantly reduces filter efficiency. The damping resistor’s value can be determined using the following calculation in Equation (14):

$$R_{sd} = \frac{1}{3\omega_{res} \times C_f} \quad (14)$$

By use of all the above-mentioned equations, the values of filter resistance  $R_f$ , filter capacitance ( $C_f$ ), resonance frequency ( $f_{res}$ ), inverter side inductance ( $L_i$ ), and grid-side inductance ( $L_g$ ) are calculated as 0.0575  $\Omega$ , 64  $\mu\text{F}$ , 1.39 MHz, 521  $\mu\text{H}$ , and 316  $\mu\text{H}$ , respectively.

### 3.3.1.5 DC-AC Inverter

A crucial element within photovoltaic (PV) systems, the DC-AC inverter, commonly referred to as a power inverter, facilitates the transformation of direct current (DC) electricity produced by solar panels into alternating current (AC) electricity, which is compatible with various appliances and devices. In this paper, a three-phase multi-level inverter is used, which is a type of power inverter used to alter direct current (DC) electricity into a three-phase alternating current (AC) with multiple voltage levels. Figure 3.17 represents the schematic diagram of a three-phase multi-level inverter. Its operation hinges on employing three distinct inverter switches, with each switch assigned to one of the three output phases. These switches are meticulously controlled to produce a balanced and synchronized AC output waveform. These



inverters offer benefits such as reduced lower switching losses and improved voltage waveform quality. The THD is calculated by measuring the root mean square (RMS) value of all harmonic components present in the waveform and expressing it as a percentage of the RMS value of the fundamental frequency.

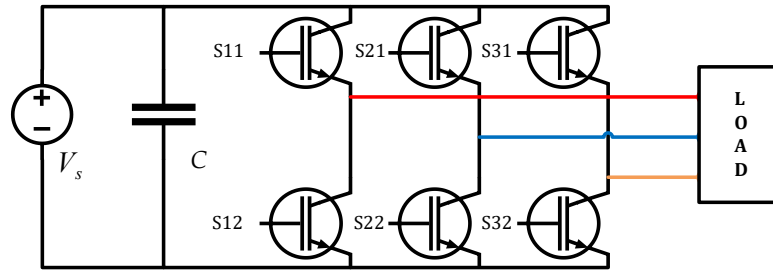


Figure 3. 17 Three-phase multi-level inverter schematic diagram.

A lower THD value indicates a waveform with less distortion and a closer resemblance to a perfect sinusoid. In the case of voltage source inverters (VSIs), which are a type of multi-level inverter, additional parameters include DC link voltage, output frequency, load current, and load impedance. The voltage source inverter (VSI) is employed to transform the 50 Hz AC voltage into DC voltage through a diode rectifier. DC link capacitors operate in parallel to store energy and regulate voltage ripples on the DC bus. Pulse width modulation (PWM) is essential for controlling both voltage and frequency.

### 3.4 Performance Analysis and Optimization of the Intended Hybrid Power System

#### 3.4.1 Performance Analysis of System Using PVsyst Software

The performance ratio serves as a key metric for assessing PV efficiency, with values varying based on factors like environmental conditions, mounting setup, and electrical design. PVsyst, developed in Geneva, is a simulation software utilized for analyzing and optimizing PV system operations. It aids in configuring system setups and estimating energy output, considering geographical location. The simulation results may offer insights into system performance across different time scales, and the “Loss Diagram” feature identifies potential design weaknesses [40]. The following is the scheme of work in the

performance analysis of the system using PVsyst software.

### 3.4.2 Orientation

The orientation part in PVsyst 7.4 software serves the purpose of determining the optimal orientation for solar panels to maximize energy production. Field parameters like tilt angle and azimuthal angle are important factors that will assess the yearly incident radiation (transportation factor, loss factor concerning optimum, global on collector plan). The tilt angle of solar panels has been set at  $34^\circ$  to obtain maximum efficiency and a lower loss factor. Figure 3.18 shows the orientation of PV panels using PVsyst software.

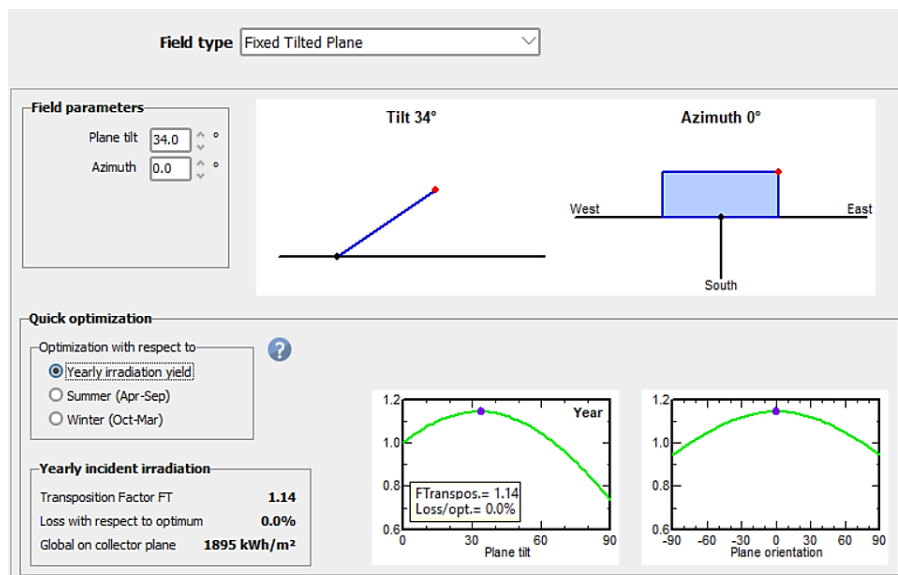


Figure 3. 18 Orientation of the PV Panels.

### 3.4.3 Simulation in PVsyst

PVsyst offers a detailed analysis of irradiance, array, and system losses, allowing users to consider module quality, string mismatches, soiling, wiring, inverter, transformer, and auxiliary losses. It uniquely models degradation and aging effects, which is vital for long-term energy and economic assessment. The projected system aims for a yearly global horizontal radiation of 1657.8 kWh/m<sup>2</sup> and a diffuse horizontal radiation of 702.48 kWh/m<sup>2</sup>, with an average ambient temperature of 14.29 °C. Moreover, the data underscores the efficiency challenges posed by inverter operation point shifts, indicating the need for optimized system configurations to maximize energy output. The considerable surplus energy of 35.93 MWh/year, coupled with the low fuel consumption estimate of 5551 L for backup generators compared

to the community’s actual usage of over 75,000 L, highlights the potential for solar power to not only meet but exceed the community’s energy needs sustainably. These findings emphasize the importance of ongoing monitoring and adjustment to ensure the optimal performance and long-term viability of solar energy systems in meeting evolving energy demands.

Table 3. 4 Details of renewable energy generation and consumption based on predefined parameters.

Month	GlobHor [kWh/m <sup>2</sup> ]	GlobEff [kWh/m <sup>2</sup> ]	Diff Hor [kWh/m <sup>2</sup> ]	E Array [kWh]	E User [kWh]	Unused Energy [kWh]	Fuel BU [Liters]
January	70.7	105.4	29.42	4418	2556	1935	542
February	85.3	107.6	45.44	4510	2462	1948	452
March	123.8	138.4	67.86	5799	2868	2643	470
April	163.7	165.7	68.20	6943	2802	3479	439
May	197	179.2	78.54	7510	2978	3634	433
June	199.2	173.8	78	7282	2949	3410	413
July	183.8	163.8	90.40	6865	3057	2895	425
August	175.4	170	82.13	7125	2967	3268	447
September	161.9	179.6	59.60	7524	2881	3696	437
October	134.2	176.9	41.38	7413	2818	3855	481
November	85.2	124	34.35	5198	2507	2572	493
December	78.1	126.9	27.16	5316	2571	2600	519
Total	1658.3	1811.3	702.48	75,903	33,416	35,953	5551

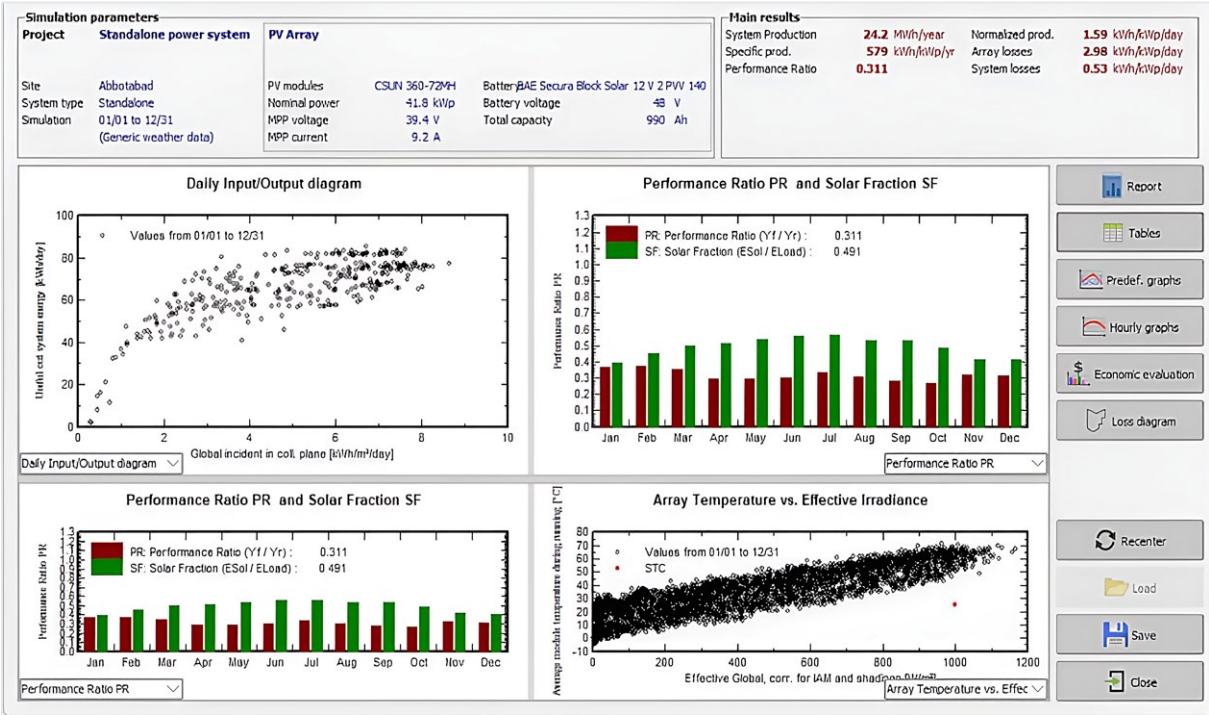


Figure 3. 19 PVsyst simulation outcomes for the proposed system.

Additionally, the comprehensive analysis provided by Figure 3.19 and Table 3.4, detailing renewable

energy generation and consumption based on predefined parameters, enhances our understanding of renewable energy dynamics, informing future planning and resource allocation strategies for resilient, environmentally friendly energy infrastructure.

### **3.4.4 HOMER Pro Simulation and Optimization**

The design of the hybrid power system is executed using HOMER Pro. HOMER Pro technology was established by the American National Renewable Energy Laboratory in 1993. It serves as a system model capable of evaluating various combinations of components for both grid-connected and off-grid systems. HOMER Pro performs three fundamental functions: simulation, optimization, and the detailed analysis of planned energy systems. During the simulation phase, HOMER Pro conducts hour-by-hour simulations throughout the year to assess the technological feasibility of the proposed systems. Additionally, it evaluates key life cycle cost aspects such as acquisition, repair, service, and maintenance. By considering factors such as energy demand fluctuations, resource variability, and component reliability, HOMER Pro aids in identifying optimal system configurations that not only meet current needs but also anticipate future requirements.

Furthermore, its ability to conduct sensitivity analyses offers valuable insights into the resilience of proposed systems, enabling stakeholders to make informed decisions amidst uncertainties in resource availability and market conditions. The flow of work of HOMER Pro is described in Figure 3.20. Initially, it simulates the system's operation across each time step of the year, considering various factors such as energy demand and resource availability. Following simulation, the software proceeds to optimize the system configuration, aiming to find feasible plans that meet specified constraints while minimizing either the net present cost (NPC) or the cost of energy (COE). Next, a sensitivity analysis is performed to assess how uncertain variables influence both system performance and cost, offering valuable insights into potential risks and opportunities. The optimization results generated by HOMER Pro software are shown in Figure 3.21.

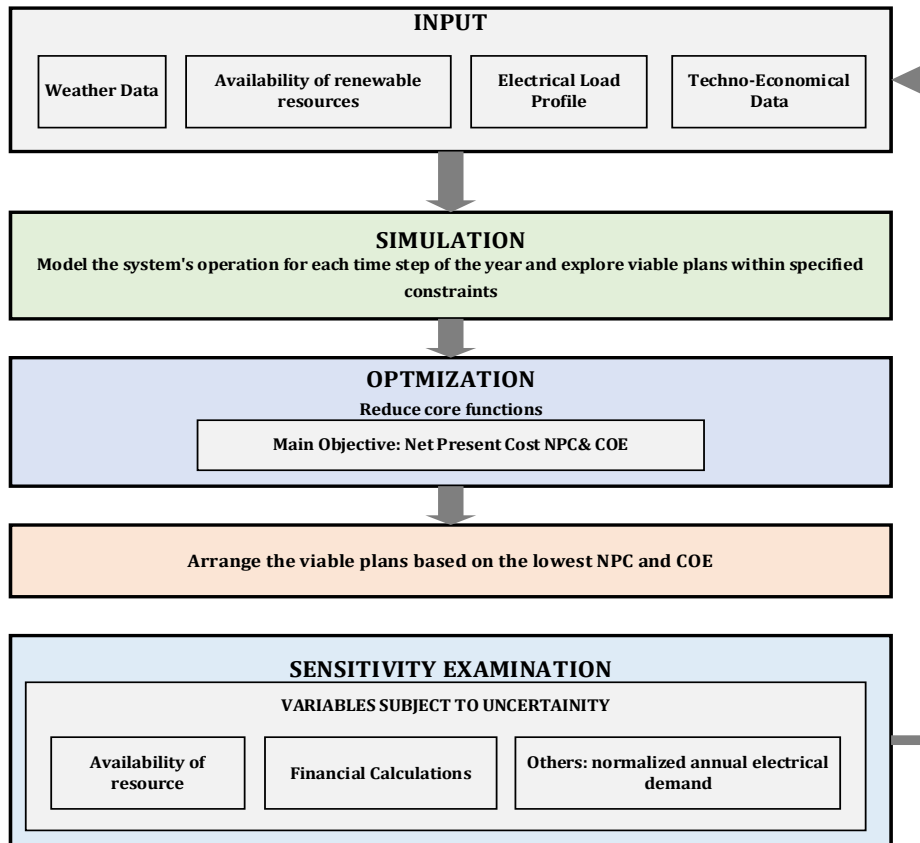


Figure 3. 20 The operational procedure of the HOMER Pro software in sequential order.

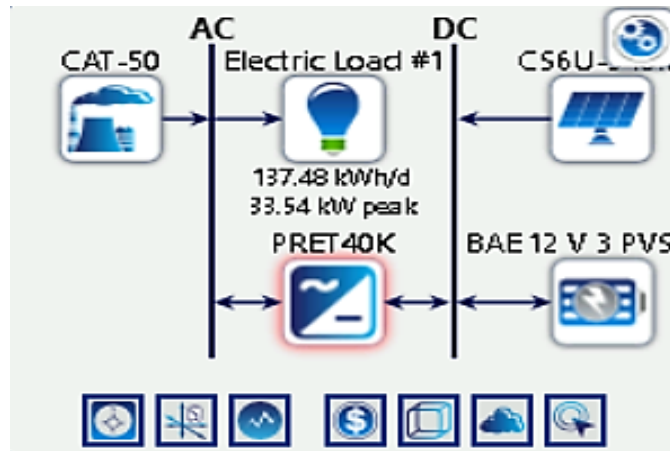


Figure 3. 21 Optimization results of HOMER Pro.

The hybrid power system includes an AC bus for conventional power sources, such as diesel generators, a DC bus connected to photovoltaic (PV) panels, and a battery pack for renewable energy and storage. The diesel generator acts as a backup for the AC bus, while the DC bus utilizes and stores solar energy.

Tables 3.5 and 3.6 provide technical specifications for the batteries and PV panels, highlighting their capacities and efficiencies.

Table 3. 5 Specifications of battery used in HPS.

<b>Model</b>	<b>BAE Secura</b>
Abbreviation	BAE 12
Nominal Voltage (V)	12
Nominal Capacity (kWh)	2.41
Maximum Capacity (Ah)	201
Rate Constant (1/hr)	2.09
Roundtrip Efficiency (%)	85
Maximum Charge Current (A)	68.4
Maximum Discharge Current (A)	342
Maximum Charge Rate (A/Ah)	1

Table 3. 6 Specifications of PV panel used in HPS.

<b>Model</b>	<b>Canadian Solar Max Power</b>
Abbreviation	CS6U-3
Nominal Max. Power (W) (Pmax)	340
Opt. Voltage (Vmp)	32.6
Opt. Current (A)(Imp)	10.43
Open Circuit Voltage (Voc)	39.6
Short Circuit Current (Isc)	10.98
Module Efficiency (%)	18.4
Cell Type	Poly-crystalline
Operating Temperature	-40 °C~+85 °C

The unit costs of the proposed system, utilized in the simulation, are presented in Table 3.7. The initial cost of PV panels for the hybrid power system is USD36,685.92, with an operation and maintenance (OM) cost of USD 1317.79 and no replacement cost. The battery bank carries an initial cost of USD 37,800, with an OM cost of USD 13,573.89 and no replacement cost. Similarly, the DC-AC inverter has an initial cost of USD 766.66, with an OM cost of USD 309.74 and no replacement cost. Figure 22 shows the results of electricity generation by HOMER Pro.

The hybrid power system was designed using HOMER Pro, simulating combinations of PV panels, batteries, converters, and diesel generators. The optimal setup—69.3 kW PV, 210 batteries, COE of USD 0.158/kWh—was selected based on NPC, COE, and operating costs. Sensitivity analyses adjusted for solar irradiance and load, while PVsyst refined the solar design for greater efficiency, ensuring the

system's economic and technical feasibility.

Table 3. 7 Per unit cost of components used in HPS.

Component Description	Capital (USD)	Replacement (USD)	OM (USD)	Total (USD)
BAE SECURA SOLAR 12 V3 PVS 210	37,800	0	13,573.89	51,373.89
Canadian solar Maxpower CS6U-340M	36,685.92	0	13,173.79	49,859.71
PRETTTL REFUso 40K	766.66	0	309.74	1076.4
<b>Total</b>	<b>75,253</b>	<b>0</b>	<b>27,057.42</b>	<b>102,310</b>

The system is designed to maximize efficiency by facilitating limitless power generation through PV modules. Simulations with HOMER Pro explored 982 configurations of power sources. Table 3.8 shows that the best configuration includes solar panels, a converter, a battery bank, and a diesel genset, resulting in the lowest net present cost (NPC) of USD 0.102 million and a cost of energy (COE) of USD 0.158. This optimal system significantly reduces costs compared to the current diesel generator cost of USD 1.06, with annual operating costs of USD 2093, saving USD 5207 annually.

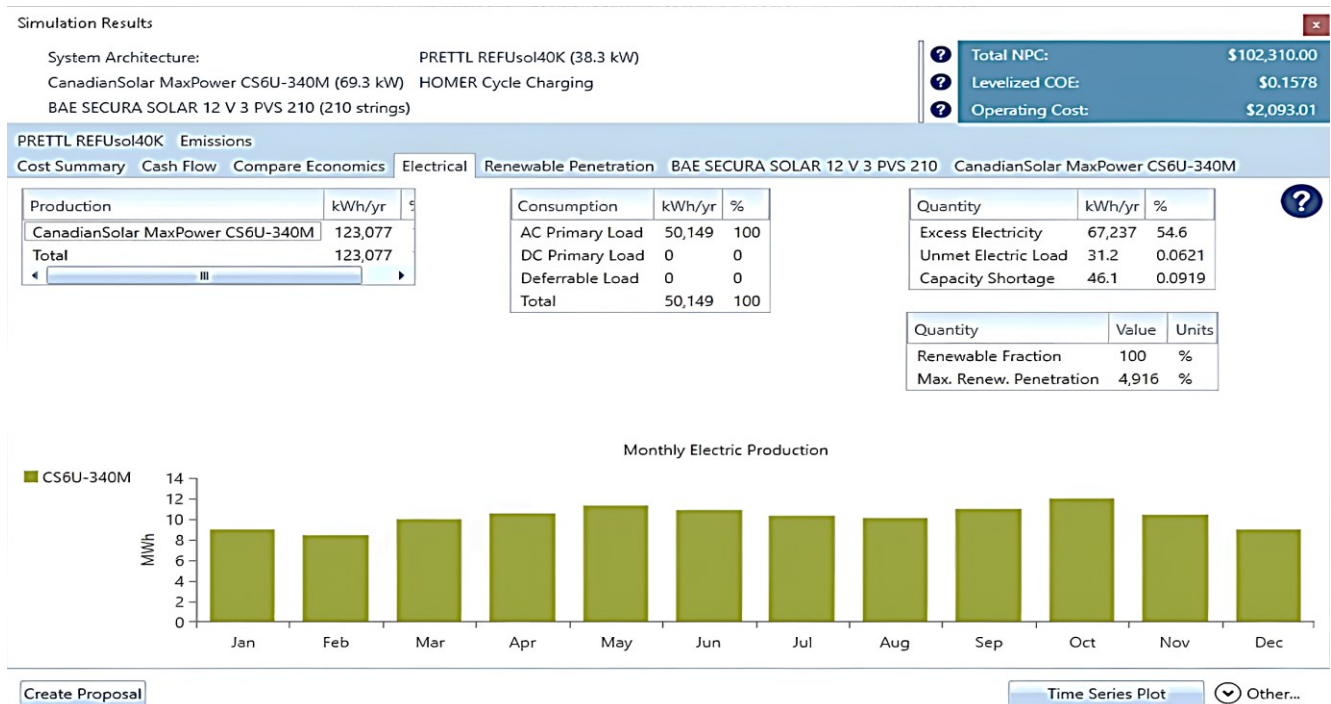


Figure 3. 22 Results of electricity generation by optimal designing of the HPS in HOMER Pro.

Table 3. 8 Results of system optimization in HOMER Pro.

System Structure	Solar Panel (kW)	Diesel Genset (kW)	Battery Bank (No.)	Converter (kW)	NPC (USD)	COE (USD)	Operating expenses (USD/Year)	Primary Investment (USD)
PV-BB-Converter	69.3		210	38.3	0.102 M	0.158	2093	75,253
PV-Genset-BB-Converter	60.5	40	187	38.1	0.104 M	0.161	2391	73,452
PV-Genset-Converter	300	40		40.4	1.70 M	2.62	118,520	166,710
Genset		40		40.4	2.44 M	3.77	188,407	166,710

To show the robustness and impact of key parameter variations on the performance and architecture of the proposed system, a comprehensive sensitivity analysis has been conducted by examining variations in solar global horizontal irradiance (GHI), as detailed in Table 3.9. This analysis helps to understand how changes in solar irradiance affect the overall system, including energy generation, inverter output, battery usage, and system costs. This approach provides valuable insights into the necessary adjustments and optimizations needed to achieve cost-effectiveness and efficiency in the solar PV system.

Table 3. 9 Sensitivity analysis of the system design by variations in the solar GHI.

Solar Irradiance (kWh/m <sup>2</sup> /day)	System Design	PV (kW)	Diesel Genset (kW)	Battery Bank (No. of Batteries)	Converter (Kw)	NPC (USD)	COE (USD/kWh)	Operating Cost (USD/year)	Initial Capital (USD)	Renewable Energy Fraction (%)	CO2 Emissions (kg/year)
0	DG	0	40	0	0	12.1 M	18.60	931,949	17,014	0	102,531
1	PV-DG-BB-Converter	404	40	216	45.6	371,294	0.572	8540	260,896	99.7	184
2	PV-BB-Converter	197	0	260	90.3	207,804	0.320	4252	152,839	100	0
3	PV-BB-Converter	115	0	273	122	152,857	0.236	3130	112,839	100	0
4	PV-BB-Converter	93.3	0	227	90	125,222	0.193	2564	92,077	100	0
5.08	PV-BB-Converter	69.3	0	210	38.3	102,310	0.158	2093	75,253	100	0
6	PV-BB-Converter	67.3	0	180	72.1	94,518	0.146	1935	69,497	100	0
7	PV-BB-Converter	55.5	0	176	54.5	84,533	0.130	1731	62,162	100	0
8	PV-BB-Converter	44.1	0	183	65.1	78,358	0.121	1605	57,612	100	0
9	PV-BB-Converter	40.8	0	176	61.9	74,174	0.114	1519	54,535	100	0
10	PV-BB-Converter	49.2	0	136	73.7	70,747	0.109	1450	52,006	100	0
11	PV-BB-Converter	43	0	136	64.9	66,039	0.102	1353	48,547	100	0

As shown in Table 3.9, variations in solar global horizontal irradiance (GHI) significantly impact the key parameters of the proposed system. When the level of solar GHI increases from the scaled annual average of the selected site, which is 5.08 kWh/m<sup>2</sup> /day, more sunlight reaches the solar panels. This increase in sunlight enhances the electrical energy generated by the PV system. Consequently, the inverter has more power to convert, leading to a higher AC output and enabling it to supply more power



to meet the demand of the connected load, thus reducing reliance on stored energy. With the increase in PV generation, there is more immediate energy available for use, which reduces the need to draw power from batteries and improves battery charging. Higher solar GHI will reduce the cost of energy (COE) and the overall cost of the proposed system. Furthermore, there will be no greenhouse gas (GHG) emissions, and the renewable energy fraction will be 100%. Conversely, if the solar GHI decreases, less sunlight is available for generating electricity. In this scenario, the inverter will have less power to convert from DC to AC, resulting in a lower AC output and requiring more power from batteries to meet the load requirements. Additionally, more batteries will be needed to store the energy, which will increase the COE as well as the overall cost of the proposed system. As seen in Table 3.7, lower solar GHI leads to higher GHG emissions and a reduced fraction of renewable energy.

### **3.5 Dynamic Modeling of Proposed Hybrid Power System in MATLAB/Simulink**

Assessing the functionality and dynamics of a system heavily relies on dynamic modeling and simulation. MATLAB Simulink simulations are conducted to delve into the dynamic behavior of the envisaged hybrid power system, with a specific emphasis on power quality, voltage fluctuations, and load impacts. The PV array's output characteristics, including V-I and V-P characteristics, exhibit non-linearity and are significantly influenced by environmental factors. These factors include solar irradiation levels, ambient temperature variations, and the extent of partial shading affecting the PV array.

The dynamic modeling of a photovoltaic (PV) system, particularly in terms of the ASTM G173 spectrum, involves simulating its performance under varying atmospheric conditions. The ASTM G173 spectrum considers factors such as air mass, ozone content, and aerosol concentration, affecting the spectral distribution of sunlight reaching the Earth's surface. In this modeling, the PV system's reaction to changes in solar irradiance and temperature is analyzed using mathematical models implemented in the software. The Simulink MATLAB design of the proposed hybrid system is shown in Figure 3.23.

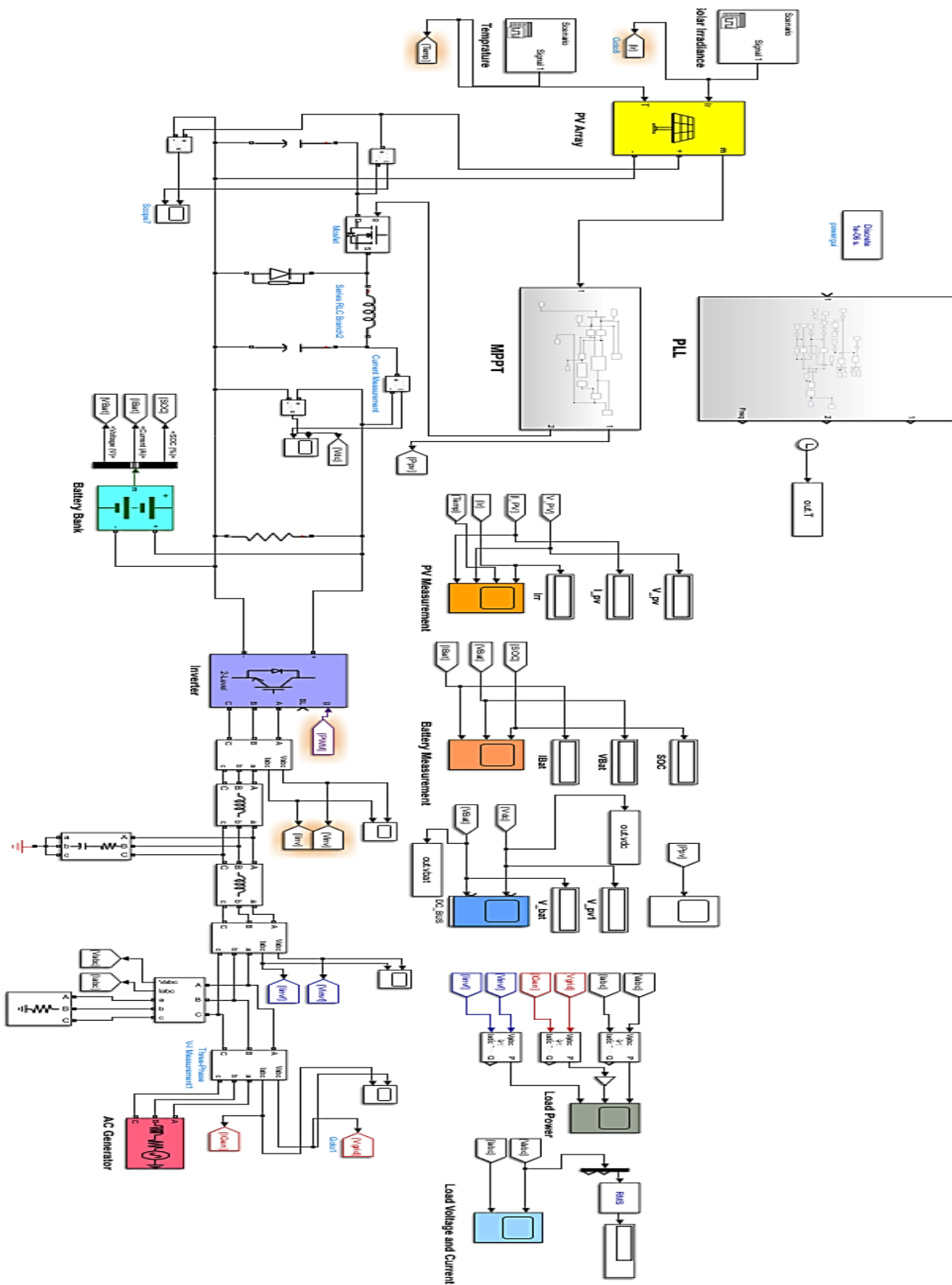


Figure 3. 23 MATLAB Simulink dynamic model for the proposed hybrid power system.

Setting the initial irradiance value to around 1000 watts per square meter (W/m<sup>2</sup>) is common practice to simulate standard solar radiation conditions. Solar cell temperatures may fluctuate within

simulations, ranging from approximately 25 °C to 60 °C. However, higher temperatures can also lead to an increase in current output due to enhanced electron excitation within the panel’s semiconductor material. These effects demonstrate the complex relationship between irradiance, temperature, voltage, and current in PV panels, ultimately impacting their overall performance and efficiency.

Table 3.10 represents the scenario of variations in solar irradiance and temperature of PV panels and how they will affect the dynamics of the proposed hybrid power system. This detailed analysis helps optimize PV system design and operation, contributing to the efficient utilization of solar energy resources and the advancement of renewable energy technologies. To visualize the effects of variations in solar global horizontal irradiance (GHI) and temperature, adjustments were made to the parameters of the PV array’s solar GHI and temperature within MATLAB Simulink. Initially, the system operated under standard conditions with a GHI of 1000 W/m<sup>2</sup> and a temperature of 25 °C. Figure 3.24 represents the variations in solar GHI and temperature and their impact on the output voltage and current of the PV panel. Subsequently, at time 0.5 s, the GHI was reduced to 400 W/m<sup>2</sup> to mimic decreased sunlight, while the temperature was incrementally increased to 35 °C. As the irradiance level decreased the voltage and current level between 0.5 to 1.5 s, at time 2 s, the temperature increased to 55 °C and the irradiance level increased to 1000 W/m<sup>2</sup>. Elevated temperatures result in a decrease in current and voltage, whereas higher GHI levels lead to an increased voltage output from the PV array. This analysis enhances the comprehension of the system’s behavior under diverse environmental conditions and facilitates performance optimization.

Table 3. 10 Scenarios of variations in solar irradiance and temperature in MATLAB Simulink.

<b>Time (Seconds)</b>	<b>Solar GHI (W/m<sup>2</sup>)</b>	<b>Temperature (°C)</b>
0	1000	25
0.5	400	25
1	400	35
1.5	1000	35
2	1000	45
2.5	1000	45

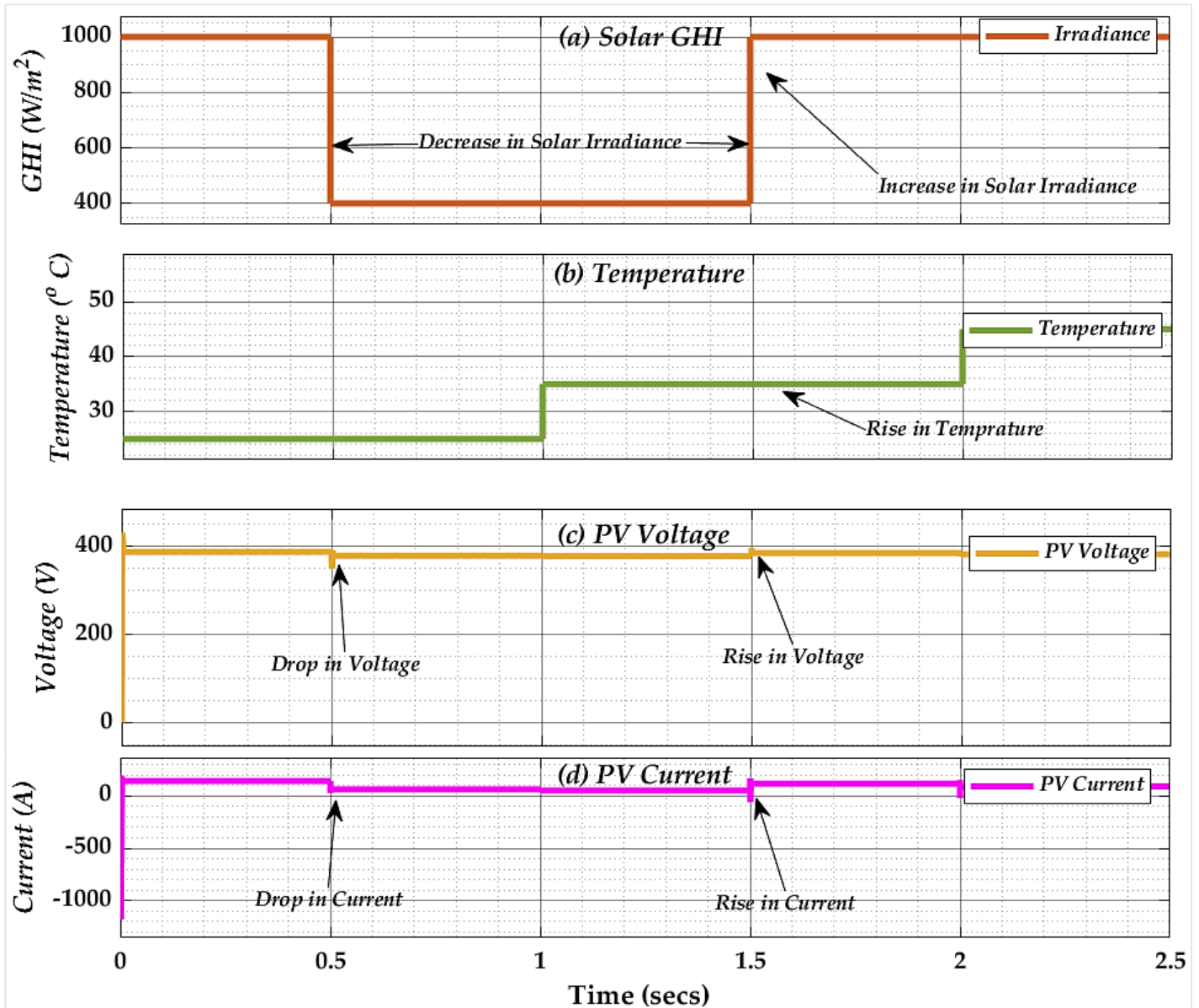


Figure 3. 24 (a) Variations in solar irradiance, (b) variations in temperature, (c) PV panel output voltage, and (d) PV panel output current due to variations in solar GHI and temperature.

The charging process of batteries in photovoltaic systems is significantly influenced by variations in irradiance and temperature. Higher levels of irradiance typically result in increased charging currents and voltages, as more solar energy is available for conversion into electrical energy. Conversely, decreases in irradiance lead to reduced charging currents and voltages.

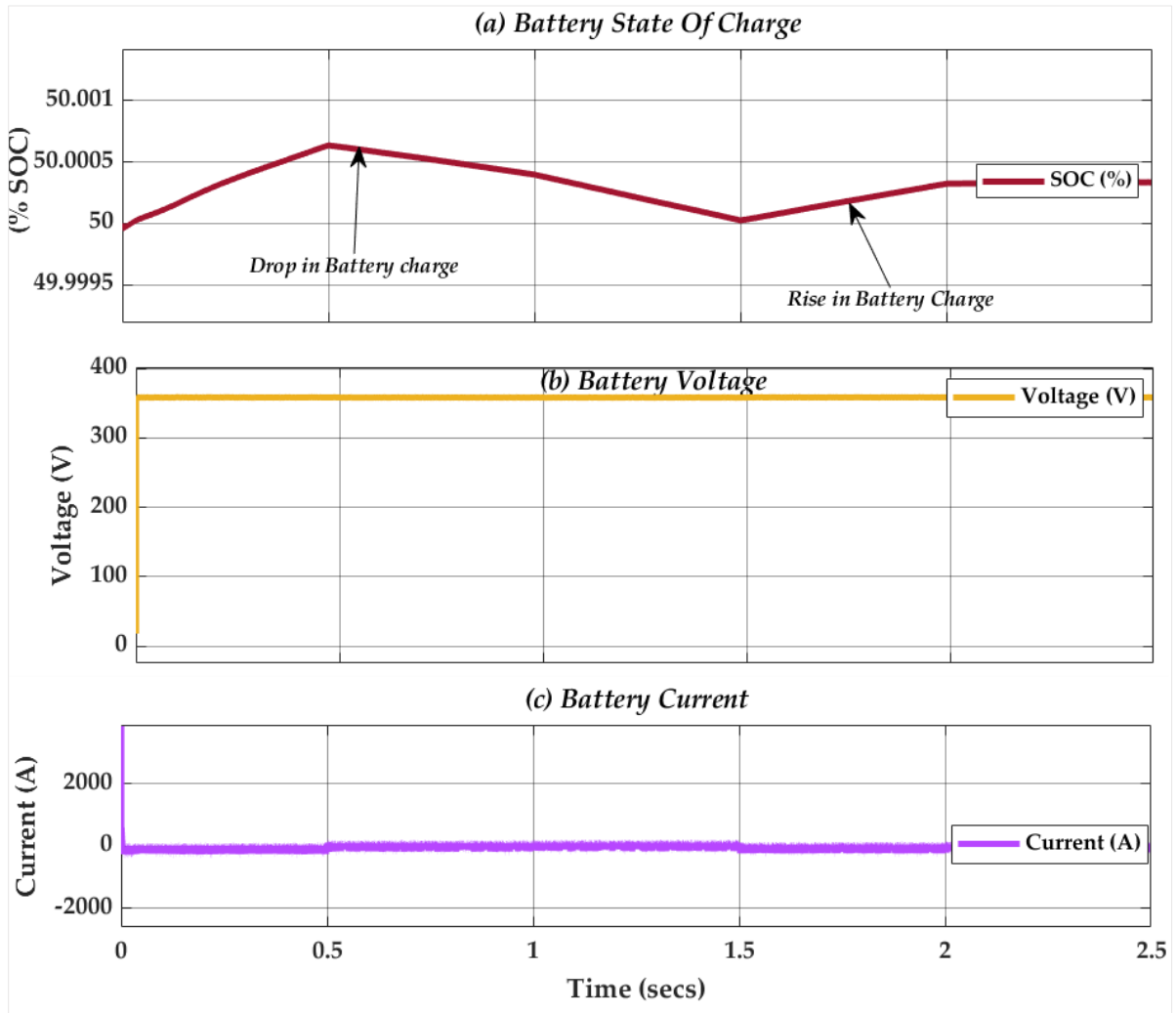


Figure 3. 25 (a) %SOC of battery bank, (b) voltage of battery bank, and (c) current of battery bank.

Temperature also plays a crucial role, with higher temperatures generally accelerating charging rates due to enhanced chemical reactions within the battery. In Figure 3.25, a shift in irradiance occurs at 0.5 s, leading to a discharge of the battery bank until 1.5 s. Subsequently, when the irradiance rises from 400 to 1000 W/m<sup>2</sup> after 1.5 s, the battery begins to recharge and stabilizes at 2 s. During a power outage, the PV system activates the generator and integrates a Phase Locked Loop (PLL) into the MATLAB simulation. The system continuously monitors power output to detect shortages, prompting immediate generator activation. Concurrently, PLL parameters, such as reference signal frequency and phase, are set. The PLL block, comprising phase detectors, filters, and oscillators, synchronizes the generator's output with the grid or reference signal. This integration within the MATLAB Simulink model ensures efficient

connectivity and interaction among system components. Figure 3.26 demonstrates the consistent phase-to-ground voltage and current delivered to the connected load through the designed HPS.

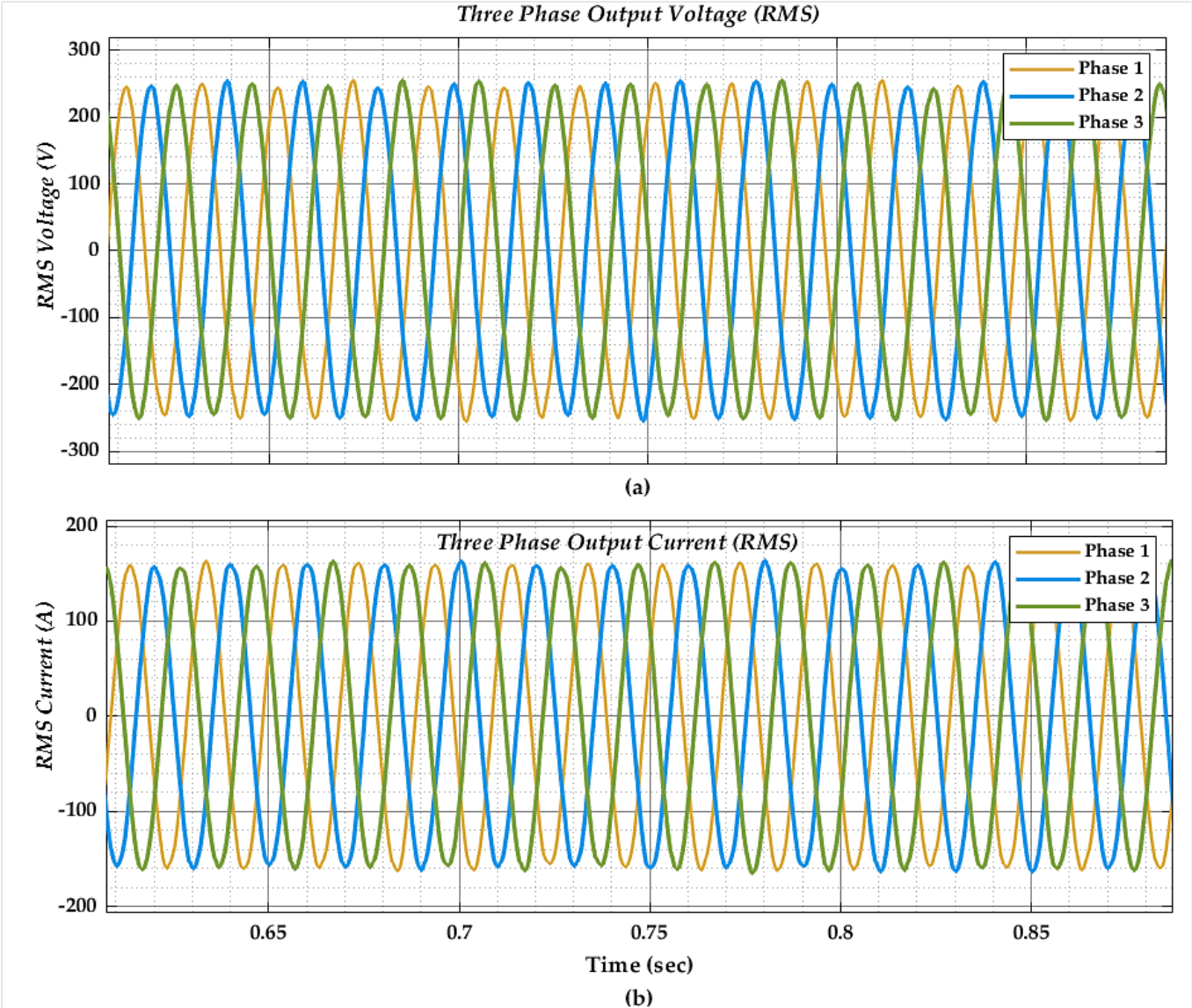


Figure 3. 26 (a) Voltage is delivered to the load in three phases (RMS). (b) Current supplied to load across three phases (RMS).

### 3.6 Experimental Validation Using Hardware in Loop

Validating a hybrid power system in real-time for a rural community is essential to verify its feasibility, reliability, and efficacy in addressing the community’s energy requirements. The OP5707XG by OPAL-

RT Technologies serves as an advanced real-time simulator, utilizing FPGA technology to ensure swift and accurate simulations with minimal latency. It excels in facilitating HIL checking for diverse applications, including photovoltaic (PV) systems. With powerful processors and precise I/O interfaces, it accurately replicates load current and voltage dynamics, which is crucial for optimizing PV system performance. Figure 3.27 shows the hardware structure of the simulator.

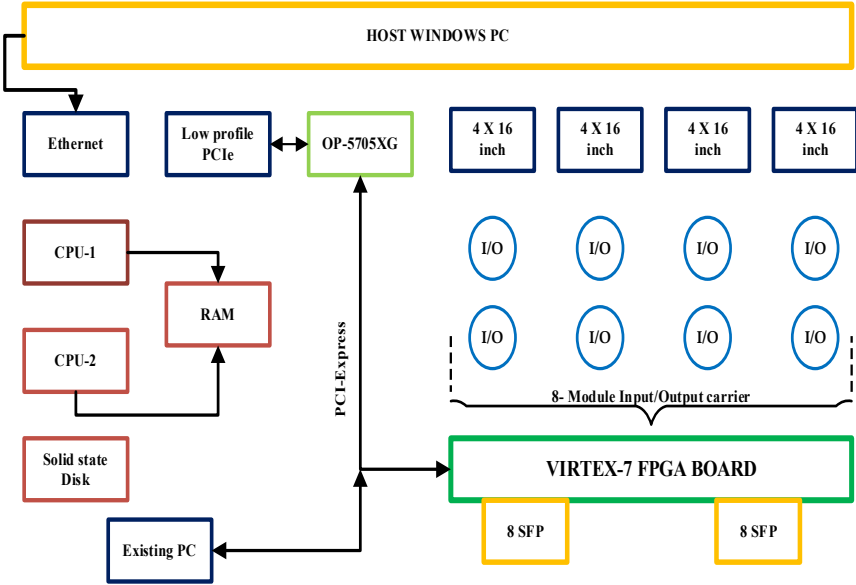


Figure 3. 27 Hardware structure of the simulator.

The OP5707XG can be integrated with MATLAB Simulink, a popular environment for modeling and simulating dynamic systems. The required model to be simulated has been created in Simulink, representing the components and behaviors. Once the model is developed, it can be compiled and executed in real-time on the OP5707XG hardware. This integration allows for HIL testing, where the simulated system interacts with the physical system as well as the design under testing along with components connected to the OP5707XG, representing real-world conditions. Real-time monitoring and logging provided by Simulink enable the analysis of the performance of the simulated system and validate its behavior. Figure 3.28 shows the hardware architecture of the OP5707XG simulator.



Figure 3. 28 OPAL-RT hardware setup.

The block set has been developed to enable distributed processing, inter-node communication, and signal input/output within the MATLAB Simulink model. Following the simulation using OPAL-RT, the system consistently provided a three-phase load voltage and current, affirming the practical applicability and efficacy of the designed system. Figures 3.29 and 3.30 display the results of the experimental validation, presenting the three-phase voltage and current output of the designed system utilizing HIL testing. Further, figures 2.13 and 2.14 are based on a connected load of 35.65 kWh/day and a peak load of 11.33 kW, whereas the system in figures 3.28 and 3.29 is designed for a connected load of 137.48 kWh/day and a peak load of 33.54 kW.

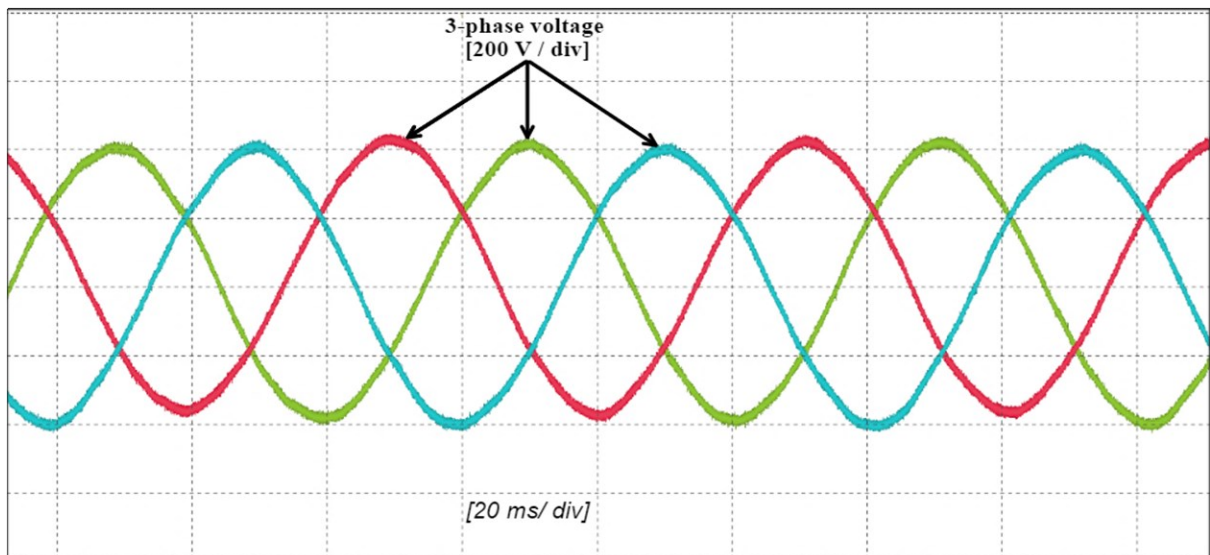


Figure 3. 29 Three-phase output load voltage because of experimental validation.



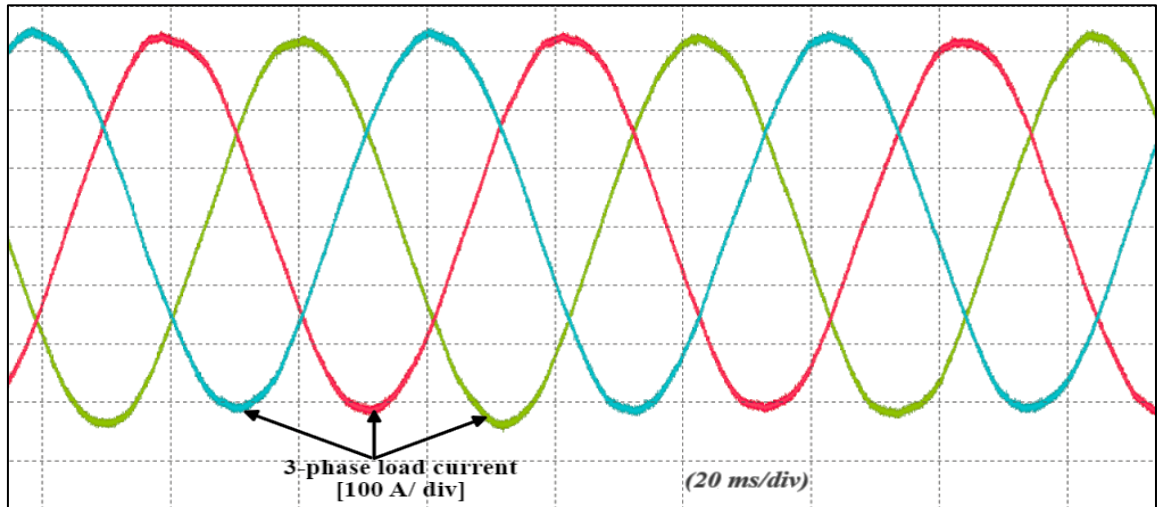


Figure 3. 30 Three-phase output load current as a result of experimental validation.

### 3.7 Findings

This research article introduces an innovative method to fulfill the energy requirements of distant and isolated communities by proposing and executing a hybrid power system. Highlighting the importance of innovative energy solutions in remote regions, the research underscores the capability of hybrid power systems to provide a reliable and enduring electricity supply. Incorporating a range of elements, the hybrid power system proposal encompasses solar panels, MPPT, a DC-AC inverter, a buck converter, a diesel generator, battery storage, and an electrical load. The performance analysis and ideal configurations are achieved using PVsyst and HOMER Pro software; the dynamic modeling of the system is conducted in MATLAB Simulink conditions to assess its performance. Additionally, experimental validation is performed via Hardware-in-the-Loop simulations using the real-time OPAL-RT Technologies' OP5707XG simulator. The primary findings of the study are summarized as follows:

- Considering the recent floods in Pakistan, attributed largely to climate change induced by greenhouse gas emissions from fossil fuels, there is an urgent call for transitioning to renewable energy sources with minimal greenhouse gas emissions. Leveraging Pakistan's ample solar global horizontal irradiance, solar photovoltaic systems play a crucial role in bolstering the electricity output

of hybrid power systems. This addresses the specific energy needs of such facilities while amplifying economic advantages, thereby making advancements consistent with broader energy sustainability goals.

- Using HOMER Pro, 982 simulations were conducted, resulting in an optimal system with a renewable energy fraction of 100%.
- The hybrid power system's energy cost is USD 0.158, resulting in substantial savings of USD 0.902 in contrast to the present expenses of USD 1.06. Additionally, the system's annual operating cost of USD 2093 signifies significant savings of USD 5207 in contrast to the current cost of USD 7300.

### **3.8 Conclusion**

This study underscores the vital role hybrid power systems can play in advancing sustainable energy solutions for rural communities. By renewable energy sources such as solar panels with traditional generators and employing advanced simulation tools like PVsyst and HOMER Pro, it has been demonstrated that it is feasible to develop reliable, cost-effective, and environmentally friendly energy systems tailored to rural needs. The dynamic modeling and validation, conducted through MATLAB Simulink and Hardware-in-the-Loop simulations, further validates the system's operational efficiency and resilience to variations in environmental conditions. The implementation of such hybrid systems not only helps in reducing the dependency on fossil fuels but also significantly mitigates greenhouse gas emissions, contributing to global efforts against climate change. Furthermore, the economic analysis reveals that the adoption of the HPS can lead to substantial savings in energy costs, enhancing the economic stability of rural communities. As rural areas continue to face unique challenges in accessing reliable energy sources, the findings of this study offer a promising pathway toward achieving energy independence through sustainable practices. It encourages stakeholders, including policymakers and renewable energy developers, to invest in hybrid systems that leverage local resources and technological advancements to meet the increasing

energy demands while fostering environmental management.

## References

1. Akhtar, S.; Hashmi, M.K.; Ahmad, I.; Raza, R. Advances and significance of solar reflectors in solar energy technology in Pakistan. *Energy Environ.* 2018, 29, 435–455. <https://doi.org/10.1177/0958305X18758487>.
2. Bakht, M.P.; Salam, Z.; Bhatti, A.R.; Ullah Sheikh, U.; Khan, N.; Anjum, W. Techno-economic modelling of hybrid energy system to overcome the load shedding problem: A case study of Pakistan. *PLoS ONE* 2022, 17, e0266660. <https://doi.org/10.1371/journal.pone.0266660>.
3. Ahmed, Md.R.; Hasan, Md.R.; Al Hasan, S.; Aziz, M.; Hoque, Md.E. Feasibility Study of the Grid-Connected Hybrid Energy System for Supplying Electricity to Support the Health and Education Sector in the Metropolitan Area. *Energies* 2023, 16, 1571. <https://doi.org/10.3390/en16041571>.
4. Martins, F.; Felgueiras, C.; Smitkova, M.; Caetano, N. Analysis of Fossil Fuel Energy Consumption and Environmental Impacts in European Countries. *Energies* 2019, 12, 964. <https://doi.org/10.3390/en12060964>.
5. Richardson, M.; Cowtan, K.; Millar, R.J. Global temperature definition affects achievement of long-term climate goals. *Environ. Res. Lett.* 2018, 13, 054004. <https://doi.org/10.1088/1748-9326/aab305>.
6. Bölük, G.; Mert, M. Fossil & renewable energy consumption, GHGs (greenhouse gases) and economic growth: Evidence from a panel of EU (European Union) countries. *Energy* 2014, 74, 439–446. <https://doi.org/10.1016/j.energy.2014.07.008>.
7. Al-Ketan, O. Potential of using olive pomace as a source of renewable energy for electricity generation in the Kingdom of Jordan. *J. Renew. Sustain. Energy* 2012, 4, 063132. <https://doi.org/10.1063/1.4769205>.
8. Malik, S.; Qasim, M.; Saeed, H.; Chang, Y.; Taghizadeh-Hesary, F. Energy security in Pakistan: Perspectives and policy implications from a quantitative analysis. *Energy Policy* 2020, 144, 111552. <https://doi.org/10.1016/j.enpol.2020.111552>.
9. Lin, B.; Raza, M.Y. Analysis of energy-related CO<sub>2</sub> emissions in Pakistan. *J. Clean. Prod.* 2019, 219,

981–993. <https://doi.org/10.1016/j.jclepro.2019.02.112>.

10. Naeem, M.K.; Anwar, S.; Nasreen, S. Empirical analysis of CO<sub>2</sub> emissions and sustainable use of energy sources in Pakistan. *Environ. Sci. Pollut. Res.* 2021, 28, 16420–16433. <https://doi.org/10.1007/s11356-020-11927-1>.

11. Sohoo, I.; Ritzkowski, M.; Kuchta, K.; Cinar, S.Ö. Environmental Sustainability Enhancement of Waste Disposal Sites in Developing Countries through Controlling Greenhouse Gas Emissions. *Sustainability* 2020, 13, 151. <https://doi.org/10.3390/su13010151>.

12. Asian Development Bank. The Impact of Infrastructure Investment on Inclusive Growth and Poverty Reduction: A Review. Available online: <https://www.adb.org/sites/default/files/publication/535821/adbi-wp1024.pdf> (accessed on 2 May 2024).

13. Alifu, H.; Hirabayashi, Y.; Imada, Y.; Shiogama, H. Enhancement of river flooding due to global warming. *Sci. Rep.* 2022, 12, 20687. <https://doi.org/10.1038/s41598-022-25182-6>.

14. Shehzad, K. Extreme flood in Pakistan: Is Pakistan paying the cost of climate change? A short communication. *Sci. Total Environ.* 2023, 880, 162973. <https://doi.org/10.1016/j.scitotenv.2023.162973>.

15. Manzoor, Z.; Ehsan, M.; Khan, M.B.; Manzoor, A.; Akhter, M.M.; Sohail, M.T.; Hussain, A.; Shafi, A.; Abu-Alam, T.; Abioui, M. Floods and flood management and its socio-economic impact on Pakistan: A review of the empirical literature. *Front. Environ. Sci.* 2022, 10, 1021862. <https://doi.org/10.3389/fenvs.2022.1021862>.

16. Khayyam, U.; Noureen, S. Assessing the adverse effects of flooding for the livelihood of the poor and the level of external response: A case study of Hazara Division, Pakistan. *Environ. Sci. Pollut. Res.* 2020, 27, 19638–19649. <https://doi.org/10.1007/s11356-020-08303-4>.

17. Qudrat-Ullah, H. A review and analysis of renewable energy policies and CO<sub>2</sub> emissions of Pakistan. *Energy* 2022, 238, 121849. <https://doi.org/10.1016/j.energy.2021.121849>.

18. Zafar, U.; Ur Rashid, T.; Khosa, A.A.; Khalil, M.S.; Rashid, M. An overview of implemented renewable energy policy of Pakistan. *Renew. Sustain. Energy Rev.* 2018, 82, 654–665.

<https://doi.org/10.1016/j.rser.2017.09.034>.

19. Guo, S.; Liu, Q.; Sun, J.; Jin, H. A review on the utilization of hybrid renewable energy. *Renew. Sustain. Energy Rev.* 2018, 91, 1121–1147. <https://doi.org/10.1016/j.rser.2018.04.105>.

20. Ji, L.; Liang, X.; Xie, Y.; Huang, G.; Wang, B. Optimal design and sensitivity analysis of the stand-alone hybrid energy system with PV and biomass-CHP for remote villages. *Energy* 2021, 225, 120323. <https://doi.org/10.1016/j.energy.2021.120323>.

21. Hussain, F.; Maeng, S.-J.; Cheema, M.J.M.; Anjum, M.N.; Afzal, A.; Azam, M.; Wu, R.-S.; Noor, R.S.; Umair, M.; Iqbal, T. Solar Irrigation Potential, Key Issues and Challenges in Pakistan. *Water* 2023, 15, 1727. <https://doi.org/10.3390/w15091727>.

22. Tamoor, M.; Bhatti, A.R.; Farhan, M.; Miran, S. Design of On-Grid Photovoltaic System Considering Optimized Sizing of Photovoltaic Modules for Enhancing Output Energy. *Eng. Proc.* 2022, 19, 2. <https://doi.org/10.3390/ECP2022-12671>.

23. Nawab, F.; Abd Hamid, A.S.; Arif, M.; Khan, T.A.; Naveed, A.; Sadiq, M.; Imad Ud Din, S.; Ibrahim, A. Solar–Biogas Microgrid: A Strategy for the Sustainable Development of Rural Communities in Pakistan. *Sustainability* 2022, 14, 11124. <https://doi.org/10.3390/su141811124>.

24. Iqbal, A.; Iqbal, M.T. Design and Analysis of a Stand-Alone PV System for a Rural House in Pakistan. *Int. J. Photoenergy* 2019, 2019, 1–8. <https://doi.org/10.1155/2019/4967148>.

25. Xu, L.; Wang, Y.; Solangi, Y.; Zameer, H.; Shah, S. Off-Grid Solar PV Power Generation System in Sindh, Pakistan: A TechnoEconomic Feasibility Analysis. *Processes* 2019, 7, 308. <https://doi.org/10.3390/pr7050308>.

26. Ur Rehman, A.; Iqbal, M.T. Design and Control of an Off-Grid Solar System for a Rural House in Pakistan. In *Proceedings of the 2020 11th IEEE Annual Information Technology, Electronics and Mobile Communication Conference (IEMCON)*, IEEE, Vancouver, BC, Canada, 4–7 November 2020; pp. 0786–0790. <https://doi.org/10.1109/IEMCON51383.2020.9284867>.

27. Elsaraf, H.; Jamil, M.; Pandey, B. Techno-Economic Design of a Combined Heat and Power Microgrid

- for a Remote Community in Newfoundland Canada. *IEEE Access* 2021, 9, 91548–91563. <https://doi.org/10.1109/ACCESS.2021.3091738>.
28. Kumar, K.; Kumar, M.; Soomro, A.M. To Design an off Grid PV System for an electrified area of District Tharparkar, Pakistan. *Int. J. Green Energy* 2021, 18, 920–932. <https://doi.org/10.1080/15435075.2021.1884867>.
29. Ali, F.; Ahmar, M.; Jiang, Y.; AlAhmad, M. A techno-economic assessment of hybrid energy systems in rural Pakistan. *Energy* 2021, 215, 119103. <https://doi.org/10.1016/j.energy.2020.119103>.
30. Rehmani, A.M.; Akhter, P. Techno-Economic analysis of hybrid renewable energy systems for rural area energization in Pakistan. In *Proceedings of the 2019 3rd International Conference on Energy Conservation and Efficiency (ICECE)*; IEEE, Lahore, Pakistan, 23–24 October 2019; pp. 1–6.
31. Abdullah, F.B.; Iqbal, R.; Jawaid, M.; Ahmad, S. Addressing unaccounted-for-gas (UFG): Proactive techniques for optimal management and control. *Energy Strategy Rev.* 2024, 53, 101397. <https://doi.org/10.1016/j.esr.2024.101397>.
32. Qazi, U.; Jahanzaib, M. An integrated sectoral framework for the development of sustainable power sector in Pakistan. *Energy Rep.* 2018, 4, 376–392. <https://doi.org/10.1016/j.egyr.2018.06.001>.
33. Dhimish, M.; Silvestre, S. Estimating the impact of azimuth-angle variations on photovoltaic annual energy production. *Clean Energy* 2019, 3, 47–58. <https://doi.org/10.1093/ce/zky022>.
34. Solaris. Solar Resource Information and PV Power Potential. Available online: <https://apps.solaris.com/prospect/detail/3lirckDVsvHfKB5n/info> (accessed on 2 May 2024).
35. Wang, Z.; Crawley, J.; Li, F.G.N.; Lowe, R. Sizing of district heating systems based on smart meter data: Quantifying the aggregated domestic energy demand and demand diversity in the UK. *Energy* 2020, 193, 116780. <https://doi.org/10.1016/j.energy.2019.116780>.
36. Al-Shahri, O.A.; Ismail, F.B.; Hannan, M.A.; Lipu, M.S.H.; Al-Shetwi, A.Q.; Begum, R.A.; Al-Muhsen, N.F.O.; Soujeri, E. Solar photovoltaic energy optimization methods, challenges and issues: A comprehensive review. *J. Clean. Prod.* 2021, 284, 125465. <https://doi.org/10.1016/j.jclepro.2020.125465>.

37. Podder, A.K.; Roy, N.K.; Pota, H.R. MPPT methods for solar PV systems: A critical review based on tracking nature. *IET Renew Power Gener.* 2019, 13, 1615–1632. <https://doi.org/10.1049/iet-rpg.2018.5946>.
38. Madhukumar, M.; Suresh, T.; Jamil, M. Investigation of Photovoltaic Grid System under Non-Uniform Irradiance Conditions. *Electronics* 2020, 9, 1512. <https://doi.org/10.3390/electronics9091512>.
39. Cai, Y.; He, Y.; Zhou, H.; Liu, J. Design Method of LCL Filter for Grid-Connected Inverter Based on Particle Swarm Optimization and Screening Method. *IEEE Trans. Power Electron.* 2021, 36, 10097–10113. <https://doi.org/10.1109/TPEL.2021.3064701>.
40. Baqir, M.; Channi, H.K. Analysis and design of solar PV system using Pvsyst software. *Mater. Today Proc.* 2022, 48, 1332–1338. <https://doi.org/10.1016/j.matpr.2021.09.029>.

# Chapter 4

## Open Source IoT-Based SCADA System for PV Monitoring and Control Using HTTP and TCP/IP Protocols

### Preface

*A version of this manuscript has been published in MDPI Energies Journal, (Energies 2024, 17(16), 4083; <https://doi.org/10.3390/en17164083>). I am the primary author, and have carried out most of the research work, performed the literature reviews, and carried out the system design, modeling, and analysis of the results. I also prepared the first draft of the manuscript and subsequently revised the final manuscript based on the feedback from the supervisor. The co-authors, Dr. Mohsin Jamil and Dr. Ashraf Ali Khan, supervised the research, acquired, and provided the research guide, reviewed and corrected the manuscript, and contributed research ideas in the actualization.*



# Abstract

This study presents a cost-effective IoT-based Supervisory Control and Data Acquisition system for real-time monitoring and control of photovoltaic systems in a rural Pakistani community. The system utilizes the Blynk platform with Arduino Nano, GSM SIM800L, and ESP-32 microcontrollers. The ZMPT101B voltage sensor, ACS712 current sensors, and a Maximum PowerPoint Tracking module for optimizing power output are key components. The system operates over both Global system for Mobile communication and Wi-Fi networks, employing Universal asynchronous receiver transmitter serial communication and using Transmission control protocol/ Internet Protocol and Hypertext transfer Protocol for data exchange. Testing showed that the system consumes only 3.462 W of power, making it highly efficient. With an implementation cost of CAD 35.52, it offers an affordable solution for rural areas. The system achieved an average data transmission latency of less than 2 seconds over Wi-Fi and less than 5 seconds over GSM, ensuring timely data updates and control. The Blynk app provides data retention capabilities, allowing users to access historical data for performance analysis and optimization. This open-source SCADA system demonstrates significant potential for improving efficiency and user engagement in renewable energy management, offering a scalable solution for global applications

**Keywords:** Renewable Energy, IoT, SCADA (Supervisory Control and Data Acquisition), Arduino Nano, GSM SIM800L, ESP-32, TCP/IP (Transmission control protocol/ Internet Protocol), HTTP (Hypertext transfer Protocol), UART (Universal asynchronous receiver transmitter), the Blynk, Arduino IDE 1.8.19, Sensors, Low cost and Low powered.

## 4.1 Introduction

In recent years, global energy demand has surged due to population growth and rapid industrial advancement. As a result, renewable energy sources have gained widespread adoption in both industrial and residential sectors [1]. Solar energy, being endless, eco-friendly, and secure, is a highly sought-after form of

green energy [2]. Global photovoltaic (PV) capacity has dramatically increased over the past twenty years, from 1,288 MW in 2000 to 1,177,000 MW in 2022, reflecting a significant rise in solar energy use[3]. Pakistan receives abundant solar irradiance, averaging 2400 kWh/m<sup>2</sup> annually and 5-7 kWh/m<sup>2</sup> daily, with over 2300-2700 sunshine hours and more than 300 sunny days per year. Leveraging this resource could significantly address the country's energy shortfall[4]. Pakistan's energy sector faces severe power shortages about 2.5 outages daily, lasting 13.2 hours each. Over 75% of businesses cite unreliable electricity as a major obstacle, primarily due to technical malfunctions [5]. Load shedding severely affects Pakistan's industrial sector, reducing GDP by 2-3% annually, or \$7.5 to \$11.25 billion. The textile industry, responsible for 60% of exports, loses about \$1.3 billion yearly due to power shortages, decreasing manufacturing output by 15-20%. Industries spend over \$1 billion annually on diesel for generators, with backup systems costing \$5,000 to \$100,000 each. Small and Medium Enterprises (SMEs) face revenue declines of 20-30%, with 10-15% closing or downsizing. Load shedding also results in the loss of over 400,000 jobs each year and deters \$1-2 billion in foreign investment, highlighting the urgent need for reliable energy solutions to support economic stability[6].

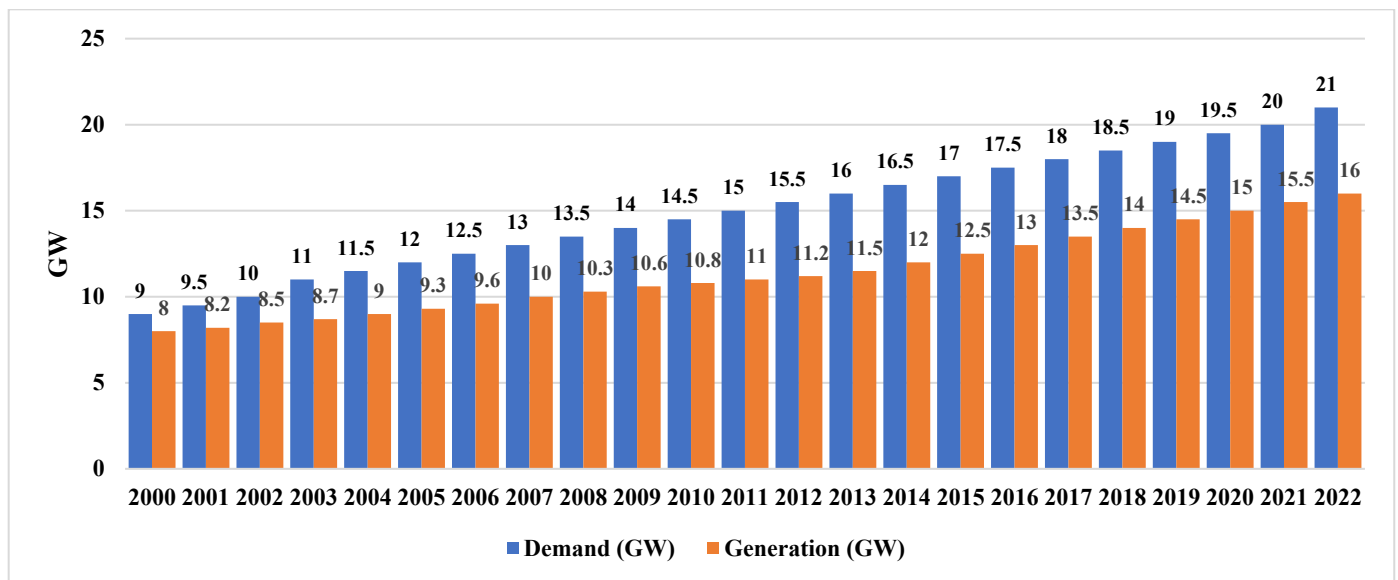


Figure 4. 1 Electricity demand and Generation of Pakistan [7].

Figure 4.1 shows the electricity demand and generation in Pakistan. In Pakistan, 24% of the population,

about 51 million people, lack reliable electricity access and often rely on expensive fossil fuels. To address this, cost-effective distributed renewable sources like PV systems are increasingly used to power these remote areas [8]. A standalone PV system for rural homes offers reliable, off-grid electricity with solar panels, batteries, charge controllers, and inverters. Ideal for remote areas, it provides a sustainable, cost-effective alternative to fossil fuels, powering appliances and lighting [9].

There's growing interest in smart homes with interconnected devices for remote control. Users can monitor and manage lighting, climate, entertainment, and appliances via smartphone from anywhere. IoT energy monitoring devices offer remote control and data transmission over the Internet [10]. SCADA (Supervisory Control and Data Acquisition) technology retrieves data from remote facilities and administers limited control commands [11] which integrates sensors, actuators, and software like Human Machine Interface (HMI) for data collection, networked communication, display, and monitoring/control. It uses Remote Terminal Units (RTUs) such as microcontrollers and Master Terminal Units (MTUs) like Arduino IoT Cloud, alongside communication networks [12]. SCADA systems are typically categorized as proprietary or open source. Proprietary systems use components from a single manufacturer, which can limit flexibility and pose vulnerabilities if the supplier fails [13].

The Internet of Things (IoT) connects physical entities via sensors and software for online data exchange. Originating from the RFID community, IoT has expanded with advances in communication and cloud computing. Billions of devices, from household items to industrial machinery, communicate over IP networks, enabling real-time monitoring, enhanced security, and intelligent decision-making [14]. It supports real-time identification, location tracking, monitoring, and event automation[15]. The IoT platform integrates smart sensors, PLCs, actuators, and IEDs from industrial control systems (ICS) and SCADA networks [16]. Home PV systems utilize IoT for real-time monitoring of voltage, current levels, and safety via sensors, enhancing energy production and usage. Wireless data transmission facilitates analysis to optimize solar capture and efficient battery storage management through automated controls and intelligent algorithms [17]. This proactive approach allows for timely interventions such as maintenance or

adjustments to optimize performance and minimize disruptions [18]. Remote access via smartphone apps or web interfaces enables homeowners to manage PV systems from anywhere with internet access, enhancing convenience and facilitating informed decisions on energy usage, troubleshooting, and cost-effectiveness optimization. Communication protocols are crucial in heterogeneous systems, providing a standardized framework for device interaction. Key protocols for machine-to-machine (M2M) communication and IoT systems include MQTT, AMQP, HTTP, and CoAP [19] and TCP/IP-based framework to connect devices to designated applications, enabling data transfer over networks like the Internet, Intranet, WiFi, WiMax, and LTE to control centers for processing and management [20]. Figure 4.2 depicts the SCADA system structure and layers scheme of SCADA.

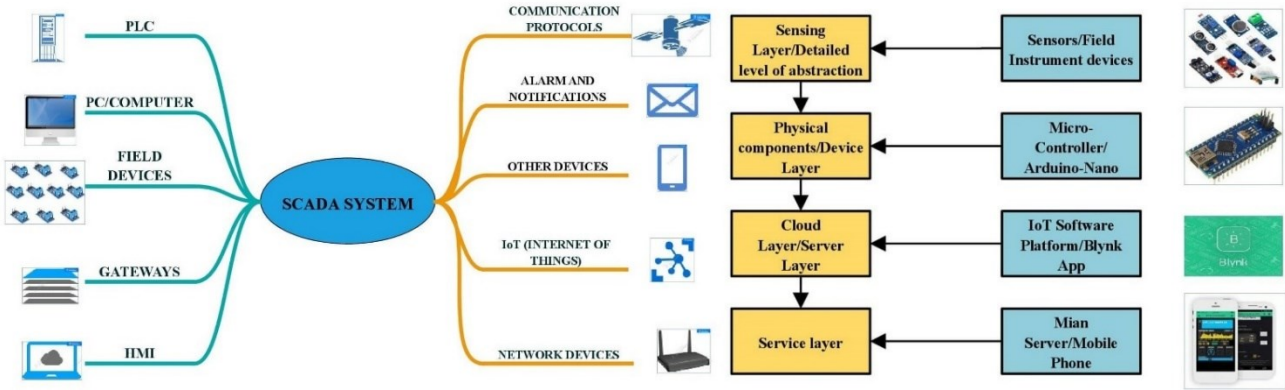


Figure 4. 2 (a)Structure of SCADA System. (b) Layer Scheme of SCAD system.

Given the escalating environmental impact of greenhouse gas (GHG) emissions from fossil fuels, evidenced by events like floods and climate change, the development of a Hybrid Power System (HPS) for rural communities in Pakistan focuses on integrating renewable energy sources, particularly solar power, with conventional generators. This aims to reduce GHG emissions while enhancing energy accessibility in rural areas. The HPS includes components such as a Buck converter (DC-DC), Maximum Power Point Tracking (MPPT), LCL Filter, and DC-AC inverter. Advanced software tools like PVsyst and HOMER Pro are used for system sizing, evaluating energy usage patterns, and optimization under site-specific conditions. Dynamic modeling in MATLAB/Simulink and hardware-in-the-loop (HIL) validation assesses the system's performance in response to changes in solar irradiance and temperature, ensuring operational efficiency and reliability. An open-source SCADA system utilizing the Blynk app enables real-

time monitoring, local data storage, and integration with GSM and Wi-Fi networks.

The paper is outlined in the following sequence, A literature review and proposed system comparison are presented in section 2, an overview of the system is in section 3 and the components used are discussed in section 4, the implementation method and the presentation of experimental setup/hardware and results are detailed in section 5, the analysis in section 6, and the conclusion is provided in section 7.

## 4.2 Literature Review and Proposed System Comparison

A considerable amount of work has been carried out in the field of IoT-based SCADA systems for its improvement in terms of communication and data transfer. Table 4.1 shows a brief overview of the work previously done during recent years in the field of IoT SCADA.

Table 4. 1 An overview of prior work in the field of IoT SCADA.

Ref./Year	Methodology
[12] 2021	A grid-independent IoT SCADA system at a BTS site uses ESP32 and Arduino IoT Cloud for monitoring current, voltage, temperature, and humidity data over Wi-Fi.
[21] 2022	An economical SCADA system for a PV plant using Arduino, Raspberry Pi, sensors, serial cables, and an open-source web interface on Debian OS via Emoncms, processing and displaying data.
[22] 2022	An ESP32 microcontroller as the RTU and the Cayenne IoT platform with MQTT protocol enabled efficient wireless data transfer, power allocation, and detailed performance insights.
[23] 2022	An open-source SCADA system for solar-powered reverse osmosis uses FIDs, RTU, and MTU with Node-Red on Grafana.
[24] 2023	An affordable IoT-based SCADA system monitors offshore aquaculture HPS using sensors, Arduino Leonardo RTU, and LoRa gateway.
[25] 2023	A cost-effective IoT monitoring system was developed for an off-grid PV system in Algeria's Sahara region, supporting a small greenhouse farm.
[26] 2024	With three voltage and three current sensors, the system uses an ESP32-E to transmit data to a Banana Pi M4 via MQTT, while Node-RED on the BPI-M4.

Throughout this research, an extensive review of existing literature in the field of IoT-based SCADA systems has been conducted. Despite this thorough examination, it has been determined that no low-cost, low-powered SCADA system has been developed or identified that incorporates both GSM and Wi-Fi

communication, utilizes TCP/IP and HTTP protocols, and provides monitoring and control of a photovoltaic (PV) system via the Blynk app and web dashboard. Furthermore, this system aims to be open source, making it accessible for widespread adoption and customization. Table 4.2 presents a detailed comparison of the proposed SCADA system with previous work, highlighting its unique combination of features and capabilities not found in other systems.

Table 4. 2 A detailed comparison of the proposed SCADA system with previous work.

Proposed SCADA System		[12]	[21]	[22]	[23]	[24]	[25]	[26]
SCADA Platform	Blynk	Things Speak	Emoncms's	Grafana, Node Red	Cayenne Server	Grafana, AWS	Locally Developed	Node-Red
Open Source	✓	✓	✓	✓	✓	✓	✓	✓
Power Consumption (W)	3.462	Not Mentioned	32.31	Not Mentioned	Not Mentioned	Not Mentioned	13.5	3.19
Cost (\$)	35.52	88.34	761.72	N.A	N.A	N.A	107.77	94.5
Comm. Protocol	HTTP, TCP/IP	MQTT	MQTT, HP	MQTT	MQTT	LORA, QTT	MQTT	MQTT
Control	✓	X	X	✓	X	X	✓	✓
Delay(ms)	50~300	50~300	50~500	50~500	50~500	50~100	160~180	50~500
GSM	✓	X	X	X	X	X	X	X
Wi-Fi	✓	✓	✓	✓	✓	✓	✓	✓
Micro-Controller	Arduino Nano, ESP-32, GSM SIM800L	ESP-32	Arduino Mega 2586	Arduino Mega 2560	ESP-32	Arduino Leonardo	ESP-8266	ESP-32

The proposed SCADA system, developed as part of this research, introduces a novel approach with several distinctive features:

**I.System Architecture:** The proposed SCADA system employs an Arduino Nano as the RTU, utilizing voltage and current sensors as Field Instruments (FIDs), and GSM SIM800L, ESP-32 works to extend the RTU communication.

**II.Utilization of Open Source Platforms:** The system offers thorough monitoring of essential photovoltaic (PV) parameters and enables remote control of electrical loads to optimize energy usage. Open-source SCADA platforms, such as the Blynk app and console, exemplify this capability. Through remote access via smartphone applications or web interfaces, users can achieve real-time data access and system management, thereby enhancing user engagement and operational efficiency.

**III.Data Transfer Mechanism:** Data transfer in the SCADA system uses an Arduino Nano communicating with GSM SIM800L and ESP-32 via UART. TCP/IP and HTTP protocols ensure secure, reliable, and encrypted data transfer from RTU to MTU (Blynk), guaranteeing robust and seamless integration with web infrastructure.

**IV.Low Cost and Low Powered:** The developed SCADA system is designed to be low-cost, with a total expense of CAD 35.52 and low power consumption of 3.462 W. This makes it an affordable solution for rural communities, promoting wider adoption and accessibility. The use of open-source platforms like Arduino IDE further enhances its accessibility and encourages community-driven innovation.

**V.Dual-Mode Communication:** Traditional SCADA systems often rely on single-mode communication and proprietary components, resulting in higher costs and lower flexibility. The system supports both GSM and Wi-Fi communication, ensuring reliable data transfer under various network conditions. This dual-mode capability enhances the flexibility and robustness of the system, making it suitable for diverse environments.

## **4.3 Site and System Description**

### **4.3.1 Site Description**

The chosen location, "Berru Bandi," is a small community of 10 houses in the rural area of Abbottabad District, around 25 km from Abbottabad city, Pakistan. Positioned on a mountain at coordinates 34°16'38" N 73°15'18" E and an elevation of 1456.79 meters above sea level, accessing this site is

difficult due to the absence of road infrastructure and basic amenities. Figure 4.3 shows an overview of the selected site from Google Maps.



Figure 4. 3 Site overview from Google Maps [27].

### 4.3.2 PV System Description

The PV system envisioned for the chosen location integrates multiple elements, such as a solar photovoltaic system, MPPT controller, battery bank, DC-DC buck converter, DC-AC inverter, LCL filter, and AC power source. This setup features both AC and DC buses for increased operational versatility and easier upkeep, ensuring uninterrupted power provision. The system is configured with a DC-AC inverter that converts the DC electricity generated by the solar panels into AC electricity for use in standard applications. A three-phase multi-level inverter is used, which offers benefits such as reduced switching losses and improved voltage waveform quality. The PV system also includes a battery bank with a maximum capacity of 201 Ah and a round-trip efficiency of 85%. The battery bank's maximum charge and discharge currents are 68.4 A and 342 A, respectively. The PV system's orientation and tilt angle are optimized using PVsyst software, with a tilt angle set at 34° to maximize energy production. This ensures maximum efficiency and minimizes loss factors associated with solar radiation incidence on the panels. The designed system has a load of 137.48



kWh/d and a peak load of 33.54 kW. To optimize performance and cost-effectiveness, the system design includes simulations conducted with HOMER Pro software. This simulation explored 982 different configurations of power sources, with the best setup incorporating solar panels, a converter, a battery bank, and a diesel genset, leading to a low net present cost (NPC) of USD 0.102 million and a cost of energy (COE) of USD 0.158.

The Maximum Power Point Tracking (MPPT) technique employed for the PV system in this study is the Incremental Conductance Algorithm (ICA). The ICA is chosen for its ability to dynamically adjust the operating voltage and current of the photovoltaic system to ensure operation at or near its Maximum Power Point (MPP). This optimization is crucial for maximizing the efficiency and power output of the PV system, especially under varying environmental conditions such as changes in solar irradiance and temperature. Unlike simpler algorithms like Perturb and Observe (P&O), the ICA evaluates both the instantaneous conductance and the incremental changes in conductance of the PV array. This allows it to more accurately track the MPP and respond effectively to rapid changes in weather conditions.

### **4.3.3 System Description**

Software and hardware components are essential and integral to the design of the proposed system, ensuring its successful and smooth operation. In this SCADA system designed for monitoring and controlling a PV system in a rural community, electrical parameters are continuously monitored by voltage and current sensors located at key points within the system. Figure 4.4 depicts the brief of the proposed SCADA system.

The proposed management and operation algorithm enhances the SCADA system for photovoltaic (PV) microgrids by integrating advanced data acquisition, processing, and control mechanisms. It is monitored by sensors, including the ZMPT101B for voltage and the ACS712 for current, as well as a relay for monitoring voltage and current at the PV panel and battery storage unit. These sensors interface with an Arduino Nano microcontroller, serving as an RTU, which processes the acquired data.

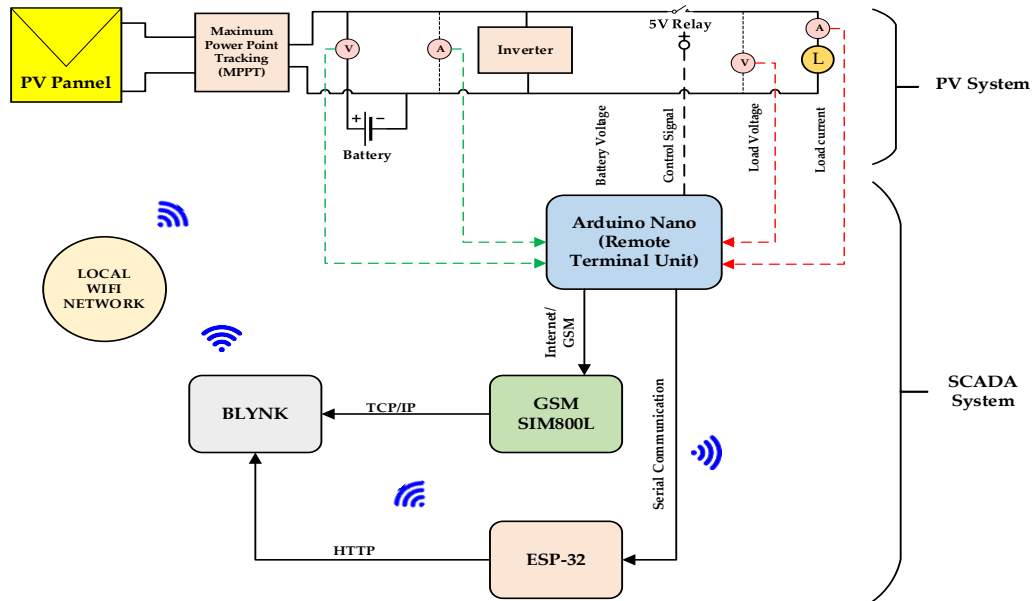


Figure 4. 4 Brief of the proposed SCADA system.

The RTU then transmits the processed data to an MTU at a central monitoring station via the SIM800L GSM module or the ESP-32. The MTU, implemented using a cloud-based server interfaced with the Blynk, aggregates and visualizes the data for real-time monitoring and control. In the absence of GSM connectivity, the ESP-32 transmits the processed data to the central monitoring unit using a Wi-Fi network through HTTP interfacing with the Blynk. At the central monitoring station, a SCADA software platform receives and processes the data, employing communication protocols such as TCP/IP over the GSM network and HTTP in the case of ESP-32 to integrate seamlessly with the Blynk app and web console. Through Blynk, users can remotely oversee and manage the PV system using their smartphones or computers visualizing real-time data. Additionally, the system offers control capabilities, allowing users to control electrical devices, and manage the operation of the PV system for optimal performance and energy efficiency. This integration supports essential functionalities, including dynamic load management and threshold alerts for critical parameters, helping to maintain system stability.

#### 4.3.4 Components used in the proposed SCADA system

This section discusses the hardware components of the proposed SCADA system. It uses an Arduino Nano as the RTU, with voltage (ZMPT101B) and current (ACS712) sensors for measuring electrical

parameters and relay for control. The SIM800L GSM module and ESP-32 facilitate remote data transmission and control, ensuring efficient SCADA system operation.

### 4.3.4.1 Arduino Nano

The microcontroller is a digital system extensively used in both household and industrial electronics. Its popularity stems from its affordability. Microcontrollers are commonly employed for control systems, signal processing, instrumentation, and a range of other applications [28]. The Arduino Nano has been selected for the SCADA system because of its compact size, cost-effectiveness, and versatile features. Its small form factor facilitates easy integration into systems with limited space, while its affordability makes it a practical choice for large-scale deployments. Compared to other microcontrollers, such as the Raspberry Pi Pico, the Arduino Nano is distinguished by its simplicity and ease of use, making it an ideal solution for developers seeking a straightforward and reliable option.

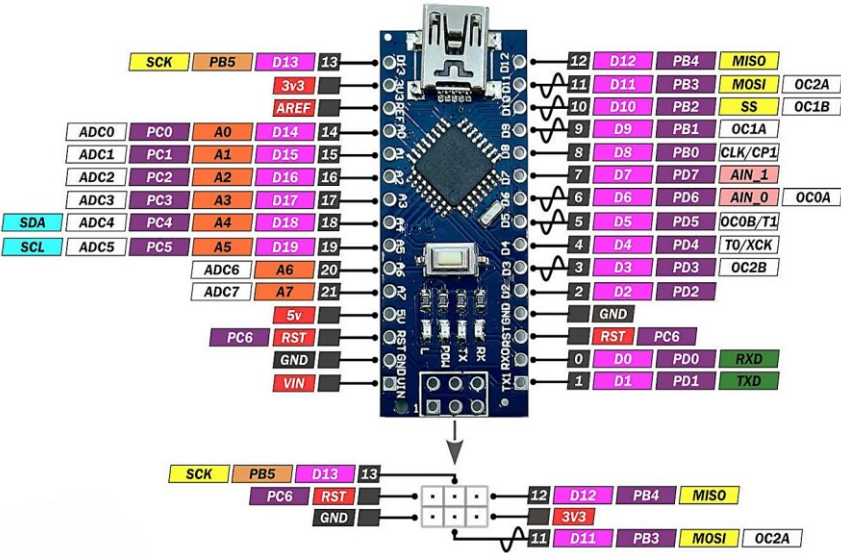


Figure 4. 5 Pin layout of Arduino nano [29].

Figure 4.5 shows the pinout diagram of Arduino Nano and Table 4.3 shows the technical specifications of the Arduino Nano.

Table 4. 3 Technical specifications of Arduino Nano.

Specifications	Details
Microcontroller	ATmega328P
Operating Voltage & clock speed	5V & 16 MHz
Input Voltage	7-12 V
Digital I/O pins	14 (of which 6 provided PWM)
PWM digital I/O pins	6 (D3, D5, D6,D9,D10,D11)
Analog Input pins	8 (A0 to A7)
Flash memory	32 KB of which 2 KB used by the bootloader
EPR0M	1 KB (ATmega328P)
Communication	UART,12C, SPI, Mini-USB

#### 4.3.4.2 Voltage Sensor ZMPT101B

The ZMPT101B is a high-precision voltage sensor module designed for measuring DC voltages ranging from 0 to 25V, with an analog output voltage proportional to the input, readable by an Arduino's ADC[30]. Ideal for applications such as battery level monitoring, and power supply voltage tracking, requires precise voltage measurements. Interfacing with an Arduino involves connecting the sensor's VCC to 5V, GND to ground, and the output to an analog input pin (e.g., A0). In the Arduino code, the sensor value read from the analog pin is converted to the input voltage using a calibration factor, mapping the 0-5V output to the 0-25V input range. The ZMPT101B voltage sensor is widely used for real-time monitoring in applications such as battery monitoring, power supply verification, and solar systems.

#### 4.3.4.3 Current Sensor ACS712

The ACS712 current sensor, utilizing Hall-effect technology, is essential in PV systems for precise measurement of DC and AC currents within  $\pm 5A$ ,  $\pm 20A$ , or  $\pm 30A$  ranges. It outputs 66 to 185 mV per ampere and operates on a single 5-volt supply. This sensor detects current through a conductor via a magnetic field, converted to voltage by its integrated Hall IC [31]. In conjunction with an Arduino Nano microcontroller board, the ACS712 becomes a vital component for monitoring current flow within the system. The Arduino Nano's analog input pins facilitate easy interfacing with the ACS712 sensor, enabling the reading of analog voltage output proportional to the measured current. Using Arduino programming, it converts the voltage into precise current values. These values can be displayed on LCD screens, transmitted

wirelessly for remote monitoring, or used for tasks like load balancing and fault detection in PV systems.

#### **4.3.4.4 Buck Converter LM2596**

Buck converters are DC-DC step-down switching regulators known for their high power efficiency, especially when the input voltage exceeds the desired output voltage [32]. Essential in PV systems, they adjust the output of PV modules to match load specifications [33]. The LM2596 is a popular type of buck converter IC used with charge controllers in PV systems to regulate panel voltage. The LM2596 efficiently steps down high DC voltage from PV panels to a stable level suitable for battery charging or powering loads. This is crucial for optimal battery performance and longevity, preventing overcharging and over-discharging. Adjusting its output voltage to match the charge controller and load requirements enhances system efficiency and reliability.

#### **4.3.4.5 Inverter (DC to AC)**

In a PV system, an inverter plays a key role in converting the direct current (DC) electricity generated by PV panels into alternating (AC) electricity at 220V, which is suitable for operating household appliances and devices. The process initiates with the DC electricity produced by the solar panels being supplied to the input of the inverter. Inside the inverter, electronic components such as transistors, capacitors, and diodes work together to convert the DC electricity into an AC signal using pulse-width modulation (PWM) or square-wave modulation techniques. This AC signal is then passed through a transformer to increase the voltage to the required 220V, while also ensuring isolation and safety. Finally, the output undergoes filtering and shaping to produce a clean and stable AC output, ready for use in powering lights, appliances, and other electrical devices within the household.

#### **4.3.4.6 Liquid Crystal Display**

The LCD (Liquid Crystal Display) with an I2C module is an external device used to display output on a screen[34]. In PV applications, an LCD is commonly used alongside an Arduino Nano to provide a user-

friendly interface for monitoring and controlling the system. The Arduino Nano collects data from various sensors, such as voltage and current sensors, which measure the performance and status of the PV system. This data is then processed and displayed on the LCD screen, allowing users to easily read important information such as the current output, battery charge level, and system status.

#### **4.3.4.7 Single Channel Relay 5V**

A 5V single-channel relay is an electromechanical switch used to control high-power devices with a low-voltage signal from microcontrollers like Arduino Nano or Raspberry Pi. It operates on a 5V DC supply, switching up to 250V AC or 30V DC at 10A. A microcontroller's digital signal activates its internal coil, altering the contact states to control components such as motors, lights, and household appliances [35]. Featuring Normally Open (NO) and Normally Closed (NC) contacts, it provides flexibility in managing various loads. A 5V single-channel relay, when integrated with an Arduino Nano, provides intelligent control and automation for PV systems, enhancing overall performance and reliability.

#### **4.3.4.8 GSM Module SIM800L**

GSM is a global standard for digital cellular communication, defining functionalities and interface requirements in networks like Base Station Systems (BSS), Switching Systems (SS), and Operation and Support Systems (OSS) [36]. The SIM800L module enables data communication over GPRS in Machine-to-Machine (M2M) systems [37], supporting voice calls, SMS, and GPRS on GSM frequencies (850/900/1800/1900 MHz). It communicates with microcontrollers via UART. To interface with an Arduino Nano, connect SIM800L's VCC to 5V, GND to ground, TX to Arduino RX, and RX to Arduino tx.

### 4.3.4.9 ESP-32 System on Chip (SOC) Microcontroller

The ESP-32, developed by Espressif Systems, is a versatile, low-cost System-On-Chip (SOC) microcontroller known for its integrated Wi-Fi and dual-mode Bluetooth capabilities. Launched in 2016 as a successor to the ESP8266, it features a dual-core Tensilica Xtensa LX6 microprocessor, clock speeds up to 240 MHz, and advanced power management with various sleep modes, making it ideal for energy-efficient IoT applications. Figure 4.6 shows the pinout of the ESP-32 and Table 4 shows the technical details of the ESP-32.

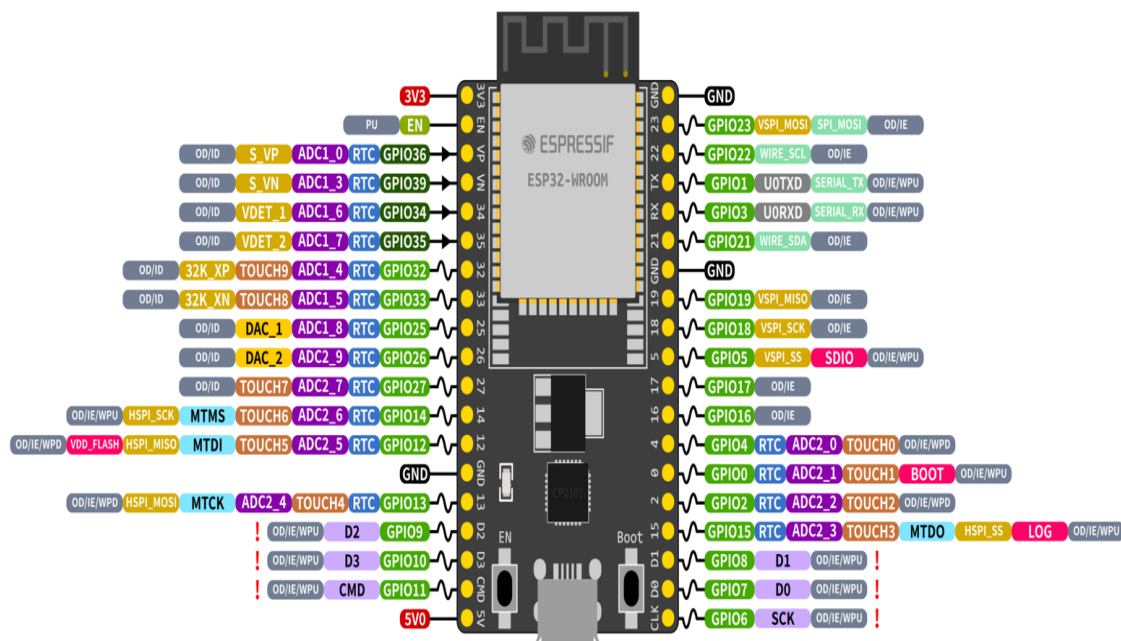


Figure 4. 6 Pin layout of the ESP32 [38].

Table 4. 4 Technical specifications of the ESP-32.

Specifications	Details
Processor	Xtensa dual-core 32-bit LX6, up to 240 MHz
Wi-Fi	IEEE 802.11 b/g/n, 2.4 GHz
Supply Voltage	3.3 Volts
GPIO Pins	34 GPIO pins
Analog Channels	18 channels (12-bit SAR ADCs)
Digital to Analog	2 channels (8-bit DACs)
Communication Interfaces	SPI, I2C, I2S, UART, CAN, PWM, ADC, DAC

The ESP-32 is widely used in home automation, wearable electronics, industrial automation, and smart energy devices, and can be programmed using multiple development frameworks like Arduino, Micro Python, and ESP-IDF, making it a favored option for both hobbyists and professional developers[39].

## 4.4 Implementation Approach

To implement the proposed SCADA system, the following strategy was employed. The designed system followed two approaches:

1. The IoT system has been developed using an Arduino with a GSM module SIM800L interfaced with the Blynk app.
2. The IoT system has been developed using an Arduino serially interfaced with an ESP-32, utilizing the Blynk console.

The process starts with creating a circuit diagram using EasyEDA software, incorporating components like Arduino Nano, GSM SIM800L, ESP-32, current and voltage sensors, relay, buck converters, and LCD. Components are then soldered onto the PCB. Next, the Blynk app, an open-source SCADA design system, is configured. Arduino code is developed to manage SCADA system parameters, uploaded via Arduino IDE 1.8.19, and verified using the serial monitor. Hardware testing follows to enable live data monitoring from FIDs and control of electrical loads using the IoT Blynk app and Blynk console Web dashboard. Figure 4.7 shows the flow chart of the system's working.



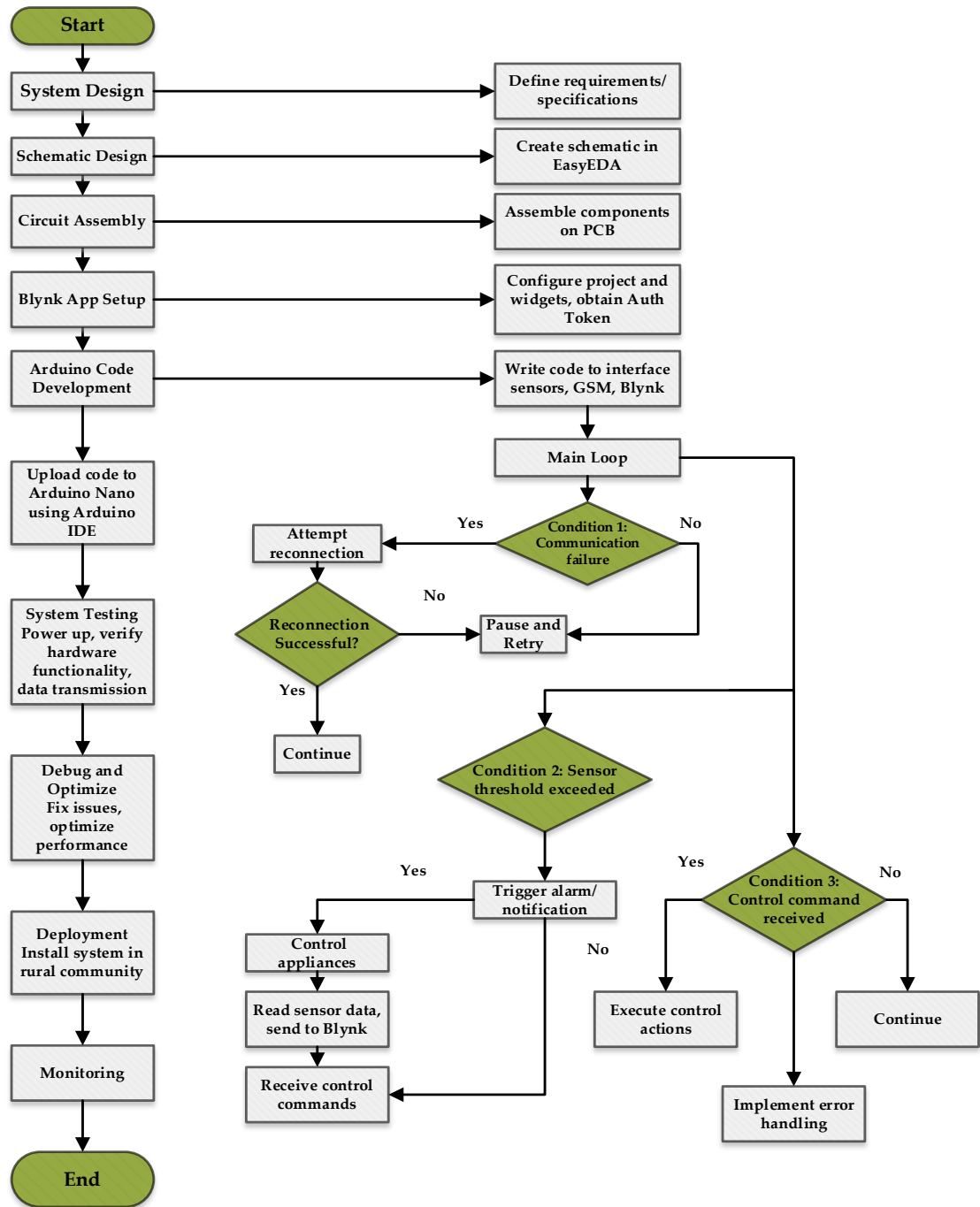


Figure 4. 7 Flow chart of SCADA System Working.

## 4.5 SCADA-based PV System Design Using Arduino Nano and GSM SIM800L

### 4.5.1 Schematic Design

The schematic design of the SCADA System has been implemented on EasyEDA (Electronic Design

Automation). EasyEDA is an online tool that facilitates the design, simulation, and creation of schematics and printed circuit boards (PCBs)[40].

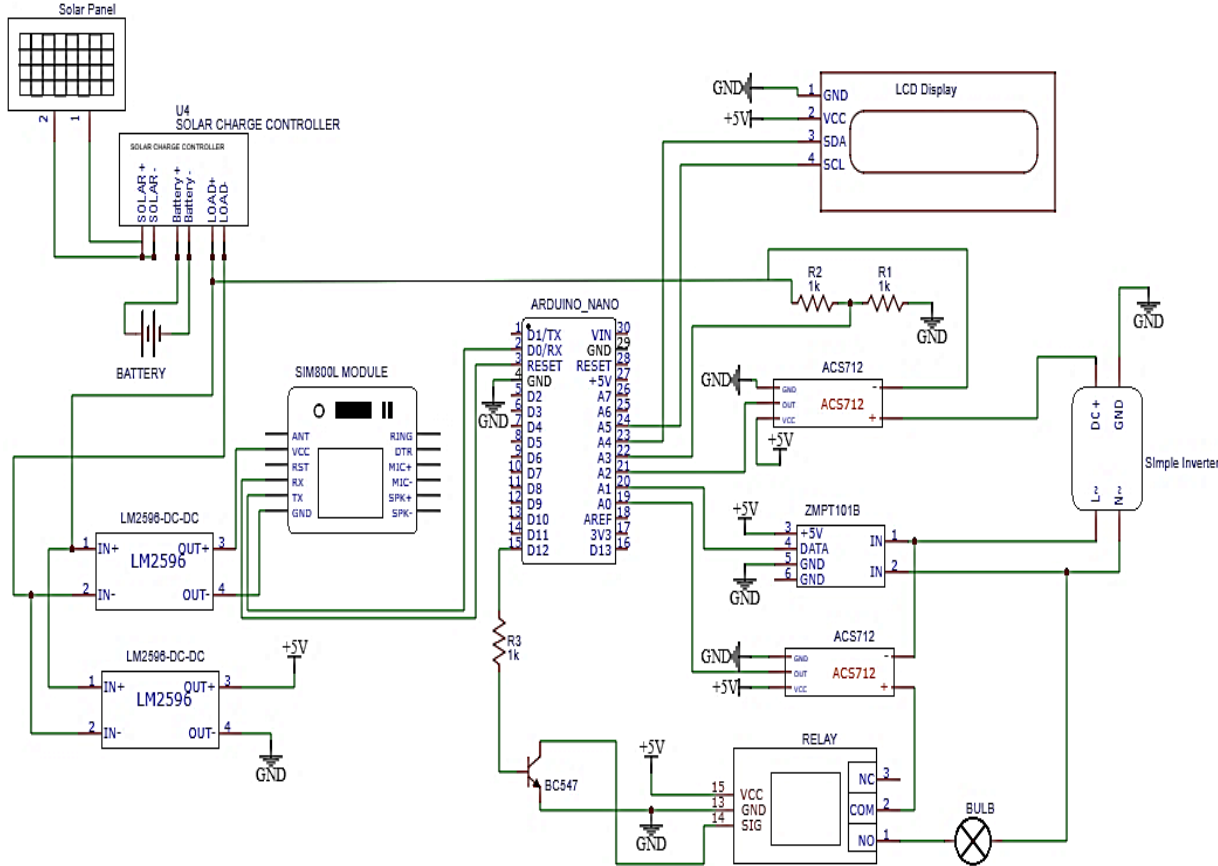


Figure 4. 8 Circuit Diagram of proposed SCADA system using Arduino Nano and GSM Sim800L.

The platform includes an extensive component library, allowing users to access a wide variety of electronic parts and symbols. Figure 4.8 shows the schematic diagram of the proposed SCADA system using Arduino Nano and GSM SIM800L. The solar panel is interfaced with a solar charge controller, which in turn is connected to a 12-volt, 5-ampere battery. The output from the charge controller is directed to two LM2596 buck converters, tasked with stepping down the higher voltage from the PV panel to a stable lower voltage (from 12V to 5V). Table 4.5 shows the connections of FIDs to the RTU.

Table 4. 5 FIDs connections with Arduino Nano and GSM SIM800L

Component #	Description	Ana- log/Digital	Arduino Nano Pin#
1	GSM SIM800L	Digital	2,3
2	PV Voltage	Analog	22
3	LCD Display	Analog	23,24
4	ACS 712 Current sensors	Analog	21,19
5	ZMPT101B	Analog	20
6	5V Relay	Digital	15

Furthermore, a basic inverter is integrated to convert DC to AC, essential for the site's location in Pakistan, where the standard operating voltage is 220V AC. A 5V relay is connected to an Arduino through a transistor and resistor, along with a load to switch on and off as needed. The Arduino operates on a 5-volt power supply, with all necessary sensors connected to it. To implement the design in EasyEDA, the project is initiated in the schematic editor. Subsequently, electronic components including the Arduino Nano, ZMPT101B voltage sensor, ACS712 current sensor, resistors, SIM800L GSM module, 5V relay, and buck converter are selected from the extensive library and placed accordingly. Following component placement, connections are established between them using the wiring tool.

## 4.5.2 Blynk App Setup

Blynk is a versatile IoT platform enabling users to create custom mobile apps for remote hardware monitoring and control. It supports a wide range of microcontrollers including Arduino, Raspberry Pi, ESP32, and others. With Blynk, users can easily design graphical interfaces using a drag-and-drop interface on smartphones or tablets. These interfaces communicate with connected hardware via the Blynk Cloud, enabling real-time data exchange and control. Figure 4.9 depicts the Blynk app setup with Arduino Nano and GSM SIM800L. Integrating Blynk enhances PV system functionality and user experience by aggregating sensor data on solar panel output and battery status. Data is transmitted to the Blynk app via Wi-Fi or GSM, enabling real-time visualization and control of components via smartphones or tablets.

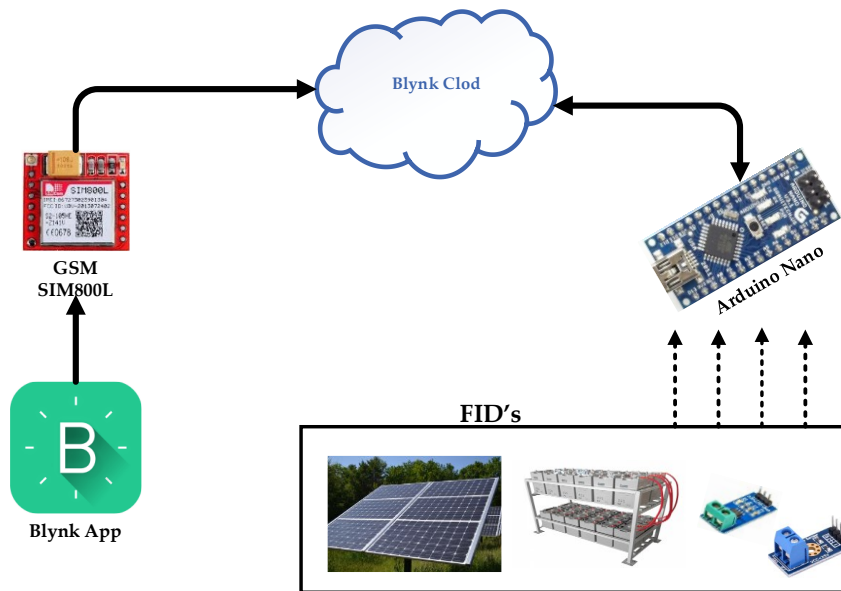


Figure 4. 9 Blynk App setup using Arduino Nano and GSM SIM800L.

### 4.5.3 Arduino Code Development

The Arduino IDE allows programming in Sketch, a C-based language. Arduino microcontrollers feature a Bootloader for communication with the Arduino compiler during development [41]. The free, open-source Arduino IDE runs on Java and works on Mac, Windows, and Linux. Supporting C and C++, it simplifies program uploads and communication with Arduino hardware [42]. To write and upload a program, launch the IDE and create a new sketch. Code is written using the Arduino programming language, derived from C/C++, which simplifies development with built-in functions and libraries.

It initializes a SoftwareSerial interface (gsm) for communication with the SIM800 modem and an LCD for local display and Blynk authentication details are defined for connection to the Blynk cloud server. Sensors for AC and DC voltage and current readings are interfaced using analog inputs (ACvolpin, AC-curpin, DCvolpin, DCcurpin). Data is transmitted to Blynk using `Blynk.virtualWrite()` in the `blynkupdate()` function for real-time monitoring on the Blynk mobile app. Additionally, the system allows remote control of a relay connected to a relay pin through Blynk app commands (V4), enabling remote switching of connected devices. After writing the code, verify it by clicking the checkmark icon to detect syntax errors. Plug the Arduino Nano into the computer using a USB cable, and select the "Arduino

Nano" board and the appropriate COM port from the "Tools" menu.

---

---

### **GSM, Voltage and Current Sensor Data Reading Algorithm**

---

---

#### **1. Start**

1. Initialization
  - 1.1 Include necessary libraries (ZMPT101B, Tiny Gsm Client, Blynk Simple Tiny GSM, Software Serial, LiquidCrystal\_I2C), Set pin modes for sensor and relay pins.
  - 1.2 Define constants and pins (Blynk authentication token, APN settings, sensor, and relay pins).
  - 1.3 Initialize the GSM module, LCD, and modem, Set sensitivity for the voltage sensor.
2. Setup Function
  - 2.1 Begin serial communication at 9600 bps, initialize GSM and LCD, Display "Initializing GSM" on LCD, Initialize the modem, and print modem info to the serial monitor.
  - 2.2 Connect to Blynk with the provided credentials, Display "Connecting To BLYNK" on LCD.
  - 2.3 Set pin modes for AC and DC voltage/current pins and relay pins, Turn off the relay initially.
3. Main Loop (Loop Function)
  - 3.1 Run Blynk.
  - 3.2 Call function `takeDCvol` to measure DC voltage, `takeDCcur` to measure DC current.
  - 3.3 Call function `takeACvol` to measure AC voltage, `takeACcur` to measure AC current.
  - 3.4 Call function, Update LCD with the latest sensor values using `LCD update`.
4. Function: takeDCvol
  - 4.1 Read DC voltage from an analog pin, Calculate actual DC voltage
  - 4.2 Delay for 500ms.
5. Function: takeDCcur,
  - 5.1 Read DC from analog pin, calculate actual DC, Print DC to the serial monitor, Delay for 500ms.
6. Function: takeACvol
  - 6.1 Get RMS voltage from the voltage sensor, Adjust AC voltage to be within the specified range.
  - 6.2 Print AC voltage to the serial monitor, Delay for 500ms.
7. Function: takeACcur
  - 7.1 Get peak-to-peak voltage for AC using `getVPP1`, Calculate RMS voltage and current.
  - 7.2 Adjust AC to be within the specified range, Print AC to the serial monitor, Delay for 500ms.
8. Function: blynkupdate
  - 8.1 Update Blynk virtual pins with DC voltage, DC current, AC voltage, and AC current.
9. Function: LCD update
  - 9.1 Clear LCD, Display DC voltage and current on the first row,
  - 9.2 Display AC voltage and current on the second row.
10. BLYNK\_WRITE Function
  - 10.1 Check if the value from pin V4 is 1, If true, turn on the relay, Else, turn off the relay.
11. Function: getVPP1
  - 11.1 Initialize variables for reading sensor values, Start timing for sampling period (500ms).
  - 11.2 While the sampling period is not over: Read sensor value.
  - 11.3 Update max and min values if the current reading is higher or lower than the current max or min.
  - 11.4 Calculate peak-to-peak voltage. 12.5. Return peak-to-peak voltage.

---

---

#### **12. End**

Click the upload arrow icon to compile and transfer the code to the Arduino board. The IDE will compile the code, establish communication with the board, and upload the program. The above Algorithm represents the pseudocode

programmed using Arduino IDE in Arduino Nano and GSM SIM800L.

#### 4.5.4 Hardware Setup and Commissioning with Blynk App

Hardware development is essential in research involving physical systems. It enables real-world validation, prototyping, and testing, ensuring functionality and performance. In the proposed system the Hardware setup has been implemented by connecting the Charge controller, MPPT, Arduino Nano Microcontroller, FIDs, 10 Watts PV panel, and 12V DC battery. The circuit gets powered from the DC voltage produced by the PV panels that have been stored by the 12V DC battery connected through the MMPT. There is also a simple inverter that will convert the 12VDC to 220V AC.

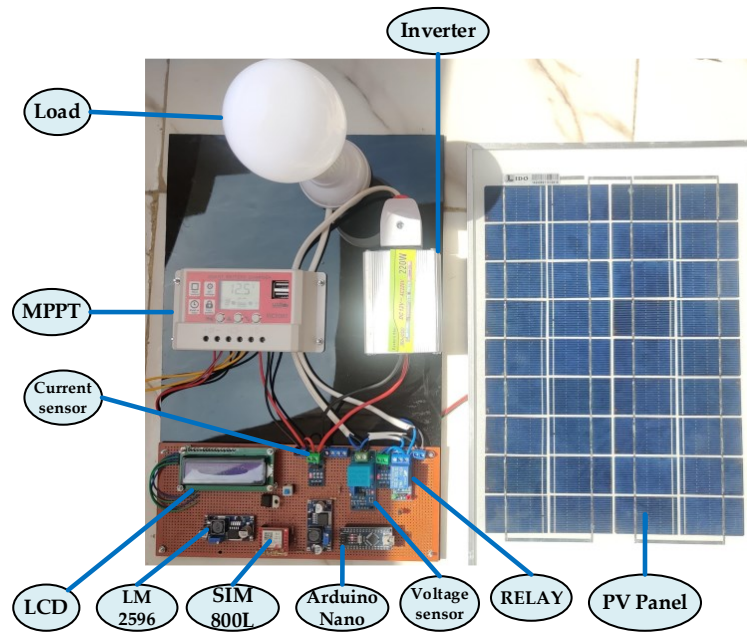


Figure 4. 10 Hardware setup using Arduino Nano and GSM SIM800L.

This setup enables the SIM800L to communicate with the Blynk app, transmitting real-time data from the PV system, including voltage and current measurements, to the Blynk cloud. Figure 4.10 shows the Hardware setup using Arduino Nano and GSM SIM800L. When no load is connected to the power source, the terminal voltage is at its maximum, 12V known as the open-circuit voltage ( $V_{oc}$ ), while the current is effectively zero due to the lack of a closed path for current flow. Upon switching on a load through the Blynk app, the voltage across the terminals drops from its open-circuit value due to the internal resistance

of the power source and the voltage drops across the load. Concurrently, the current begins to flow through the circuit, with its magnitude determined by the load's resistance and the applied voltage according to Ohm's Law. Figure 4.11 shows the display of FIDs parameters on LCD.



Figure 4. 11 Display of FIDs values on LCD.

The SIM800L module uses GSM for data communication, connecting to the internet via the cellular network using the APN credentials provided by the SIM card carrier. Communication between the micro-controller and the SIM800L is established through AT commands sent over a serial interface. Figure 4.12 shows the PV systems FID values on the Blynk App Dashboard in the “ON” and “OFF” states.



Figure 4. 12 PV system FIDs values on the Blynk App Dashboard.

Upon successful internet connection, the microcontroller firmware's Blynk library facilitates data transfer to the Blynk cloud server, utilizing the TCP/IP protocol over the GSM network for reliable transmission. The Blynk app presents real-time data of the PV system, including DC and AC voltage readings and current measurements, providing a comprehensive view of system performance. Furthermore, the Blynk app enables remote control of the load connected to the PV system. The app's interface enables live monitoring, allowing for real-time observation of electrical parameters and load status as shown in Figure 4.13.

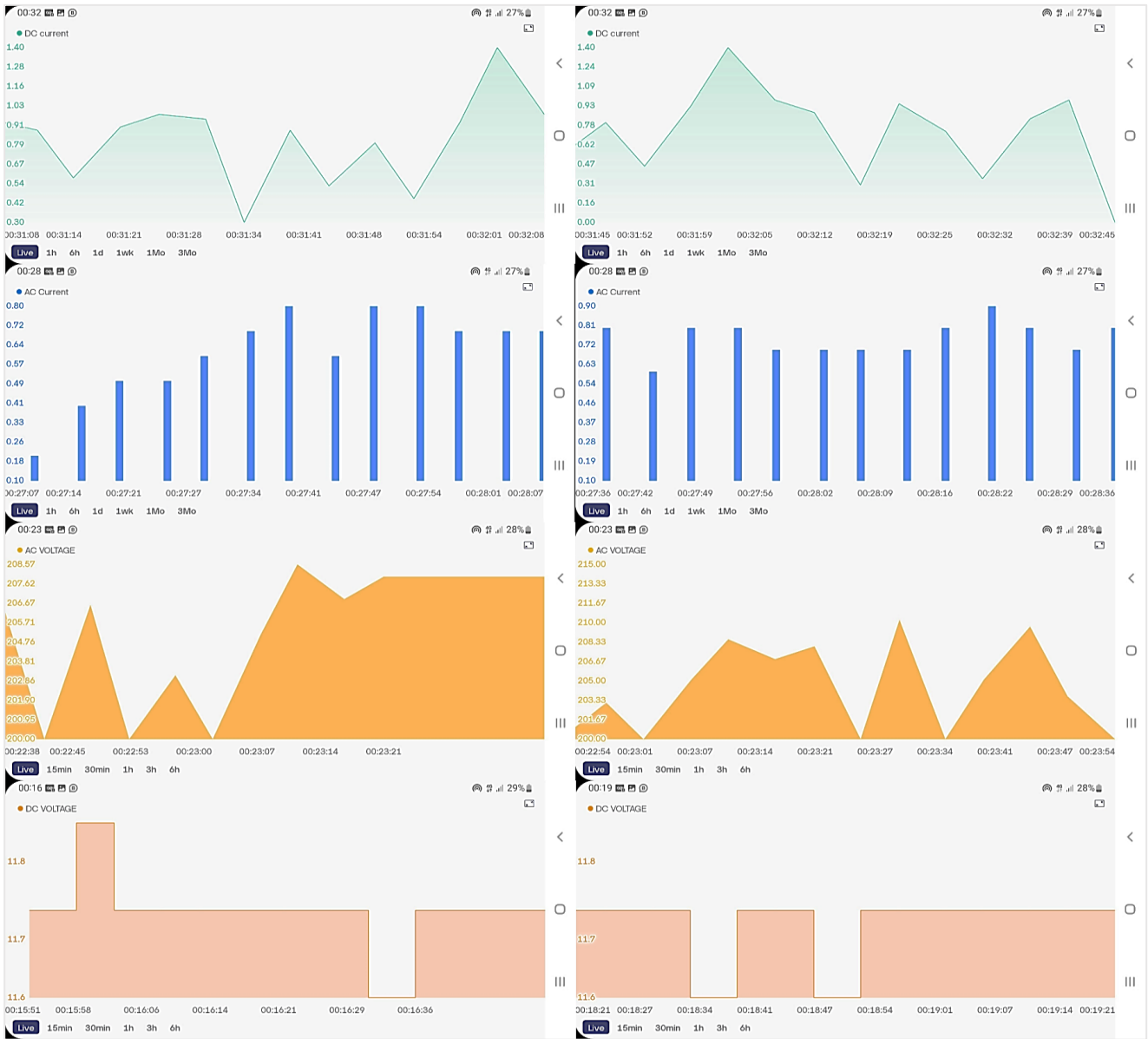


Figure 4. 13 PV system FIDs Monitoring on the Blynk App mobile interface.

The connected load is turned “ON” or “OFF” directly through the app, using virtual pins mapped to



specific digital pins on the microcontroller that control relays or switches connected to the load.

On and off the connected load, is managed by the `Serial2.write(val);` command within the `BLYNK_WRITE(V4)` function. By this function, the Arduino receives a value from the Blynk application and forwards this value to the relay for switching the load. Here's how this works in terms of controlling a load such as a relay:

- **Receiving Input from Blynk App:** The `BLYNK_WRITE(V4)` function is activated when a widget linked to virtual pin V4 in the Blynk app is interacted with, such as a button press. The state of this widget (usually 0 or 1) is then passed as a parameter to the function.
- **Load Control on the Receiving Device:** The Arduino code controls a relay by sending a digital signal at a specific voltage level. In the `setup()` function, the relay pin is configured as an output and initially set to LOW, ensuring the relay is off. In the main `loop()`, the code continuously checks for incoming data via the `SoftwareSerial` connection. When a command is received, it reads the value; if the value is 0, it sets the relay pin to LOW (0 volts), turning the relay off, and if the value is 1, it sets the relay pin to HIGH (5 volts), turning the relay on. This means the Arduino operates the relay using a digital signal of either 0 volts (to turn it off) or 5 volts (to turn it on). This control logic allows the Arduino to dynamically manage the relay's state based on external input.

## **4.6 SCADA-based PV System Design Using Arduino Nano and ESP-32**

### **4.6.1 Schematic Design**

The schematic diagram of the proposed system was generated using EasyEDA software. This diagram mirrors Figure 4.12, with the SIM800L being substituted by the ESP-32. While the circuit requires a 5V power supply, the ESP-32 operates at 3V.

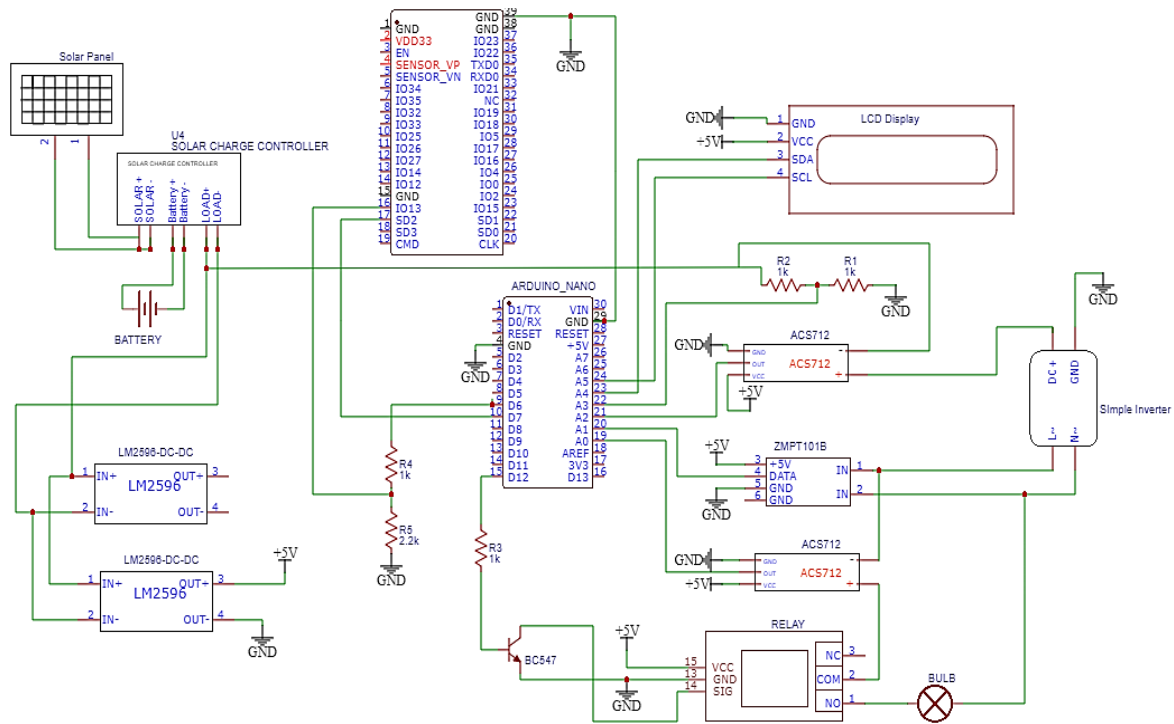


Figure 4. 14 Circuit Diagram of proposed SCADA system using Arduino Nano and ESP-32.

Hence, to provide the ESP-32 with the requisite voltage, a voltage divider comprising 1kΩ and 2kΩ resistors is employed. Figure 4.14 shows the circuit diagram of the Arduino Nano interface with ESP-32 for Wi-fi connectivity. To facilitate communication between the two microcontrollers, serial communication via UART (Universal Asynchronous Receiver-Transmitter) is utilized. UART serves as a protocol specifically designed for direct device communication, enabling data exchange through dedicated transmit (TX) and receive (RX) pins. Pin 10 of the Arduino Nano is directly connected to pin 17 of the ESP-32, while pin 9 of the Arduino Nano is linked to pin 16 of the ESP-32 via a voltage divider. Both devices are configured to operate at the same baud rate of 9600 bps for serial communication, ensuring seamless data transfer. The Arduino Nano sketch employs the serial or Software Serial library to transmit data to the ESP32, whereas the ESP32 sketch utilizes the Hardware Serial library to receive incoming data from the Arduino Nano, facilitating efficient inter-device communication.

#### 4.6.2 Arduino IDE Code Development for ESP-32

To code for the ESP-32 using the Arduino IDE 1.8.19, start by adding the ESP-32 Board Manager URL

in the IDE Preferences under "Additional Board Manager URLs." Install the ESP32 package from the Boards Manager and connect the ESP-32 to your computer via USB, selecting the appropriate COM port. Use the Library Manager to install Wi-Fi, Blynk, and HTTP Client libraries for Wi-Fi connectivity, sensor readings, and app communication. In your Arduino sketch, configure the setup function to initialize connections and settings, and use the loop function for continuous operations. This setup is tailored for a load monitoring system with an ESP32 microcontroller, integrating with the Blynk platform over Wi-Fi. The system connects to the Blynk cloud server via HTTP on port 80 using the BlynkSimpleEsp32.h library, with Wi-Fi credentials set for network access. The sketch processes JSON data received via Software Serial (Serial2), containing DC voltage (DC vol), DC (DC cur), AC voltage (AC vol), and AC (AC cur) readings. These values are displayed on the serial monitor for debugging and updated in real-time on the Blynk app using Blynk.virtualWrite() in the blynk update() function. Furthermore, the sketch handles commands from the Blynk app through virtual pin V4, enabling remote control of connected devices. This ensures accurate programming and operational functionality across diverse applications.

The Arduino code handles control commands and implements safety mechanisms through a structured approach, with robust error handling integrated into the system. During initialization, the setup function sets up serial communication, LCD display, and sensor pins, ensuring the relay starts in a safe, known state by explicitly setting it to LOW. In the main loop function, the code checks for incoming data from the ESP module using espSerial.available() and reads the data with espSerial.read(). Based on the received value (0 or 1), the relay is controlled via digitalWrite(relay, HIGH) or digitalWrite(relay, LOW), allowing for remote operation.

The error-handling mechanisms are embedded in the sensor calibration functions, such as takeDCvol(), takeDCcur(), takeACvol(), and takeACcur(). These functions read analog values from sensors and convert them to accurate voltage and current readings using calibration constants. The code includes checks for spurious readings; for example, in takeDCvol(), if the DC voltage reading is below 0.1V, it is set to 0.0V. This prevents erroneous low readings from affecting system operations. Further, error handling is

reinforced by the design of the `lcdupdate()` function, which updates the LCD display with real-time sensor values, ensuring continuous and accurate monitoring. The `senddata()` function transmits sensor data, possibly to a remote monitoring system, allowing for real-time data logging and error detection. Additionally, the initial state setting and continuous monitoring help in identifying and mitigating errors promptly, maintaining the reliability and safety of the system. These comprehensive error-handling strategies ensure that the Arduino code manages control commands effectively, maintains accurate sensor data, and prevents incorrect operations due to spurious or erroneous inputs. The complete code for the ESP-32 is available in Appendix A, providing further insight into the implementation details.

### 4.6.3 Hardware Setup

To evaluate the performance of the proposed Supervisory SCADA system using ESP-32, the experimental setup has been established within the Electrical and Computer Engineering Laboratory at Memorial University of Newfoundland and Labrador (MUN), Canada. On the rooftop of the building, twelve PV panels each generate 130 Watts with a maximum current of 7.6 Amperes. For the SCADA system implementation, two PV panels are used to evaluate performance in monitoring and controlling the electrical load.



Figure 4. 15 PV Panels installation at the rooftop of the ECE building.

The system also includes Maximum Power Point Tracking (MPPT) and a battery bank of six 12V, 25A lead-acid batteries to enhance operational efficiency and effectiveness. Figure 4.15 illustrates the

installation of the PV panels on the rooftop of the ECE building at MUN and Figure 4.16 shows the Hardware setup in the ECE Lab. The battery is connected to the circuit's input to power the entire system. A multimeter is attached to verify the voltage supply to the circuit. The GSM SIM800L has been removed from the circuitry and ESP-32 has been installed in the circuit using a voltage divider. The Arduino Nano acts as the main controller interfacing with the FIDs and relays while ESP-32 will provide the Wi-Fi connectivity for remote monitoring and control via the Blynk app. In the case when there is no load “OFF” then the DC voltage is 13V, DC 0A, AC Voltage 220V, and AC is 0.1A as shown in Figure 4.17.

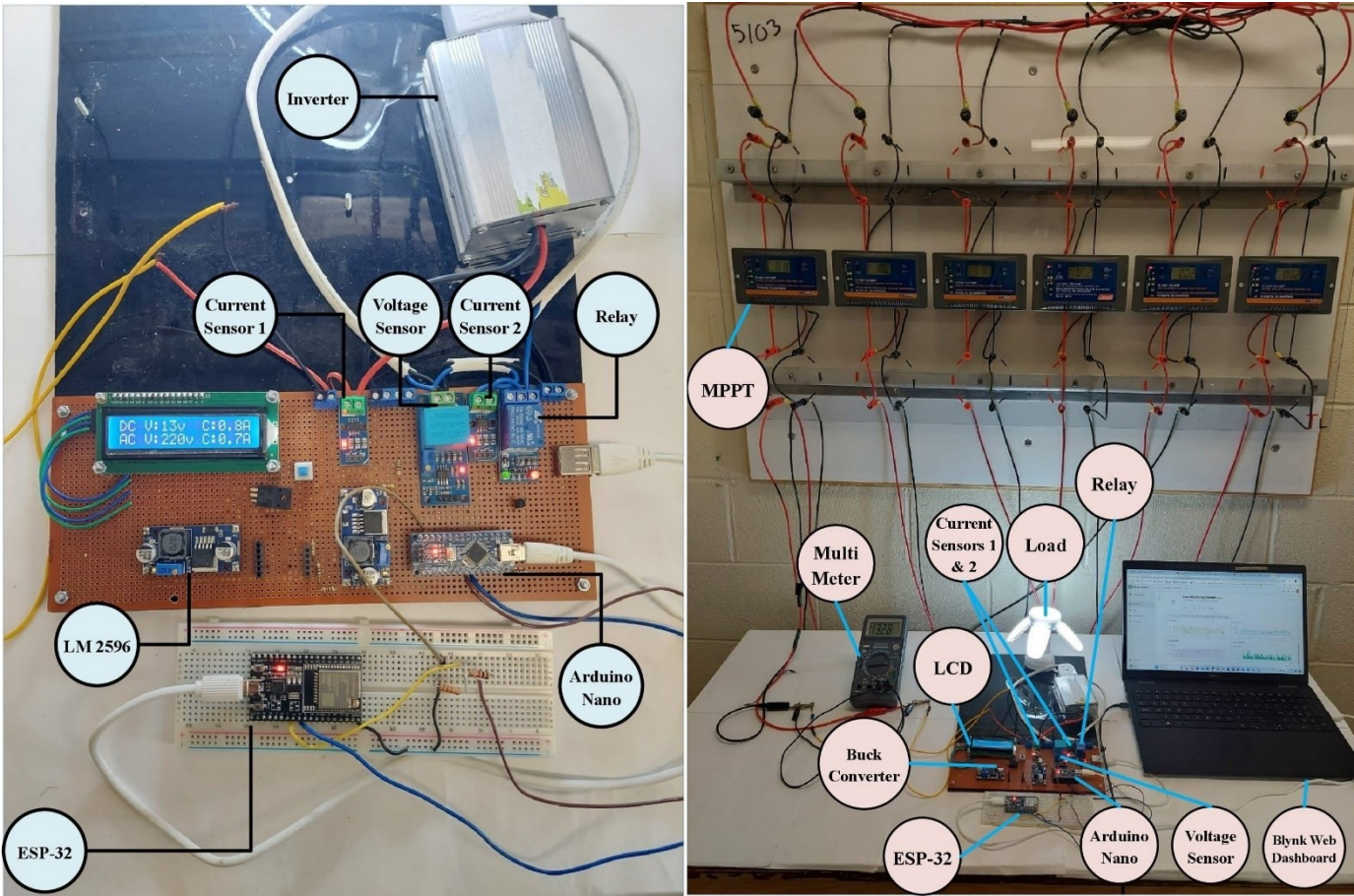


Figure 4. 16 Experimental setup at MUN ECE Building.



Figure 4. 17 FIDs parameters on the LCD in the “OFF”.

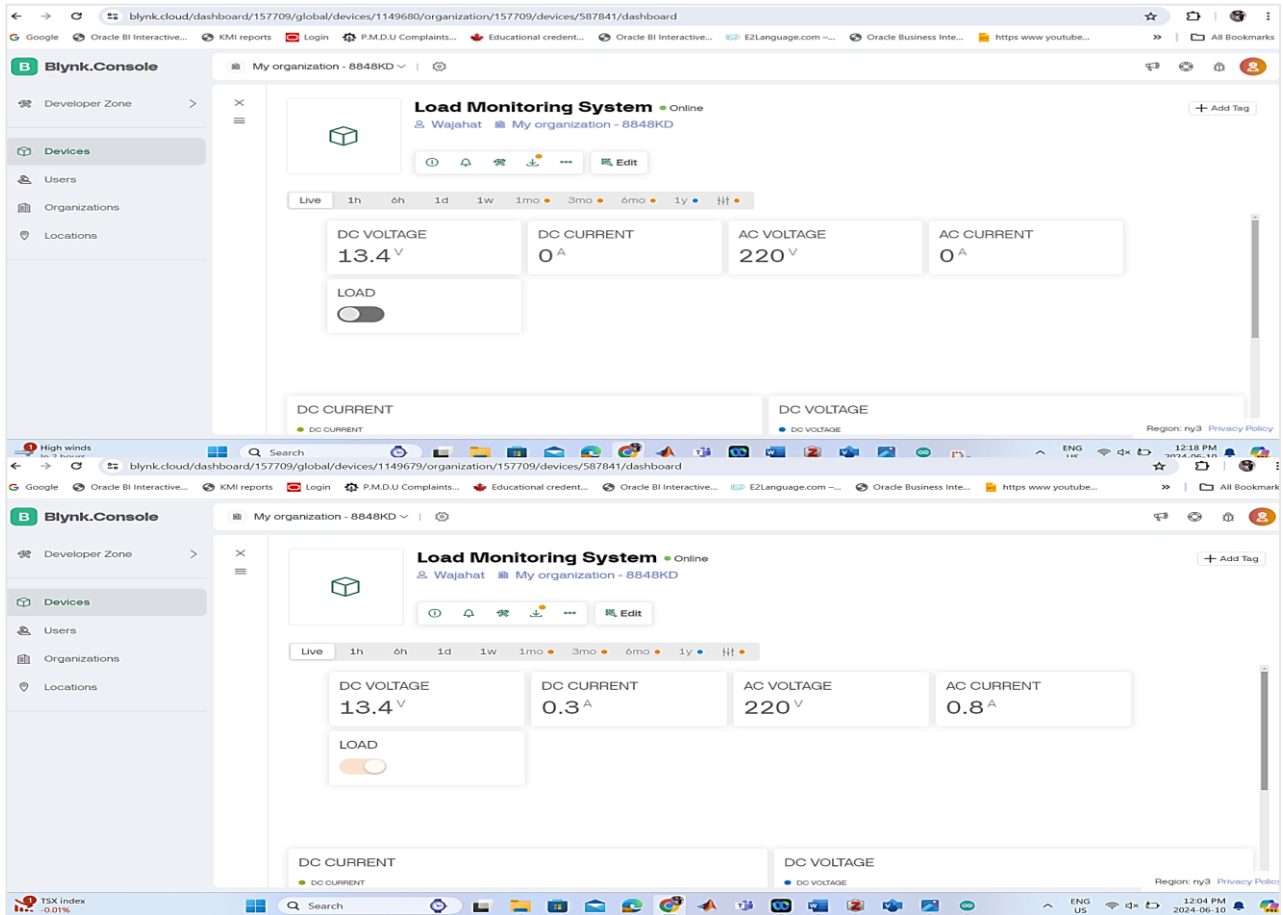


Figure 4. 18 The status of the Blynk web dashboard interface in the “OFF” and “ON” states.

As soon as the load is “ON” by the Web-Interface of the Blynk, the current starts flowing through the circuit and there is a drop of the voltage at the Load side. Figure 4.18 shows the status of the Blynk console. The LCDs FIDs values of DC voltage are 13V, DC 1.3A, AC Voltage 217V, and AC 0.5A. The voltage and current sensors measure the data and transmit it to the analog pins of the Arduino Nano which processes these analog signals to determine the actual voltage and current values using the necessary conversion factors. Based on this data, the Arduino Nano controls load switching through a 5V relay. The processed data is then transmitted to the ESP-32 via a UART interface, with data packets sent at a baud rate of 9600 bps between the two microcontrollers. The ESP-32 receives the data from the Arduino Nano, processes it, and prepares it for transmission over the Wi-Fi network. Communication with the Blynk cloud server is established using HTTP protocols, enabling the ESP-32 to send FIDs data to the Blynk server, which updates the user interface on the Blynk console in real-time. Control commands such as "ON" and "OFF" from the Blynk console are sent to the ESP-32, which then relays the commands to the Arduino Nano via the serial interface. The Blynk console displays real-time

voltage and current readings of the PV panels, load, and battery, facilitating monitoring and control of the PV system and identifying anomalies. Figure 4.19 shows the live monitoring and Control of PV data on Blynk Console.

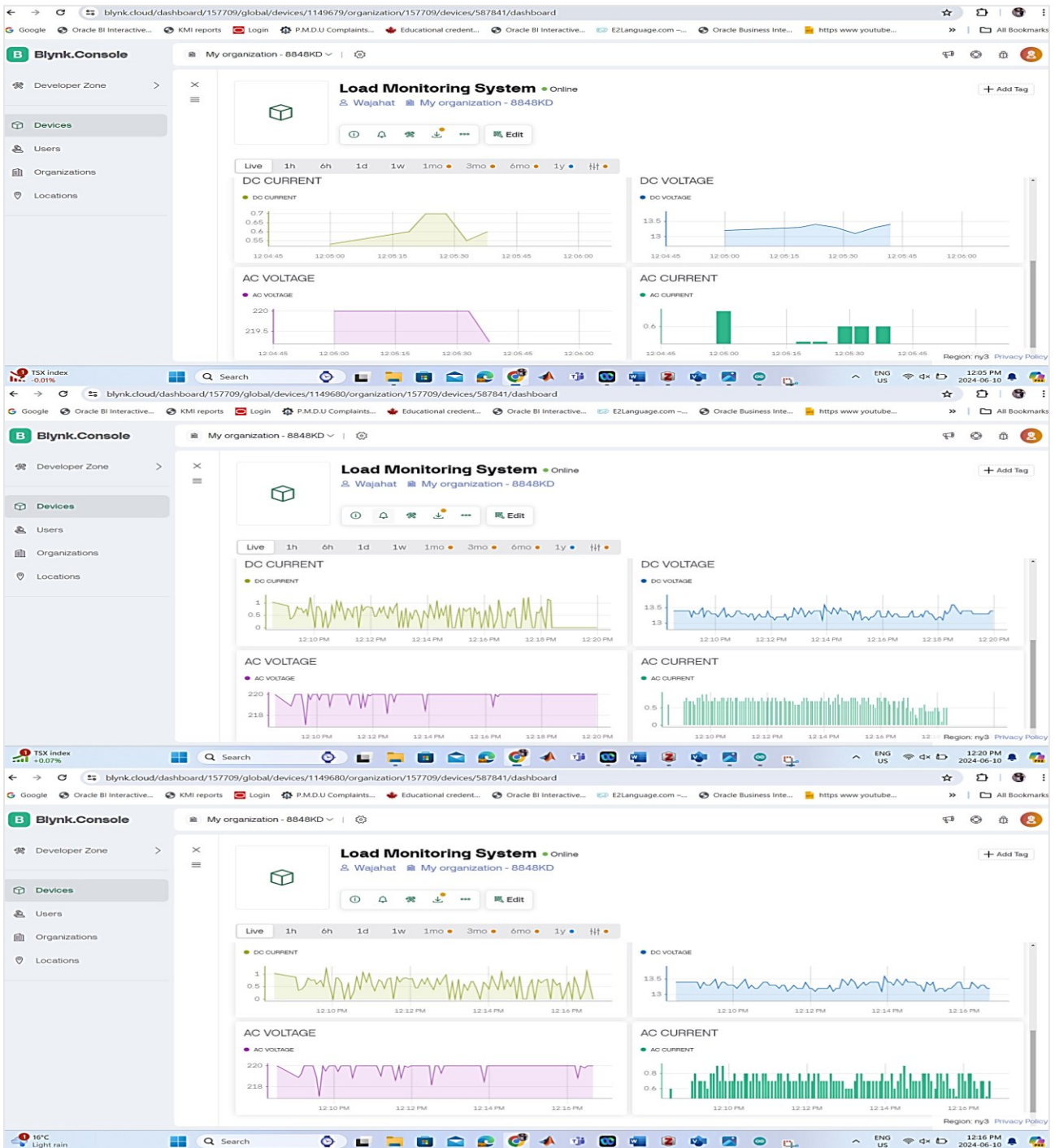


Figure 4. 19 Monitoring and Control of PV system on Blynk Console Dashboard using ESP-32 and Arduino Nano.

The system was tested during a time of day when sunlight exposure was minimal, specifically in the evening, as shown in the attached figure. As the sunlight began to diminish, noticeable fluctuations in the

DC voltage were observed, starting at approximately 6:58 PM. These fluctuations caused the DC voltage to drop from an initial value of 11 V to 10.8 V, and this downward trend continued as the light exposure further decreased. Figure 4.20 illustrates the system's performance under these reduced sunlight conditions.

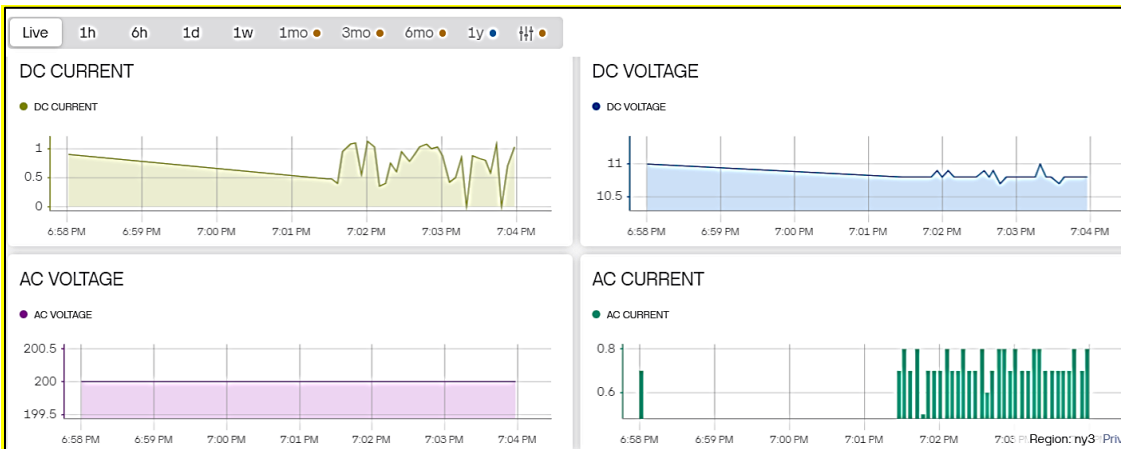


Figure 4. 20 PV system parameters under reduced sunlight.

This reduction in DC voltage directly impacted the DC current, which also began to exhibit abrupt fluctuations. The graph clearly shows a correlation between the decrease in DC voltage and the instability of the DC current. As the voltage continued to drop, the current became increasingly erratic, reflecting the instability in the power generation due to the reduced sunlight.

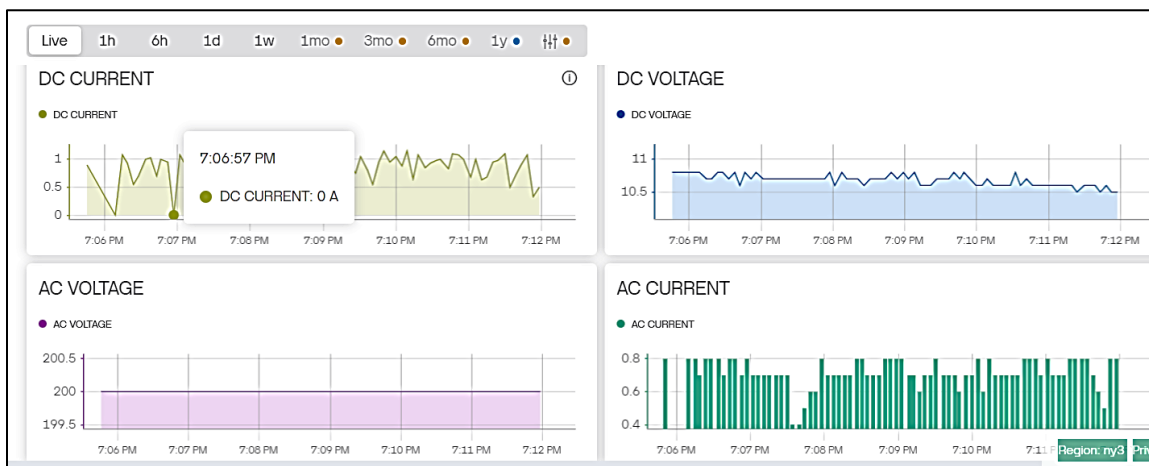


Figure 4. 21 Status of DC Voltage and DC current.



Figure 4.21 shows the status of voltages and currents as a result of low PV exposure. These observations underline the sensitivity of the PV system to changes in environmental conditions, such as varying sunlight intensity. The fluctuations in both DC voltage and current demonstrate the dynamic nature of the system's performance under less-than-optimal lighting conditions, providing valuable insights into how the system behaves in real-world scenarios.

#### **4.6.4 Notification of PV system parameters**

The designed system is fully capable of notifying users about the PV system parameters both through SMS notifications and via visual inspection using an LCD installed in the circuit. The LCD provides a real-time display of critical parameters, including DC and AC voltage, as well as DC and AC current. Any malfunction or abnormal behavior in the system is immediately displayed, enabling the user to identify and rectify faults promptly. In addition to on-site monitoring, the system also supports remote notification via SMS, ensuring that users can stay informed about system performance even when they are away. This functionality is enabled through the integration of the Twilio platform, an open-source cloud communications service. Twilio's robust Application Program Interface (API) allows seamless integration of messaging, voice, and video capabilities into applications. Specifically, within this SCADA system, Twilio's SMS API is utilized to send real-time alerts regarding system status, faults, or operational changes directly to the user's mobile phone, ensuring timely awareness and response. By incorporating Twilio's services, the system significantly enhances its monitoring and communication capabilities, facilitating more responsive and efficient management of the PV system's operational environment. Figure 4.22 shows the notification of system parameters via SMS under testing conditions. The `sendTwilioMessage()` function is designed to transmit an SMS containing critical electrical measurements—such as AC and DC voltage and current readings—to a specified phone number via the Twilio API. Initially, the function verifies the presence of an active WiFi connection; if WiFi is not connected, it exits and notifies the user via the serial monitor.

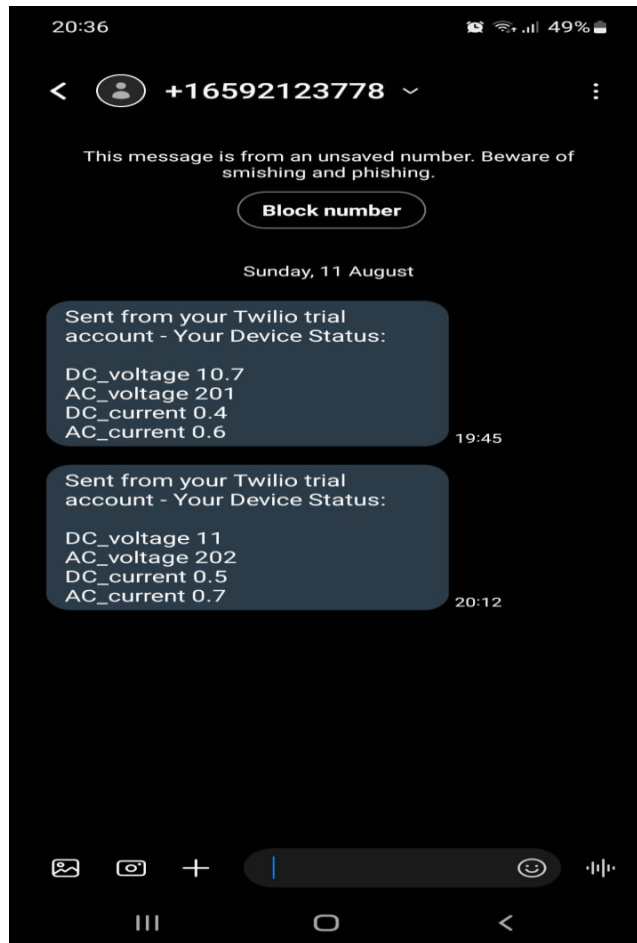
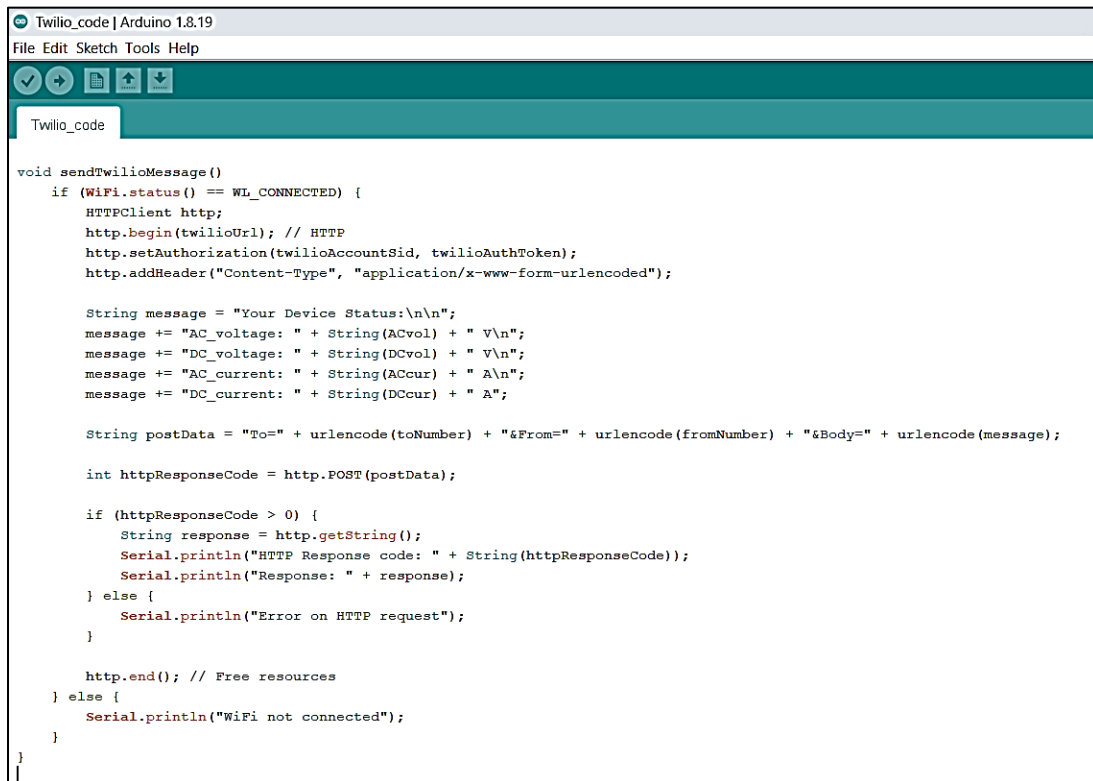


Figure 4. 22 Notification of PV system parameters via SMS under testing conditions.

If connected, the function proceeds by preparing the necessary components for message transmission. This includes constructing the Twilio API endpoint URL and encoding the account SID and authentication token for authorization. The electrical measurements are formatted into a clear and readable message, which is then embedded in the body of the HTTP POST request alongside the recipient's and sender's phone numbers. Upon sending the HTTP request to Twilio's API, the function captures and outputs the response status code and content to the serial monitor, providing feedback on the success of the message transmission. If the WiFi connection is absent, the function immediately reports the issue without attempting to send the SMS. Figure 4.23 illustrates the Arduino IDE code implementation of the Twilio function.



```
void sendTwilioMessage()
  if (WiFi.status() == WL_CONNECTED) {
    HTTPClient http;
    http.begin(twilioUrl); // HTTP
    http.setAuthorization(twilioAccountSid, twilioAuthToken);
    http.addHeader("Content-Type", "application/x-www-form-urlencoded");

    String message = "Your Device Status:\n\n";
    message += "AC_voltage: " + String(ACvol) + " V\n";
    message += "DC_voltage: " + String(DCvol) + " V\n";
    message += "AC_current: " + String(ACcur) + " A\n";
    message += "DC_current: " + String(DCcur) + " A";

    String postData = "To=" + urlencode(toNumber) + "&From=" + urlencode(fromNumber) + "&Body=" + urlencode(message);

    int httpResponseCode = http.POST(postData);

    if (httpResponseCode > 0) {
      String response = http.getString();
      Serial.println("HTTP Response code: " + String(httpResponseCode));
      Serial.println("Response: " + response);
    } else {
      Serial.println("Error on HTTP request");
    }

    http.end(); // Free resources
  } else {
    Serial.println("WiFi not connected");
  }
}
```

Figure 4. 23 Arduino IDE code of the Twilio API

## 4.7 Discussion

Building upon the successful experimental outcomes, here are key attributes of the proposed IoT-enabled SCADA system for overseeing and managing the PV system.

- **Framework:** The proposed SCADA system represents the latest IoT-based framework, incorporating essential components for a SCADA system. It consists of FIDs (ZMPT101B, ACS712, relay), and a RTU built on an Arduino Nano. A GSM SIM800L, and an ESP-32, all serially interfaced (UART) with the RTU for communication over GSM and Wi-Fi. Additionally, it features an MTU configured via the Blynk and the TCP/IP for GSM and HTTP protocol over a local network.

- **Graphical User Interface (GUI):** The Blynk platform is utilized in the development of the SCADA framework, simplifying the intricate process of data communication via HTTP and the HMI design, thereby enabling straightforward implementation of the proposed SCADA system.
- **Remote Supervision and Monitoring:** The proposed IoT-driven SCADA system incorporates remote monitoring and Control features. Users can access the SCADA system through the Blynk app and console HMIs via the local network and mobile application.
- **Reliability of system:** The sensors and relays (FIDs) are interfaced with the Arduino Nano (RTU), ensuring that the Blynk (MTU) remains isolated from the PV system. This setup prevents potential damage to the RTU during extreme conditions.
- **Data Retention:** The proposed SCADA system integrates local storage via a Blynk enabling visualization of historical data through its graphical user interface (GUI). This feature facilitates the analysis of essential data trends to support informed decision-making.
- **Enhanced Remote Monitoring and Notification System:** The system successfully integrates a function to send real-time SMS alerts containing critical electrical measurements, such as AC and DC voltage and current, directly to the user. This capability enhances remote monitoring and ensures immediate notification of system parameters, significantly improving the responsiveness and overall reliability of the PV system.
- **Cost-effective and Open-source:** By integrating the Blynk platform with the Arduino IDE, our SCADA system optimizes cost-effectiveness through freely available open-source software. This strategy eliminates the burden of costly proprietary licenses while providing a flexible framework for development and maintenance. Hardware components such as FIDs and the RTU are readily accessible in local markets, streamlining deployment and enhancing economic viability. The

detailed cost breakdown in Table 4.6 reveals a total system cost of CAD 33.39, coupled with a low average power consumption of 3.39 watts, ensuring efficient, sustainable operation 24/7.

Table 4. 6 Price and Power consumption of elements used in the SCADA system.

Quantity (No.)	Elements	Price (CAD)	Power consumption(W)
1	Arduino Nano	4.91	0.2
1	ESP-32	7.37	0.66
1	LCD Display	1.39	0.135
2	ACS 712 Current	6.38	0.012
1	ZMPT101B	2.45	0.025
1	GSM-SIM800L	5.92	1.5
1	5V Relay	2.28	0.05
2	Buck Converter LM2596	4.82	0.88
	<b>Total</b>	<b>35.52</b>	<b>3.462</b>

## 4.8 Conclusion

Rural communities in Pakistan face electricity shortages due to high initial infrastructure costs. Given these communities' diverse terrains, Photovoltaic (PV) systems are crucial for electrification—components like PV panels, MPPT controllers, batteries, inverters, and loads from the PV system. Field Interface Devices (FIDs) monitor and control PV parameters, aiding effective electrical consumption management. There's a growing need for a versatile, scalable system to handle these tasks efficiently. The study achieves significant technical milestones in developing an economical IoT-based SCADA system for PV monitoring and control. Integrating IoT technology with traditional SCADA functionalities, the system enables remote monitoring and control through the Blynk app and console, leveraging Arduino Nano, GSM SIM800L, and ESP-32 microcontrollers. It offers a cost-effective solution with a total expense of CAD 35.52 and low power consumption of 3.462 W, making it an affordable alternative for rural communities. The dual-mode communication capability via GSM and Wi-Fi ensures reliable data transfer in various network conditions, enhancing flexibility and robustness. Utilizing open-source platforms like Blynk and Arduino IDE promotes accessibility and customization, encouraging community-driven innovation. The system provides comprehensive monitoring of critical PV parameters, allows remote control of electrical loads, and features real-time SMS

notifications for critical system alerts, ensuring immediate user awareness and quick response to any issues. Real-world validation demonstrated its reliability and effectiveness, particularly in rural settings. The user-friendly interface of the Blynk app and web dashboard facilitates easy access to real-time data and system management, enhancing user engagement and operational efficiency. These achievements underscore the potential of IoT-based SCADA systems to revolutionize renewable energy management, particularly in underserved areas. Future research should focus on enhancing the system's ability to integrate a broader range of energy sources and leverage advanced predictive analytics to optimize energy usage and generation. Additionally, there is significant potential to support the cybersecurity measures of IoT components, ensuring the reliability and security of the energy management system. Although the current user interface is functional, it would benefit from improved visualization tools to facilitate the interpretation of complex data. Research should also explore the system's scalability by deploying it in larger environments and implementing advanced cybersecurity protocols to protect against unauthorized access and data breaches. Developing solutions for long-term data storage and incorporating machine learning algorithms for predictive maintenance and optimization will further enhance the system's efficiency. Moreover, expanding the system to include redundancy features and automated fault detection will significantly improve its reliability and robustness.

# Arduino- ESP-32 Code (Appendix A)

```
#define BLYNK_PRINT Serial

#include <WiFi.h>

#include <BlynkSimpleEsp32.h>

#include <ArduinoJson.h>

#define BLYNK_TEMPLATE_ID "TMPL2th_r2ugs"

#define BLYNK_TEMPLATE_NAME "Load Monitoring System"

#define BLYNK_AUTH_TOKEN "6EF9dE0xZalWaVG-AtZ-q9ZHGcGtuvUa"

char auth[] = "6EF9dE0xZalWaVG-AtZ-q9ZHGcGtuvUa";

char ssid [] = "Galaxy M513EFF";

char pass [] = "xzoe6621";

float DCvol, DCcur, ACvol, ACcur;

void setup () {

  Serial. Begin (9600);

  Serial2.begin(9600);

  Blynk. Begin (auth, ssid, pass,"blynk.cloud",80);

}

void loop () {

  Blynk. Run();

  if (Serial2.available() > 0) {

    // Read the data from Arduino

    String Json String = Serial2.readStringUntil('\n');

    // Parse JSON

    DynamicJsonDocument doc (200);

    deserializeJson(doc, jsonString);
```

```

DCvol = doc["DCvol"] ;
DCcur = doc["DCcur"];
ACvol = doc["ACvol"];
ACcur = doc["ACcur"];

// Extract values

Serial.print("DCvol = ");
Serial.println(DCvol,1);
Serial.print("DCcur = ");
Serial.println(DCcur,1);
Serial.print("ACvol = ");
Serial.println(ACvol,1);
Serial.print("ACcur = ");
Serial.println(ACcur,1);

blynkupdate();

}

delay (1000); // Adjust delay as needed

}

void blynkupdate()
{
  Blynk.virtualWrite(0, DCvol);
  Blynk.virtualWrite(1, DCcur);
  Blynk.virtualWrite(2, ACvol);
  Blynk.virtualWrite(3, ACcur);
}

BLYNK_WRITE(V4) {

```



```
int val = param.asInt();  
Serial.print("Recieved ");  
Serial.println(val);  
Serial2.write(val);  
}
```

## References

1. Ahmed, M.M.; Qays, M.O.; Abu-Siada, A.; Muyeen, S.M.; Hossain, M.L. Cost-Effective Design of IoT-Based Smart Household Distribution System. *Designs* **2021**, *5*, 55. <https://doi.org/10.3390/designs5030055>.
2. Abouobaida, H.; De Oliveira-Assis, L.; Soares-Ramos, E.P.P.; Mahmoudi, H.; Guerrero, J.M.; Jamil, M. Energy Management and Control Strategy of DC Microgrid Based Hybrid Storage System. *Simulation Modelling Practice and Theory* **2023**, *124*, 102726. <https://doi.org/10.1016/j.simpat.2023.102726>.
3. He, W.; Iqbal, M.T. A Novel Design of a Low-Cost SCADA System for Monitoring Standalone Photovoltaic Systems. *J. Electron. Electr. Eng.* **2024**. <https://doi.org/10.37256/jeee.3120244132>.
4. Stökler, S.; Schillings, C.; Kraas, B. Solar Resource Assessment Study for Pakistan. *Renew. Sustain. Energy Rev.* **2016**, *58*, 1184–1188. <https://doi.org/10.1016/j.rser.2015.12.298>.
5. Grainger, C.A.; Zhang, F. Electricity Shortages and Manufacturing Productivity in Pakistan. *Energy Policy* **2019**, *132*, 1000–1008. <https://doi.org/10.1016/j.enpol.2019.05.040>.
6. Asian Development Bank. “Energy Crisis in Pakistan: Implications for Economic Growth”, *Asian Development Outlook April 2023*, Asian Development Bank, 2023. Available: <https://www.adb.org/sites/default/files/publication/863591/pak-ado-april-2023.pdf> (accessed on 31 July 2024).
7. International Energy Agency (IEA). *Energy Policies Beyond IEA Countries: Pakistan 2022*; IEA: Paris, France, 2023. Available online: <https://www.iea.org/reports/energy-policies-beyond-iea-countries-pakistan-2022> (accessed on 31 July 2024).
8. Khan, H.A.; Ahmad, H.F.; Nasir, M.; Nadeem, M.F.; Zaffar, N.A. Decentralized Electric Power Delivery for Rural Electrification in Pakistan. *Energy Policy* **2018**, *120*, 312–323. <https://doi.org/10.1016/j.enpol.2018.05.054>.

9. Nasir, M.; Anees, M.; Khan, H.A.; Khan, I.; Xu, Y.; Guerrero, J.M. Integration and Decentralized Control of Standalone Solar Home Systems for Off-Grid Community Applications. *IEEE Trans. Ind. Appl.* **2019**, *55*, 7240–7250. <https://doi.org/10.1109/TIA.2019.2911605>.
10. Akhtar, T.; Rehman, A.U.; Jamil, M.; Gilani, S.O. Impact of an Energy Monitoring System on the Energy Efficiency of an Automobile Factory: A Case Study. *Energies* **2020**, *13*, 2577. <https://doi.org/10.3390/en13102577>.
11. Aghenta, L.O.; Iqbal, M.T. Development of an IoT-Based Open-Source SCADA System for PV System Monitoring. In Proceedings of the 2019 IEEE Canadian Conference of Electrical and Computer Engineering (CCECE), Edmonton, AB, Canada, 5–8 May 2019; pp. 1–4. <https://doi.org/10.1109/CCECE.2019.8861827>.
12. Oton, C.N.; Iqbal, M.T. Low-Cost Open Source IoT-Based SCADA System for a BTS Site Using ESP32 and Arduino IoT Cloud. In Proceedings of the 2021 IEEE 12th Annual Ubiquitous Computing, Electronics & Mobile Communication Conference (UEMCON), New York, NY, USA, 1–4 December 2021; pp. 0681–0685. <https://doi.org/10.1109/UEMCON53757.2021.9666691>.
13. Kao, K.-C.; Chieng, W.-H.; Jeng, S.-L. Design and development of an IoT-based web application for an intelligent remote SCADA system. *IOP Conf. Ser. Mater. Sci. Eng.* **2018**, *323*, 012025. <https://doi.org/10.1088/1757-899X/323/1/012025>.
14. Pramudhita, A.N.; Asmara, R.A.; Sirajuddin, I.; Rohadi, E. Internet of Things Integration in Smart Grid. In Proceedings of the 2018 International Conference on Applied Science and Technology (iCAST), Manado, Indonesia, 26–27 October 2018; pp. 718–722. <https://doi.org/10.1109/iCAST1.2018.8751518>.
15. Wang, Q.; Zhu, X.; Ni, Y.; Gu, L.; Zhu, H. Blockchain for the IoT and industrial IoT: A review. *Internet Things* **2020**, *10*, 100081. <https://doi.org/10.1016/j.iot.2019.100081>.
16. Huda, S.; Yearwood, J.; Hassan, M.M.; Almogren, A. Securing the operations in SCADA-IoT platform based industrial control system using an ensemble of deep belief networks. *Appl. Soft Comput.* **2018**, *71*, 66–77. <https://doi.org/10.1016/j.asoc.2018.06.017>.

17. Al-Ali, A.R.; Zualkernan, I.A.; Rashid, M.; Gupta, R.; Alikarar, M. A smart home energy management system using IoT and big data analytics approach. *IEEE Trans. Consum. Electron.* **2017**, *63*, 426–434. <https://doi.org/10.1109/TCE.2017.015014>.
18. Devi, M.; Muralidharan S.; Elakiya R.; Monica M. Design and Implementation of a Smart Home Energy Management System Using IoT and Machine Learning. *E3S Web Conf.* **2023**, *387*, 04005. <https://doi.org/10.1051/e3sconf/202338704005>.
19. Moraes, T.; Nogueira, B.; Lira, V.; Tavares, E. Performance Comparison of IoT Communication Protocols. In Proceedings of the 2019 IEEE International Conference on Systems, Man and Cybernetics (SMC), Bari, Italy, 6–9 October 2019; pp. 3249–3254. <https://doi.org/10.1109/SMC.2019.8914552>.
20. Jaloudi, S. Open-source software of smart city protocols status and challenges. In Proceedings of the 2015 International Conference on Open-Source Software Computing (OSSCOM), Amman, Jordan, 10–13 September 2015; pp. 1–6. <https://doi.org/10.1109/OSSCOM.2015.7372690>.
21. Ahsan, L.; Baig, M.J.A.; Iqbal, M.T. Low-Cost, Open-Source, Emoncms-Based SCADA System for a Large Grid-Connected PV System. *Sensors* **2022**, *22*, 6733. <https://doi.org/10.3390/s22186733>.
22. Duair, J.J.; Majeed, A.I.; Ali, G.M. Design and Implementation of IoT-Based SCADA for a Multi Microgrid System. *ECS Trans.* **2022**, *107*, 17345–17359. <https://doi.org/10.1149/10701.17345ecst>.
23. Uddin, S.U.; Baig, M.J.A.; Iqbal, M.T. Design and Implementation of an Open-Source SCADA System for a Community Solar-Powered Reverse Osmosis System. *Sensors* **2022**, *22*, 9631. <https://doi.org/10.3390/s22249631>.
24. Asgher, M.N.; Iqbal, M.T. Development of a Low-Cost, Open-Source LoRA-based SCADA System for Remote Monitoring of a Hybrid Power System for an Offshore Aquaculture Site in Newfoundland. *Eur. J. Electr. Eng. Comput. Sci.* **2023**, *7*, 65–73. <https://doi.org/10.24018/ejece.2023.7.6.589>.
25. Hamied, A.; Mellit, A.; Benghanem, M.; Boubaker, S. IoT-Based Low-Cost Photovoltaic Monitoring for a Greenhouse Farm in an Arid Region. *Energies* **2023**, *16*, 3860. <https://doi.org/10.3390/en16093860>.

26. He, W.; Baig, M.J.A.; Iqbal, M.T. An Open-Source Supervisory Control and Data Acquisition Architecture for Photovoltaic System Monitoring Using ESP32, Banana Pi M4, and Node-RED. *Energies* **2024**, *17*, **2295**. <https://doi.org/10.3390/en17102295>.
27. Khalid, W.; Awais, Q.; Jamil, M.; Khan, A.A. Dynamic Simulation and Optimization of Off-Grid Hybrid Power Systems for Sustainable Rural Development. *Electronics* **2024**, *13*, **2487**. <https://doi.org/10.3390/electronics13132487>.
28. Santosa, E.S.B.; Waluyanti, S. Teaching Microcontrollers using Arduino Nano Based Quadcopter. *J. Phys. Conf. Ser.* **2019**, *1413*, 012003. <https://doi.org/10.1088/1742-6596/1413/1/012003>.
29. Arduino Nano Pinout. Available online: <https://www.electronicshub.org/arduino-nano-pinout/> (accessed on 2 June 2024).
30. El Hammoumi, A.; Motahhir, S.; Chalh, A.; El Ghzizal, A.; Derouich, A. Low-Cost Virtual Instrumentation of PV Panel Characteristics Using Excel and Arduino in Comparison with Traditional Instrumentation. *Renew. Sustain. Energy Rev.* **2018**, *5*, 3. <https://doi.org/10.1186/s40807-018-0049-0>.
31. Omidi, S.A.; Baig, M.J.A.; Iqbal, M.T. Design and Implementation of Node-Red Based Open-Source SCADA Architecture for a Hybrid Power System. *Energies* **2023**, *16*, 2092. <https://doi.org/10.3390/en16052092>.
32. Alsumady, M.O.; Alturk, Y.K.; Dagamseh, A.; Tantawi, M. Controlling of DC-DC Buck Converters Using Microcontrollers. *Int. J. Circuits Syst. Signal Process.* **2021**, *15*, 197–202. <https://doi.org/10.46300/9106.2021.15.22>.
33. Abidin, Z.; Muttaqin, A.; Maulana, E.; Ramadhan, M.G. Buck Converter Optimization Using P&O Algorithm for PV System Based Battery Charger. *Int. J. Power Electron. Drive Syst. IJPEDS* **2020**, *11*, 844. <https://doi.org/10.11591/ijped.v11.i2.pp844-850>.
34. Zaveri, K.A.; Amin, M.H.; Amin, M.S.; Patel, M.R. IoT Based Real Time Low Cost Home Quarantine Patient Aid System Using Blynk App. *J. Phys. Conf. Ser.* **2007**, 012014. <https://doi.org/10.1088/1742-6596/2007/1/012014>.

35. Jamlos, M.A.; Moorali, J.; Mustafa, W.A.W.; Idrus, S.Z.S. Automotive Collision Avoidance System (ACAS) Application. *J. Phys. Conf. Ser.* **2021**, *1874*, 012037. <https://doi.org/10.1088/1742-6596/1874/1/012037>.
36. Budijono, S. Margareta Smart Warning System Using SIM800L and ESP32. *IOP Conf. Ser. Earth Environ. Sci.* **2021**, *794*, 012132. <https://doi.org/10.1088/1755-1315/794/1/012132>.
37. Sugiyanti, I. Design of ATM Crime Monitoring System Based on MQTT Protocol Using SIM800L and Arduino Mega 2560. *INA-Rxiv Pap.* **2019**. <https://doi.org/10.31227/osf.io/jwqgn>.
38. Espressif. ESP-IDF Programming Guide: Get Started with ESP32 DevKitC. Available online: <https://docs.espressif.com/projects/esp-idf/en/stable/esp32/hw-reference/esp32/get-started-dev-kitc.html> (accessed on 8 June 2024).
39. Hercog, D.; Lerher, T.; Truntič, M.; Težak, O. Design and Implementation of ESP32-Based IoT Devices. *Sensors* **2023**, *23*, 6739. <https://doi.org/10.3390/s23156739>.
40. Hossain, J.; Algeelani, N.A.; Al-Masoodi, A.H.H.; Kadir, A.F.A. Solar-Wind Power Generation System for Street Lighting Using Internet of Things. *Indonesia. J. Electr. Eng. Comput. Sci.* **2022**, *26*, 639. <https://doi.org/10.11591/ijeecs.v26.i2.pp639-647>.
41. Vidhya, R.G.; Rani, B.K.; Singh, K.; Kalpanadevi, D.; Patra, J.P.; Srinivas, T.A.S. An Effective Evaluation of SONARS Using Arduino and Display on Processing IDE. In Proceedings of the *2022 International Conference on Computer, Power and Communications (ICCPC)*, Chennai, India, 14–16 December 2022; IEEE: New York, NY, USA, 2022; pp. 500–505. <https://doi.org/10.1109/ICCPC55978.2022.10072229>.
42. Divya, P.; Bhavana, N.; George, M. Arduino Based Obstacle Detecting System. *SSRN Electron. J.* **2020**. <https://doi.org/10.2139/ssrn.3621950>.

# Chapter 5

## Conclusion and Future Work

### 5.1 Conclusion

This study presents a novel approach to meeting the energy needs of remote and isolated sites through the development and implementation of a hybrid power system. Emphasizing the significance of innovative energy solutions in these areas, the research highlights the potential of hybrid power systems to deliver a consistent and sustainable electricity supply. The proposed hybrid power system integrates various components, including solar panels, MPPT, a DC-AC inverter, a buck converter, a diesel generator, battery storage, and an electrical load. Performance analysis and optimal configurations are determined using PVsyst and HOMER Pro software, while the system's dynamic modeling is performed in MATLAB Simulink to evaluate its performance. Furthermore, experimental validation is conducted through Hardware-in-the-Loop simulations using the OP5707XG simulator from OPAL-RT Technologies.

In the first phase, Hybrid Power System Design and Dynamic Modeling of a Signal Repeater Station on a Natural Gas Transmission Network has been carried out. Using HOMER Pro software, the system combines photovoltaic panels, a DC-AC inverter, a natural gas generator (Genset), a battery bank (BB), and electrical loads. Extensive simulations result in an optimal system with a 100% renewable energy fraction and zero CO<sub>2</sub> emissions. The hybrid power system targets an energy cost of \$0.199 per kWh, an annual operating cost of \$653.44, a Net Present Cost of \$33,434, and an initial capital cost of \$24,987. Analysis of solar irradiance variations reveals their impact on energy cost and total system cost, highlighting the system's sensitivity to changes in solar radiation. Additionally, dynamic modeling and simulation with MATLAB/Simulink, along with real-time experimental validation using an OPAL-RT simulator, confirm the system's reliability in delivering consistent power. Overall, the hybrid power

system provides sustainable and cost-effective energy solutions, meeting the energy needs of isolated repeater stations and improving the sustainability of energy infrastructure.

In the second phase the design and simulation of a Hybrid power system has been carried out for a remote community has been carried out. Considering the recent floods in Pakistan, which are largely attributed to climate change driven by greenhouse gas emissions from fossil fuels, there is an urgent need to shift to renewable energy sources with minimal greenhouse gas emissions. Given Pakistan's abundant solar global horizontal irradiance, solar photovoltaic systems are pivotal in enhancing the electricity output of hybrid power systems. This approach not only addresses the specific energy needs of these facilities but also increases economic benefits, aligning with broader goals for energy sustainability. Using HOMER Pro, a total of 982 simulations were performed, leading to the identification of an optimal system with a renewable energy fraction of 100%. The hybrid power system's energy cost is USD 0.158 per kWh, leading to significant savings of USD 0.902 compared to the current cost of USD 1.06 per kWh. Furthermore, the system's annual operating cost of USD 2,093 represents substantial savings of USD 5,207 compared to the current annual cost of USD 7,300.

A comprehensive SCADA system that integrates FIDs, an RTU, an MTU, and a reliable communication protocol (HTTP) to effectively monitor and manage data flow for the proposed HPS has been carried out in the third phase. This advanced SCADA configuration employs GSM SIM800L and ESP-32 interfaces with Arduino Nano via UART for remote monitoring and control of electrical loads. The system has shown exceptional performance in both field and laboratory tests, enabling real-time monitoring of key parameters such as battery and load voltage and current, thus facilitating remote load management. The PV system is managed and controlled through the Blynk app and Blynk console, with an LCD displaying FID values within the circuit. Additionally, the system offers user-friendly data visualization via Blynk, enhancing operational reliability. This SCADA implementation not only provides an economical monitoring solution—with a total cost of CAD 35.52, no ongoing expenses, and power consumption of



3.462 W—but also demonstrates versatility and accuracy in handling real-time data in demanding environments. This research contributes to the academic and practical understanding of IoT-based SCADA systems and aligns with global efforts to adopt more sustainable and renewable energy sources by offering an effective tool to manage and optimize these resources.

## 5.2 Research Contribution/Problem Solutions

The contribution of this research work is to find the best solution to the problem enumerated in section 1.6 summarized below.

1. Two remote sites have been chosen for conducting the feasibility of a Hybrid Power system. The HP's sizing and economic feasibility have been done in the HOMER PRO and PVsyst software. Different scenarios have been discussed and the most feasible has been selected for the following sites:

- For a remote Natural Gas repeater station with a connected load of 33.65 kWh/day and a peak load of 11.33 kW, the proposed hybrid power system provides a reliable and sustainable solution for electricity supply, substantially reducing environmental impact.
- For a remote community the analysis of a connected load of 137.48 kWh/d and a peak load of 33.54 kW demonstrates the system's promise for reliable electricity.
- The control and dynamics of the proposed system are modeled in MATLAB/Simulink, with real-time simulation conducted using the OPAL-RT hardware-in-the-loop simulation platform.
- For monitoring and controlling the designed system, a low-power, cost-effective, open-source IoT-based SCADA system is utilized, employing HTTP and TCP/IP protocols. This SCADA system leverages the Blynk app and web console for remote electric load management. It is compatible with both GSM and Wi-Fi, increasing its feasibility for areas with limited or intermittent internet access. Field instrument devices (FIDs), including the ZMPT101B voltage

sensor and ACS712 current sensor, are used to collect field data, thereby enhancing the system's interoperability.

## 5.3 Future Work

Building upon the current research, several avenues for future work have been identified to further enhance the performance and scope of the hybrid power and IoT-based SCADA systems.

1. **Advanced Optimization Techniques:** Future research will explore the integration of advanced optimization algorithms, such as genetic algorithms, machine learning, and artificial intelligence, to improve the accuracy of energy forecasting and system performance. These techniques can help optimize energy generation, storage, and distribution while reducing costs and increasing system efficiency.
2. **Incorporation of Energy Storage Innovations:** The next step will involve integrating cutting-edge energy storage technologies, such as supercapacitors and advanced lithium-ion batteries, to enhance the reliability of energy storage, especially during periods of low renewable energy generation. This will ensure a more consistent and stable power supply for remote sites.
3. **Expansion of the SCADA System:** Future work will focus on expanding the IoT-based SCADA system to support multiple renewable energy sources, including wind and hydroelectric power, alongside solar energy. Enhancing real-time data analytics and predictive maintenance capabilities using IoT and big data tools will also improve operational decision-making and system management.
4. **Cybersecurity Enhancements:** Given the increasing reliance on IoT and remote monitoring systems, further research will address strengthening cybersecurity measures to safeguard against

potential cyber threats. Developing robust security protocols for data transmission and storage will be essential to ensure the secure operation of SCADA systems in critical infrastructure.

5. **Field Deployment and Long-Term Monitoring:** Finally, implementing large-scale field tests and long-term monitoring of the system's performance under different environmental conditions will provide valuable insights into its real-world effectiveness. These trials will help refine system configurations and further improve hybrid energy solutions' economic and technical feasibility in remote locations.

## Articles in Refereed Publications

- Khalid, W.; Awais, Q.; Jamil, M.; Khan, A.A. Dynamic Simulation and Optimization of Off-Grid Hybrid Power Systems for Sustainable Rural Development. *Electronics* 2024, 13, 2487. <https://doi.org/10.3390/electronics13132487>.
- Khalid, W.; Jamil, M.; Khan, A.A.; Awais, Q. Open-Source Internet of Things-Based Supervisory Control and Data Acquisition System for Photovoltaic Monitoring and Control Using HTTP and TCP/IP Protocols. *Energies* 2024, 17, 4083. <https://doi.org/10.3390/en17164083>.

## Refereed Conference Publications

- W. Khalid and M. Jamil, "Hybrid Power System Design and Dynamic Modeling of Signal Repeater Station on Natural Gas Transmission Network," *2024 12th International Conference on Smart Grid (icSmartGrid)*, Setubal, Portugal, 2024, pp. 412-417, doi: 10.1109/icSmart-Grid61824.2024.10578153.